UNIVERSITÀ DEGLI STUDI DI PALERMO
Dottorato in Scienze della Terra e del Mare
Dipartimento di Scienze della Terra del Mare (DiSTeM)
Settore Scientifico Disciplinare GEO/08

Noble gas geochemistry in seismic (Umbria, Italy) and volcanic (Grand Comore Island, Indian Ocean) regions: New methodologies and implications

IL DOTTORE
CLAUDIO VENTURA BORDENCA

IL COORDINATORE
Prof. ALESSANDRO AIUPPA

IL TUTOR
Prof. ALESSANDRO AIUPPA

I CO-TUTOR
Prof. RAPHAËL PIK
Dott. ANTONIO CARACAUSI

CICLO XXXII
ANNO CONSEGUIMENTO TITOLO 2018/2019

UNIVERSITÀ DEGLI STUDI DI PALERMO

To my little nephew Nicolò….
...May you always have the sunshine by your side and the courage
to break down the walls you will find on your way…

TABLE OF CONTENTS

CHAPTER III

The role of gas-water interaction in controlling the chemistry of volatiles emitted in a seismic region: The central Apennines case (Italy)

CHAPTER IV

Geochemistry of noble gas and radiogenic isotopes of ultramafic mantle xenoliths from La Grille volcano (Grand Comore Island, Indian Ocean)

LIST OF FIGURES

LIST OF TABLES

LIST OF EQUATIONS

Acknowledgements

The writing of this PhD thesis has been possible through the guidance of a number of people. Through their inspiration and precious contribution, I was able to expand my knowledge about Fluid Geochemistry and to become better acquainted with the analytical methods used here.

First and foremost, the first great outstanding tribute is devoted to my INGV tutor, **Dr. Antonio Caracausi**, who wholeheartedly shared with me his never-ending knowledge and helping me out to pave the way in the context of Geochemistry as a real mentor. I thank him for teaching me the scientific method, for being always a supportive soul both in life and science, for sharing laughs, beers, trips, ships, ferryboats and flights. All the time I spent with him was worth living. He has truly believed in me and trained me like a football manager who takes the best from his players. I consider him my big brother. I dedicate to him the Oasis song "Thank you for the good times"

To **Professor Alessandro Aiuppa**, my University advisor and my former professor of Volcanology, for his helpful support and precious tips for the pursuit of my research and to have greatly improved the quality of this Thesis.

To the crew of the Istituto Nazionale di Geofisica e Vulcanologia (INGV) of Palermo:

- To **Paolo** "the Eagle" **Cosenza**, the master of the Officina Meccanca, for his marvellous assistance in developing new lab equipments and all the technical aspects of this Thesis as well as for our discussions on rock music;
- To **Mariano Tantillo** for his training in the Noble Gas Laboratory and for his patience during isotopic analyses;
- To **Maria Grazia Misseri** for helping during mineral separation procedures;
- To **Fabio Vita** for his funny ways to make me laugh;
- To **Andrea Rizzo** for his unlimited wisdom;
- To **Giorgio Capasso** and **Cinzia Federico** for precious suggestions on Rayleigh fractionation modeling;
- To the two characters **Dario** "Darius" **Buttitta** from Trabia and **Paolo** "u praticu" **Randazzo** from Tortorici villages, respectively, for our everyday stories in our office and hilarious adventures in Vienna during EGU 2019.

A special laud is also dedicated to my ex Bachelor supervisor, **Professor P. Mario Nuccio**, who, since I had the chance to know years ago, helped me to grow both from a human and professional point of view.

To the crew of the Centre de Recherches Pétrographiques et Géochimiques (CRPG) during my formation period abroad in the city of Nancy:

- To my French supervisor **Raphael Pik** for his warm welcoming at CRPG
- To my best French buddy **Antoine Cremades** and our hot debates about rock'n'roll along with a fresh beer
- To the "violinist" **Camille Cartier** and our discussions on the beauty of living a foolish life
- To all the CRPG staff and lab technicians who kindly assisted me during sample analysis (**Christophe Cloquet**, **Christiane Parmentier**, **Aimeryc Schumacher**, **Catherine Zimmerman**, **David Cividini**)

To **Bernard Marty** (CRPG, Nancy - France) and **Ying Li** (IEF-CEA, Beijing - China) for their assistance during field campaigns in Umbria for colleting gas samples

To **Andrea di Muro and the student crew from Grand Comore Island** for our wild fieldtrips on Karthala and La Grille volcanoes.

To the reviewers **Michele Paternoster** (University of Basilicata) and **Orlando Vaselli** (University of Florence) for their constructive comments on this PhD Thesis

To my rockband mates **Giuseppe** "Joseph" **Ciglietti, Leonardo** "Leopino" **Giuliana, Matteo** "Matthew" **Agricola** for our perseverance and time spent during the making of the EP record and music videos on You Tube.

To my best friends **Simon Guess, Ricky La Cover, Nat Quartuccio** and **Ciccio Blues**

Last but not least, a final honor is dedicated to the sacrifices of **my family** whose human and moral support allowed building step-by-step prospects for a solid and encouraging future.

Abstract of the PhD dissertation

The noble gases are among the most powerful geochemical tools in different geological settings. For this reason, they represent one of the most valuable tracers of geochemical processes whose variations can be straightforwardly ascribed to magmatic/crustal dynamics. In this dissertation, noble gas (He, Ne, Ar) geochemistry applied in both seismic and volcanic regions are presented.

The PhD research has firstly been devoted to the test on the field of an auto-sampler for high-frequency collection of the water samples in order to be analysed for their dissolved noble gases. Then, I developed a lab-based methodology for the in-vacuum extraction of noble gases from waters collected in the copper tubes. The auto-sampler, named S.P.A.R.T.A.H. (*Syringe Pump Apparatus for the Retrieval and Temporal Analysis of Helium*), has been installed for a period of 2 months in a seismically active sector in the Umbria region (central Apennines, Italy), and collected fluids from a natural spring for the entire duration of the deployment with the aim of obtaining short-term noble gas data. The proper functioning and successful operation of the extraction system has been tested and verified in the Noble Gas Laboratory at the Istituto Nazionale di Geofisica e Vulcanologia (INGV) of Palermo.

In second part of the PhD research, I focused my attention on the high-flux CO_2–rich gas emissions localized in the central sector of the Apennines. The sampled gases have been analyzed for their chemical and isotopic composition (e.g., noble gases). Then, I developed a background geochemical model of fluid circulation and secondary chemical processes that occur during the transfer of fluid in the shallow crustal layers. Moreover I recognize a progressive northward decrease of the mantle-derived He degassing at regional scale along the Apennines. Furthermore, this study highlighted that the variable compositions of the gas manifestations discharged across the Umbria region can be best interpreted as a result of the combination of two different chemical processes which are not mutually exclusive: 1) a mixing between a magmatic end-member (VCVD) and a shallow-sedimentary sources, and 2) solubility-controlled fractionation mechanisms taking place upon interaction with shallow subsurface waters.

Finally, the project has been also addressed to the investigation of noble gases in fluids of an active volcanic system, Grande Comore Island (Indian Ocean). The noble gases (He, Ne, Ar) from fluid inclusions in peridotite mantle xenoliths coupled to radiogenic components (Sr, Nd, Pb) have been analysed to resolve the mantle source feeding the volcanism. Here I recognized a MORB-type mantle reservoir. In particular, the $^{3}He/^{4}He$ isotope compositions (up to 7.3Ra) fall in a range that overlaps the MORB mantle signature and the SCLM. The $^{20}Ne/^{22}Ne$, $^{21}Ne/^{22}Ne$ and $^{40}Ar/^{36}Ar$ isotope ratios plot along a mixing between air and a typical MORB-type reservoir. The Sr-Nd-Pb isotope systematics shows a mixing line between Depleted MORB and Enriched Mantle reservoirs, but for two samples whose higher Sr isotope signatures point towards an EM2 source, showing isotopic similarities with carbonatite rocks from the East African Rift System and central-northern Madagascar alkaline rocks.

CHAPTER I

1. INTRODUCTION

Deep-derived fluids are continuously released to the Earth's atmosphere. The degassing of natural fluids occurring in both volcanically (e.g., Chiodini et al. 2007; Caracausi et al. 2015; Di Muro et al. 2016; Aiuppa et al. 2019) and seismically-active regions (e.g., Caracausi and Paternoster, 2015; Buttitta et al. 2020; Frondini et al. 2018; Tamburello et al. 2018) has gained an increasingly interest over the past few decades in the framework of geochemical studies as they can substantially contribute to the present-day global carbon output through the discharge of significant amount of CO_2 (e.g., Mörner and Etiope 2002; Chiodini et al. 2004; Aiuppa et al. 2010; Burton et al. 2013). The investigation of fluids emitted at regional scale is crucial for understanding challenging issues as the evolution of the atmosphere, the Earth's interior as well as to seek for potential relationships between fluids degassing and volcanic activity and seismogenic processes, and the hazards that can be posed by such dangerous events.

Natural fluids occur commonly in the form of gas manifestations (e.g., bubbling gas springs, mud volcanoes, soil degassing, mofettes, fumaroles…) as well as in gases dissolved in subsurface water bodies. Additionally, fluids are also brought up to the surface through magmatic phenomenon, and can be trapped in peridotitic xenoliths through which the intrinsic characteristics of the Earth's interior and the processes affecting volatile transfer can be identified.

Among the most powerful indicators of natural processes are the noble gases, which reveal important insights about the behaviour and transport of volatiles to the surface from deep levels within the Earth. The noble gases are a group of chemical elements with similar properties occupying the last column of the periodic table: they are helium (He), neon (Ne), argon (Ar), krypton (Kr), xenon (Xe), and radon (Rn). In particular, the $^{3}He/^{4}He$ isotopic ratio is considered the most efficient geochemical tracer whose variations can be straightforwardly ascribed to magmatic/crustal dynamics and therefore is of primary importance in volcanic and seismic forecasting .

The advantage of using noble gases in Geochemistry relies on their (a) chemical inertness and low reactivity due to their filled outer valence shell, (b) high mobility and incompatible nature in melts, (c) relatively low abundances in the solid Earth, and (d) large isotopic disparity between different terrestrial reservoirs (e.g., mantle, crust, and atmosphere). In recent years, the international geochemical community has become very sensitive to seeking new approaches, methodologies and laboratory equipments that can

help constraining the processes that modify the pristine chemical signatures of fluids in different geological systems (e.g., volcanoes, hydrothermal systems, seismic regions).

The geochemical monitoring of fluids from active natural systems is aimed at recognizing any potential signals that can be directly correlated to geochemical changes due to volcanic and seismic activity. Evaluation of the geochemical signals carried by noble gases requires solid knowledge and awareness of natural systems and the development of accurate geochemical models.

The importance of the use of noble gases in natural fluids emitted in volcanic and near-fault areas has increased in the past 20 years. The majority, if not all, of the investigations devoted to volcanic and seismic forecasting has been focused on the use of noble gases as geochemical tracers of natural processes. Some examples are here presented. Following the 2001 eruption at Mt. Etna, Caracausi et al. 2003a reported synchronous variations of helium isotope ratio over five years of gas monitoring indicating pulses of ascending magma in the plumbing system, thus providing a powerful forecasting tool for incoming volcanic eruptions. Rizzo et al. 2006 identified signals of magma ascent preceding two distinct eruptive events at Mt. Etna during the 2002-2005 period by geochemical monitoring of both chemical composition and helium isotope ratio of peripheral gas emissions around the volcano and interpreted the geochemical signals on the basis of models proposed by Caracausi et al. 2003a-b. At Stromboli Island, a geochemical surveillance program since 2000s has demonstrated the consistency and reliability of fluid geochemistry data obtained during volcano monitoring with the purpose of identifying geochemical signals predictive of impending explosive events (Carapezza and Federico 2000; Capasso et al. 2005; Federico et al. 2008; Rizzo et al. 2009, 2015). Long-term time series of chemical and isotopic composition of noble gases (He, Ne, Ar) have shown that impressive eruptions from volcanoes inactive for decades may be preceded by the increasing input of magmatic volatiles and changes in isotopic ratios as reported for Mt. Ontake in Japan (Sano et al. 2015).

In seismic regions, the primary composition of natural gas emissions can be modified upon migration to the surface as a result of secondary chemical processes at shallow levels that can mask the pristine composition of the fluids creating misunderstanding in the evaluation of the contributions due to the different sources. The long-term geochemical monitoring allows to the identification of such processes in order to constrain any potential seismicity-induced anomalies of the emitted fluids. Therefore, the acquisition of the background level in seismic areas during quiescent periods is a

fundamental requirement to investigate the behaviour of geochemical anomalies as a consequence of seismogenic processes as well as to shed light on the possible relationship between crustal degassing, fluid flow-induced seismicity, tectonics and water-gas interaction at regional scale.

Pure geochemical precursors of seismic activity are an as yet out-of-reach frontier in earthquake forecasting. However, geochemical changes or anomalies prior to seismicity have been historically recorded. For instance, Italiano et al. 2001, 2005 and 2009 evidenced seismically-induced modifications of the helium isotope ratios and other geochemical parameters in natural fluids released in the central Apennines in Italy over long-lasting geochemical monitoring. The observed temporal variations in the geochemical features of the investigated fluids were attributed to stress-driven crustal deformations affecting bulk rock permeability occurring during seismogenesis. Chiodini et al. 2011 showed that the groundwaters circulating in two regional aquifers located in the epicentral area of the 2009 L'Aquila earthquakes in the Abruzzo region (central Italy) were affected by the influx of deeply derived, CO_2-rich gases whose source was thought to be confined beneath the epicentral area of the earthquakes where high-pressure fluids were hypothesized on seismological grounds. The composition of the uprising gases was estimated by a gas-water-rock model that simulates the evolution of the groundwater composition disturbed by the input of a CO_2-rich gas. In accordance with its geographical location in central Italy, the computed gas composition appeared to be progressively enriched in radiogenic components (^4He and ^{40}Ar) and in N_2, from the peri-Tyrrhenian volcanic complexes in the west to the Apennines in the east, suggesting increasing residence time of radiogenic gases trapped at high pressure in the crust thus playing a major role in triggering Apennines earthquakes.

The noble gases have also played an important role in answering to a breadth of challenging questions in rock geochemistry over the past decades (Allègre et al. 1983; Graham et al. 1992a; Pearson et al. 2003). Mafic mantle minerals in peridotite xenoliths, such as olivines and pyroxenes, have been widely investigated in terms of their noble gas inventory (Sumino et al. 2005; Correale et al. 2012; Rizzo et al. 2018 and reference therein) as they usually contain noble gases entrapped in fluid and/or melt inclusions. Geochemical investigation of fluid inclusions in ultramafic mantle xenoliths enclosed in volcanic products is crucial to constrain mantle heterogeneity at depth and/or to shed light on the additional chemical processes that control the pristine signature of the mantle source. The coupling of noble gas (He, Ne and Ar) to radiogenic components (i.e., Sr,

Nd, Pb) strongly contributes to the understanding of the mantle dynamics providing tools that can help to trace the mechanisms acting at modifying mantle materials that are brought up to the surface.

This PhD Thesis furnishes a new additional piece of the puzzle to the comprehension of the origin and behavior of natural fluids both in seismically- (Umbria, Italy) and volcanically-active (Grand Comore Island, western Indian Ocean) settings by means mainly of noble gases and fluid geochemistry. This work can provide new elements for the geochemical monitoring in the study areas.

The Umbria region, located in central Apennines (Italy) represents a natural laboratory for exploring the possible relationship between fluid circulation, degassing and regional-scale seismicity for different reasons: 1) It is characterized by high seismicity rate and it can be considered one of the Earth's most seismically active regions (e.g., Chiaraluce et al. 2007); 2) It is strongly affected, even in absence of seismicity, by widespread degassing of CO_2 (e.g., Chiodini et al. 2004) and characterized by fluid over-pressure at depth (Miller et al. 2004); 3) Several investigations have highlighted how this sector of the Apennines is particularly sensitive to seismogenic-induced geochemical anomalies (Caracausi et al. 2005; Heinicke et al. 2000, 2011; Italiano et al. 2001, 2004, 2005, 2009; Barberio et al. 2017); 4) It is characterized by the presence of active faults (UFS=Umbria Fault System) and tectonically dominated by a regional NW-trending low-angle normal fault (dip 15°-25°) named Alto Tiberina Fault (ATF) with associated SW-dipping high-angle antithetic structures; 5) It is monitored with multidisciplinary observing system. With the aim of investigating the seismogenic potential of the Alto Tiberina Fault, the area has been instrumented through the deployment of a near-fault observatory known as TABOO (The AltotiBerina near fault ObservatOry), a multidisciplinary research infrastructure managed by the Italian National Institute of Geophysics and Volcanology (INGV). The observatory consists of a dense geophysical network equipped with multi-sensor stations (seismometers, GPS, geochemical and electromagnetic sensors) located in the central-northern Apennines (Chiaraluce et al. 2014a-b).

On the other hand, the Indian Ocean has recently received significant interest in the scientific literature as far as concern the genesis and magmatic evolution of the Comorean archipelago and Le Reunion volcanism (Class et al. 2005 and references therein; Vlastelic and Pietruszka 2016). Here are located the two most active volcanoes in the southwest Indian Ocean: Piton de la Fournaise at La Réunion Island and Karthala on Grande Comore in the Comorian archipelago. Karthala is a magnificent volcano and, although its eruptions

are less frequent than those of Piton de la Fournaise, it poses a serious threat to the population living close to its shores and around its flanks, as demonstrated by recent eruptions. Karthala, the youngest of the Comorian volcanoes, rises from the floor of the Mozambique Channel. Grande Comore rises as a volcanic doublet comprising the coalescing shields of La Grille and Karthala. There are, however, no historic eruptions from La Grille, whereas Karthala has erupted at least twenty times since records began in 1857 and three of them occurred since 2000 producing damages to the villages at Gran Comore and led to the evacuation of people. This PhD investigation aims at obtaining important results that can contribute to the geochemical dataset of the Gran Comore volcanic system (La Grille-Karthala) to be useful for future geochemical monitoring

In summary, the main objectives of this research are:

- To highlight the pristine sources of natural gas emissions discharged in a seismically active region such as central Apennines and the role of the secondary chemical processes (e.g., mixing, fractionation due to gas-water interaction, etc.) in controlling their concentrations and isotopic signatures.
- To try reducing the sampling window by acquiring high-frequency geochemical data on the field and explore the behavior of noble gases in the short-term (hourly to daily) timescales which would thus open up a new lines of research with considerable potential both in theoretical and monitoring terms.
- To provide a strong contribution to the geochemical dataset of Gran Comore Island useful for future monitoring of an active, dangerous and very poorly-explored volcanic system characterized by large mantle heterogeneity as well as controversial and long-lasting debated origin.
- To emphasize the importance of the combined use of noble gases (e.g., He, Ne, Ar), major volatiles (e.g., CO_2, N_2) and radiogenic components (e.g., Sr, Nd and Pb) which enables important assessments of the degassing history and geochemical evolution of the Earth's interior.

2. STATE OF THE ART

2.1 Geochemistry of crustal fluids

The occurrence of natural degassing far from volcanic systems, such as the Earth's regions affected by continental rifting and active tectonics, has been called to particular attention over the past few decades (e.g., Chiodini et al. 2000; Mörner and Etiope 2002; Bräuer et al. 2018). Carbon dioxide is one of the most abundant components in natural gases and large emissions of deep CO_2-rich fluids are commonly reported worldwide in seismically- and tectonically-active regions (e.g., Chiodini et al. 2004; Italiano et al. 2009; Tamburello et al. 2018; Caracausi and Sulli, 2019) as they can substantially contribute to the present-day global carbon output. Considerations about the escape of natural fluids in non-volcanic regions stem from the identification of their sources and from the mechanisms of gas transfer through the continental crust. The released gases are usually characterized by a mixture of CO_2, CH_4, N_2, SO_2, and noble gases (He, Ne, Ar) in different proportions. When approaching the surface along the main tectonic structures the uprising volatiles can interact with shallow aquifers and be sequestered for a certain amount of time, and then progressively released as a function of their relative solubilities. In this section particular emphasis has been devoted to noble gas geochemistry in crustal settings. Three are the main sources of noble gases within the continental crust: *atmospheric*, as they are introduced into the crust dissolved in groundwater, *mantle*, during episodes of magmatic activity, and, finally, by means of processes of *radioactive decay* in the crust (**Fig.1**). Additionally, interplanetary dust particles (IDPs), cosmic ray interaction with the crust and anthropogenic sources can also represent a significant contribution of noble gases in crustal materials. Early Earth's processes, such as differentiation into mantle and continental crust, degassing and atmosphere loss, have resulted in the development of different reservoirs in which the chemistry of noble gases (their abundances and isotopic compositions) has been changed. Hence, fluids originating from these different sources will preserve noble gases with isotopically distinct signatures. Noble gases are then useful tools in the comprehension on the behaviour, transport and role of fluids in different geological environments given their low natural abundance and chemical inertness together with their isotopic fingerprint allowing contributions from different sources to be resolved and quantified. Therefore, a full understanding of the processes that control the abundances and isotopic signature of the noble gases in different crustal environments is strongly required.

Noble gas isotope ratios are sensitive parameters to trace processes of chemical fractionation (i.e., the relative partitioning of the isotopes between two natural systems). In multiple-sourced natural fluids a fractionation pattern can be recorded in only one component or in another or in both providing solid constrains about the timing of processes operating either before or after mixing.

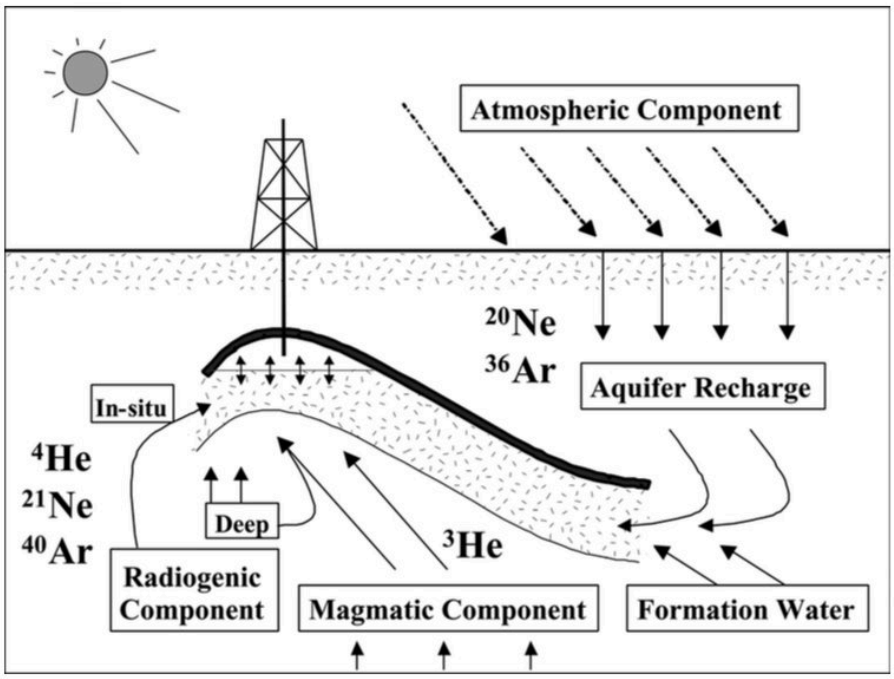

Fig. 1 – Schematic concept of a gas reservoir showing the different noble gas components in crustal fluids. Atmospheric noble gases (e.g., ^{20}Ne and ^{36}Ar) enter into the gas phase equilibrating with groundwater containing dissolved atmospheric noble gases. Radiogenic noble gases (e.g., ^{4}He, ^{21}Ne and ^{40}Ar) are produced by radioactive decay of U, Th and K in the crust and are transferred into crustal fluids. Upward transfer of deep mantle-derived noble gases (e.g., ^{3}He) may also be incorporated in crustal fluids. Image taken from Ballentine et al. 2002.

The present-day radiogenic production of ^{4}He is governed by the α-decay of ^{235,238}U and ^{232}Th and the crustal output produced in 1 g of rock per year is given by:

$$^{4}\text{He atoms g}^{-1}\text{ yr}^{-1} = (3.115\text{x}10^{6} + 1.272\text{x}10^{5})\,[\text{U}] + 7.710\text{x}10^{5}\,[\text{Th}] \quad \text{Eq. (1)},$$

where [U] and [Th] are the concentrations of ^{235,238}U, ^{232}Th in weight fraction or parts-per-million (ppm) (Ballentine and Burnard 2002). Crustal production of ^{3}He is governed by thermal neutron capture by ^{6}Li and other reactions described in Mamyrin and Tolstikhin 1984. For average crustal compositions, ^{3}He produced within the crust yields orders of magnitude lower than ^{6}Li and can, thus, be considered negligible. Neon isotopes (^{20,21,22}Ne) are almost entirely produced in the crust by nucleogenic processes through ^{17,18}O, ^{19}F, ^{22,23}Na, ^{24,25}Mg radioelements (Yatsevich and Honda 1997). Natural gases

preserved an important record of Ne isotope data in regional crustal systems. Investigations of Ne isotopes in crustal gases showed $^{21}Ne/^{22}Ne$ ratios well below those observed in radioactive elements, suggesting preferential thermal release of ^{22}Ne from minerals (Shukolyukov et al. 1973). Given that $^{21}Ne/^{22}Ne$ ratios are consistent with O/F ratios, the homogeneity of the $^{21}Ne/^{22}Ne$ production ratio in different crustal locations led Kennedy et al. 1990 to believe that the source of O/F ratios required a common mineral suite such as micas and amphiboles. The coupling of Ne to He isotopes provides a sensitive indicator of fractionation (Ballentine et al. 1991). Thus, fractionations of $^{4}He/^{21}Ne$ ratios can be caused by preferential release of noble gases from mineral production sites, transport factors such as diffusion, or gas-water-oil phase partitioning (see 5.2 Section in Chapter I).

Finally, radiogenic Argon, expressed as $^{40}Ar^{*}$, is produced in the crust by decay of ^{40}K, whose present-day production is calculated as

$$^{40}\mathbf{Ar\ atoms\ g^{-1}\ yr^{-1}} = 102.2\ [K] \quad \text{Eq. (2)},$$

where [K] is the concentration of ^{40}K, in weight fraction or parts-per-million (ppm) (Ballentine and Burnard 2002). Althought, ^{36}Ar is also production in the crust its abundance is insignificant compared to the atmosphere-derived ^{36}Ar introduced into the crust dissolved in groundwater and is usually considered negligible.

Combining the term for He radiogenic production (Eq. **1**) with that for the Ar (Eq. **2**), the total crustal He/Ar production ratio can be obtained as follows (Ballentine & Burnard 2002):

$$\mathbf{^{4}He/^{40}Ar^{*}} = \{(3.115x10^{6} + 1.272x10^{5})\ [^{235,238}U] + 7.710x10^{5}\ [^{232}Th]\} / 102.2\ [^{40}K]$$

Eq. (**3**)

Considering the average concentrations of U, Th and K, the present-day $^{4}He/^{40}Ar$ production ratio gives values of 3.09, 5.79 and 6.0 for the lower, middle and upper crust, respectively, with a weighted mean of 5.7. $^{4}He/^{40}Ar$ ratios are used to unravel processes of fractionation during thermal release from their respective mineral sites and transport related to fractionation (Ballentine et al. 1994; Mamyrin and Tolstikhin 1984). The variability of $^{4}He/^{40}Ar^{*}$ ratios in crustal gases and their deviations from the production ratio could also be explained by preferential release of He and Ar. The process of crustal degassing is characterized by the escape from the mineral in which the noble gases are trapped or produced and their transport to the surface from the respective site of

production. The transfer of radiogenic gases through structural pathways in the continental crust requires necessarily a driving force, which can result either in a concentration gradient diffusion or a pressure gradient advective fluid flow (Ballentine and Burnard 2002). The mechanism of diffusion out of crustal minerals plays an important role in the loss of noble gases at mineral scale based on gas diffusivity in minerals and is usually related to other release factors such as rock fracturing. However, the efficiency of release of He and Ar is also strongly dependant on the thermal conditions (Ballentine et al. 1994). When crustal minerals are held at thermal regimes below the He closure temperature any rare gases will diffuse out of the mineral grains, while above the Ar closure temperature the $^{4}He/^{40}Ar^{*}$ ratio will remain close to the crustal production ratio. On the other hand, elevated $^{4}He/^{40}Ar^{*}$ ratios are associated to diffusive release from minerals held at a intermediate temperature between the He and Ar closure temperatures where most of the He atoms in the rocks will be liberated compared to a minor fraction of those of the Ar (Elliot et al. 1993; O'Nions and Ballentine 1993; Ballentine et al. 1994). Previous experimental studies have shown that rare gases (e.g., He and Ar) can be released from rocks under compression (Scholz et al. 1973; Honda et al. 1982) and their fluxes in the crust are governed by rock fracturing (Torgersen and O'Donnell 1991). According to these authors, the degassing of volatiles from compressed rocks is strongly dependant to the degree of **dilatancy**, which can be attributed to the creation of new exposed surface areas due to micro-cracking which would permit the escape of atoms of rare gases away from crustal minerals. Moreover, these experimental investigations have also reported the existence of a differential release of He and Ar from rocks. Contrary to Ar, whose degassing depends on parameters other than dilatancy such as compression conditions and rock type, He is continuously released from rock under compression until fracturing. This suggests that, in accordance with Caracausi and Paternoster 2015, the development of seismogenic processes (i.e., earthquakes) could favour the releasing of He rather than Ar. Therefore, in a high-seismicity and tectonically active region such the Central Apennines in Italy there could be a relatively high potential to promote the mobility of helium accumulated in crustal levels.

2.2 Mantle Geochemistry

2.2.1 Noble Gas Isotopes as Geochemical Tracers

Owing to their volatile nature, noble gases have a strong tendency to enter gas or melt phase, thus giving them the exclusivity of being precious tracers for the origin and transport of fluids. Indeed, the noble gases have played an overwhelming role as geochemical tools to a breadth of challenging issues in fluid and rock geochemistry over the past few decades to place constrains on the evolution and structure of the Earth as well as the degassing history of the mantle (Allègre et al. 1983; Marty et al. 1989; Hilton and Porcelli 2003; Moreira 2013). The study of noble gas isotopes in mantle-derived materials (lavas, peridotite xenoliths, fluids…) is crucial to understanding the chemical heterogeneity of the Earth's mantle. In this respect, mid-ocean ridge basalts (MORBs) and ocean island basalts (OIBs) provide important examples to acquire an accurate snapshot of the Earth's interior as they may either contain high volatile contents or trap melt/fluids within magmatic phenocrysts. Detectable variations in the isotopic composition of noble gases are strictly associated to geochemical processes governing the distribution of the main Earth's heat-producing nuclides (**Table 1**).

Table 1 – List of parent nuclides of noble gases (from Graham 2002; Porcelli et al. 2002). The tracer ratios treated in this PhD Thesis are shown in red.

Parent nuclide	Daughter nuclide	Half-life	Tracer ratio	Comments
^{3}H	^{3}He	12.26 yr		Continously produced in the atm
^{238}U	^{4}He	4.46 Gyr	$^{3}He/^{4}He$	
^{238}U	$^{136,134}Xe$		$^{136,134}Xe/^{130}Xe$	Spontaneous fission
^{235}U	^{4}He	704 Ma	$^{3}He/^{4}He$	
^{232}Th	^{4}He	14 Gyr	$^{3}He/^{4}He$	
^{232}Th	^{136}Xe		$^{136}Xe/^{130}Xe$	No significant production in Earth
^{40}K	^{40}Ar	1.25 Gyr	$^{40}Ar/^{36}Ar$	
^{244}Pu	^{136}Xe	80 Ma	$^{136,134}Xe/^{130}Xe$	Extinct radioactivity
^{129}I	^{129}Xe	16 Ma	$^{129}Xe/^{130}Xe$	Extinct radioactivity
^{18}O	^{21}Ne		$^{21}Ne/^{22}Ne$	Nucleogenic reaction from U and Th decay
^{24}Mg	^{21}Ne		$^{21}Ne/^{22}Ne$	Nucleogenic reaction from U and Th decay

One of the most striking findings is that the high $^{3}He/^{4}He$ ratios, together with $^{20}Ne/^{22}Ne$ and $^{21}Ne/^{22}Ne$ ratios approaching solar values, found in mantle-derived products from ocean islands and mid-ocean ridges suggests that primordial volatiles are still outgassing from the innermost regions of the Earth. To date, the use of the He-Ne isotope systematics is the present-day solidest geochemical proof that portions of the mantle have remained rather undegassed over geologic time. High $^{40}Ar/^{36}Ar$ and $^{129}Xe/^{130}Xe$ ratios

(the latter is not treated in this PhD Thesis) in mid-ocean basalts also furnish important constrains on ancient volatile loss. Planetary outgassing, starting from formation of the Earth's ocean and atmosphere to depletion through magma generation to plate tectonic-driven recycling, leads to a wide range of parent/daughter ratios in the mantle budgets of noble gas inventory. Earth's mantle contains both primordial (e.g., ^{3}He, ^{20}Ne, ^{36}Ar, ^{130}Xe) and radiogenic isotopes (^{4}He, ^{40}Ar, ^{129}Xe, ^{136}Xe) but in different proportions. MORBs and OIBs show different isotopic ratios of these noble gases.

2.2.1.1 Helium

In the context of understanding mantle heterogeneity, analyses of helium isotopes have been carried out more than any other noble gas specie. Helium isotope measurements in mid-ridge and island basalts have provided some of the most important geochemical insights on mantle reservoirs. Helium is a reliable geochemical tracer for discriminating the crustal and mantle components due to the different origin of its two isotopes (^{3}He has a primordial origin, whereas ^{4}He is produced in the crust by radioactive α-decay of ^{235,238}U and ^{232}Th; Ballentine & Burnard 2002). The primary source of ^{3}He is degassing from Earth's interior and its presence in mantle-derived materials indicates that the Earth is still releasing volatiles that were once entrapped during accretion more than 4500 Ma ago. Understanding helium isotope variations along mid-ocean ridges and oceanic islands is essential in the context of mantle convection-driven mixing and partial melt generation in the upper mantle. The observed dichotomy in terms of ^{3}He/^{4}He ratio between MORBs and OIBs is taken as evidence for the existence of two distinct mantle source reservoirs. Several compilations of helium isotope data have been produced with the general agreement that MORBs show a relatively narrow range of ^{3}He/^{4}He (mean= 8±1 Ra), while OIBs display a much higher variability (up to 40 Ra; **Fig. 2**). This remarkable disparity has led to assume that the sources of MORBs and OIBs must have remained isolated enough for a significant time interval in Earth's history to retain isotopic differences in their respective ^{3}He/^{4}He ratios. The highest magmatic helium isotope ratios are found at ocean island localities such as Hawaii, Iceland, Galápagos, Samoa, Réunion,

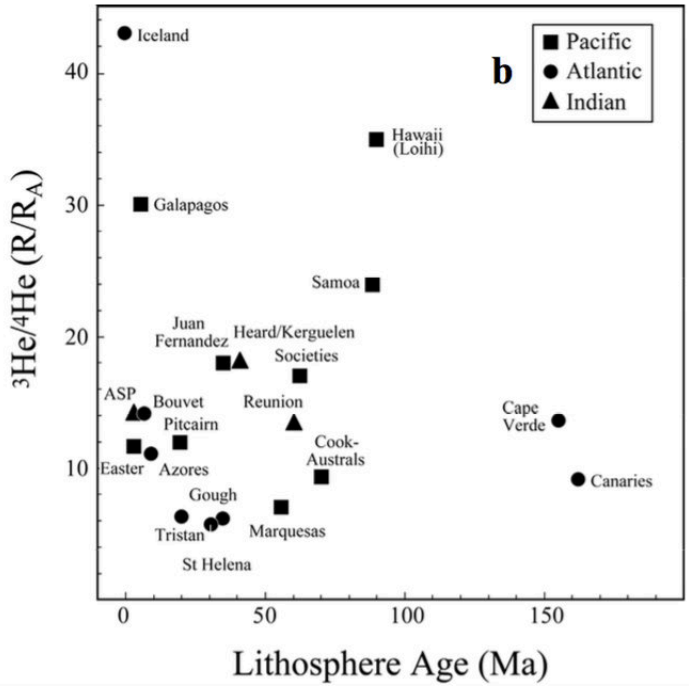

Fig. 2– Helium isotope ratios, expressed as R/Ra, in OIB lavas against the age of the lithosphere (from Graham 2002).

and Juan Fernandez (**Fig. 2**). The existence of such high $^3He/^4He$ values is coherent with the presence of mantle plume upwellings from deep remote regions in the Earth's mantle, and, thereby, less degassed, being characterized by higher time-integrated $^3He/(U+Th)$ ratio compared to the upper mantle MORB sources. However, in addition to OIB with helium isotope ratios far greater than MORB range, there is also a subcategory of OIB with $^3He/^4He$ ratios lower than MORB, such as the islands of Azores (Moreira et al. 1999) St. Helena, Gough and Tristan da Cunha (Graham et al. 1992b) and Grand Comore (Class et al. 2005), with their helium values ranging between 5 and 8 Ra. These are the so-called "low-^3He" hotspot islands, which tend to have also extreme radiogenic isotope characteristics (Zindler and Hart 1986). Indeed, these islands show a strong effect on their Sr and Pb isotope compositions along with low He isotope ratios, in accordance with the hypothesis of plume-lithosphere interaction. For instance, the association between lower $^3He/^4He$ ratios with more radiogenic $^{206}Pb/^{204}Pb$ in the Azores was interpreted by Moreira et al. 1999 as He isotope heterogeneity within mantle plume. This low $^3He/^4He$ signature at these regions may suggest addition of radiogenic contribution from crustal material recycled back into the mantle, although its origin is hotly debated.

2.2.1.2 Neon

Measurements of Ne isotopic composition of mantle-derived rocks has been considered to be challenging compared to that of helium since low abundance of Ne in the mantle and its ubiquitous presence in the atmosphere making air contamination a potential analytical drawback. Furthermore, corrections during mass spectrometer analysis for isobaric inferences on masses 20 and 22 due to doubly-charged interfering species (e.g., $^{40}Ar^{++}$ and $^{44}CO_2^{++}$) have always to be determined. So far, the most accurate Ne isotope measurements are performed by stepwise release of gas (as for Ar and Xe isotopes) by incremental crushing or by incremental heating under vacuum. Isotopic determination of Ne since late 1970s (Craig and Lupton 1976; Honda et al. 1987; Sarda et al. 1988) demonstrated that $^{20}Ne/^{22}Ne$ and $^{21}Ne/^{22}Ne$ ratios in mantle-derived rocks are far greater than Earth's atmosphere, with $^{20}Ne/^{22}Ne$ ratios approaching solar-like values, suggesting strong Ne fractionation from its terrestrial primitive composition (Porcelli and Pepin 2000). In general, Ne isotopes in mantle-derived materials have a relative large compositional range. However, MORBs and OIBs show substantial differences in their Ne isotope composition (e.g., Sarda et al. 1988; Moreira and Allegre 1998; Graham 2002; Mukhopadhyay 2012). In the Ne three isotopes diagram, MORBs samples fall along a mixing between the air value ($^{20}Ne/^{22}Ne$= 9.8 and $^{21}Ne/^{22}Ne$ = 0.029) and an end-member enriched in both $^{20}Ne/^{22}Ne$ and $^{21}Ne/^{22}Ne$. On the other hand, OIBs (such as Hawaii, Le Reunion and Iceland) show steeper arrays (**Fig. 3**). These trends reveal that the OIB mantle source, at least for these volcanic systems, have less nucleogenic Ne, hence lower $^{21}Ne/^{22}Ne$ than for the MORB mantle sources.

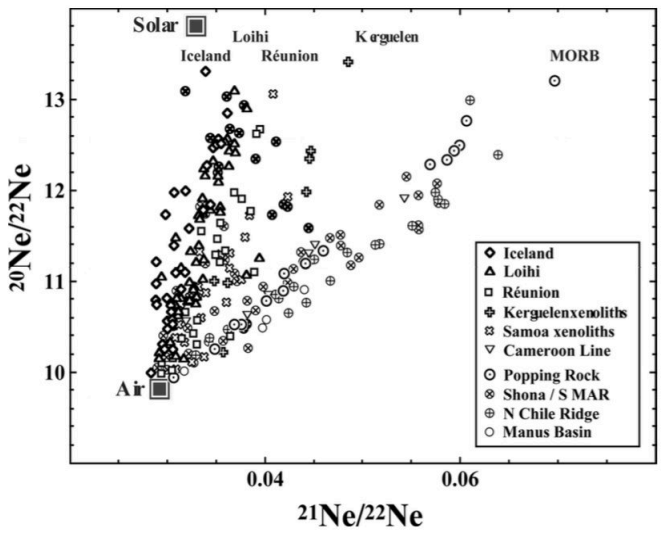

Fig. 3 - The Ne three-isotope diagram ($^{20}Ne/^{22}Ne$ vs. $^{21}Ne/^{22}Ne$). Data sources are **MORB** - Sarda et al. (1988, 2000), Hiyagon et al. (1992), Moreira et al. (1995, 1996, 1998), Moreira and Allègre (2002), Niedermann et al. (1997), Niedermann and Bach (1998), Shaw et al. (2001); **OIB** - Sarda et al. (1988), Poreda and Farley (1992), Staudacher et al. (1990), Hiyagon et al. (1992), Honda et al. (1991, 1993a-b), Valbracht et al. (1996, 1997), Dixon et al. (2000), Barfod et al. (1999), Trieloff et al. (2000), Moreira et al. (2001) and Hanyu et al. (2001). The extrapolated $^{21}Ne/^{22}Ne$ ratio, corresponding to solar $^{20}Ne/^{22}Ne$ at each locality, is 0.035 for Iceland, 0.039 for Loihi, 0.043 for Réunion, 0.053 for Kerguelen and 0.075 for MORB. Image taken from Graham 2002.

Moreover, the strong enrichment in MORB samples in $^{20}Ne/^{22}Ne$ ratio with respect to air value can be attributed by the existence of a solar neon component with $^{20}Ne/^{22}Ne > 13$ entrapped in the mantle since accretion (alike for primordial helium), suggesting that OIB source reservoirs have experienced lower degree of primitive (solar) volatile loss over geological time. The systematic divergence between MORBs and OIBs in their Ne isotope signatures results from differences in the dilution of the nucleogenic ^{21}Ne by primordial Ne, as very minor amount of ^{21}Ne can significantly alter the $^{21}Ne/^{22}Ne$ ratio in the mantle because of its scarse abundance. Furthermore, it is worth saying that the production nucleogenic ^{21}Ne in the mantle is strongly related to radiogenic ^{4}He (expressed as α-particles), as the most important pathways for ^{21}Ne, namely referred as Wetherill reactions (Wetherill 1954), require that neutrons and U-Th-derived α-particles to collide with target atoms of ^{18}O and ^{24}Mg.

2.2.1.3 Argon

Argon has three isotopes: ^{36}Ar, ^{38}Ar, and ^{40}Ar. The former two isotopes are primordial and are not produced within Earth, while ^{40}Ar is radiogenically produced by decay of ^{40}K with a relatively short half-life (1.25 Gyr) compared to the age of the Earth and, thus, providing solid constraints on the formation of the atmosphere, Earth's degassing and isotopic evolution of the mantle. As seen for Ne, measurements of Ar isotopes can be analytically difficult due to contamination by air component. The Earth's atmosphere has a $^{40}Ar/^{36}Ar$ ratio of 298 (Lee et al. 2006) and all other terrestrial material show higher values, thus $^{40}Ar/^{36}Ar$ ratios are to be considered the results of mixing between atmospheric Ar and a radiogenic component. The $^{40}Ar/^{36}Ar$ ratio of the mantle shows a variable range and this variability is due to time-integrated variations in K/Ar ratios. MORBs display $^{40}Ar/^{36}Ar$ ratios as high as 40.000 (**Fig. 4**). The highest values have been measured in popping rocks (Burnard et al. 1997) and mid-ocean glassy basalts (Marty and Humbert 1997; Sarda et al. 2000). High ratios have bee also found at ocean islands such as in xenoliths from Samoa (22.000; Farley et al. 1994), in olivine phenocrysts from Juan Fernandez (8000; Farley and Craig 1994) and basalt glasses from Loihi Seamount off the coast of the Hawaii Island (8300; Trieloff et al. 2000). According to Burnard et al. 1998, the origin of the high $^{40}Ar/^{36}Ar$ ratios in xenoliths is unknown, probably because

fluid inclusions may have been strongly suffered episodes of metasomatic overprints in the upper mantle. Any systematic correlation has been observed between argon and helium isotope ratios on MORB samples. The $^{40}Ar/^{36}Ar$ ratios in MORB are usually widely distributed over 2 orders of magnitude compared to a relatively constant $^{3}He/^{4}He$ isotope trend.

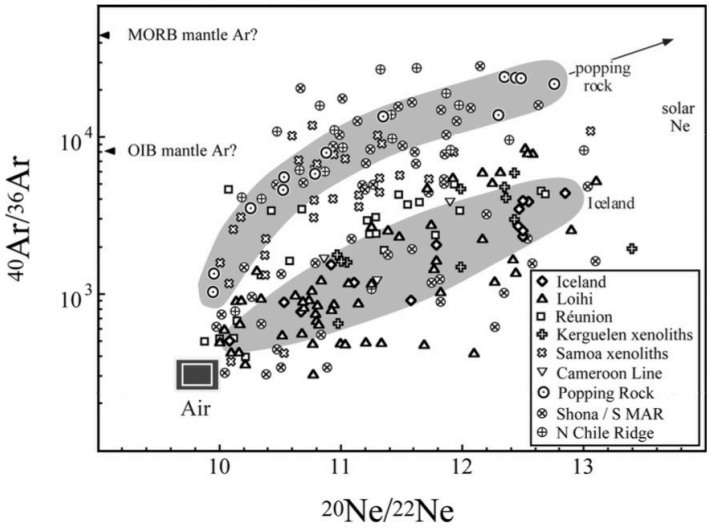

Fig. 4 – $^{40}Ar/^{36}Ar$ vs. $^{20}Ne/^{22}Ne$. Data sources are given in the caption to Fig. 3. Image taken from Graham 2002.

Interestingly, a correlation between Ar and Ne can be observed in Fig. XXX, where for the case of popping rocks the highest $^{40}Ar/^{36}Ar$ ratios are associated with the highest $^{20}Ne/^{22}Ne$ ratios, evidencing the lowest degree of atmospheric contribution for this types of rocks.

2.2.2 Radiogenic Isotopes as proxies for understanding mantle dynamics

Geochemistry of igneous rocks is based on three main lines of investigation:

1) ***Major element chemistry***. A chemical element is expressed as "major" when it represents an essential constituent of the rock-forming minerals, such as Mg, Fe, Ca, Na, O, Al. On the basis of major-element composition of an igneous rock, a mantle source can be defined as *Fertile* (a source that has never or very slightly suffered partial melting) or *Depleted* (a residual source after extraction of partial melts).

2) ***Trace element chemistry***. A chemical element is defined as "trace" when its concentration is very low and does not represent a mineral constituent. On the basis of their partitioning coefficient, trace elements can be *compatible* or *incompatible* with the solid or liquid phase, respectively. Thus, a mantle source can be defined either *Depleted* or *Enriched* in trace element contents.

3) ***Radiogenic isotope geochemistry***.

Radiogenic isotope geochemistry is considered a powerful tool to study the chemistry, history and evolution of Earth's mantle reservoirs over geological time.

Amongst the long-lived radioactive parent-daughter isotope lines (**Table 2**), the most commonly used in mantle geochemistry are Rb-Sr, Sm-Nd, and U-Th-Pb systematics.

Table 2 – List of long-lived radionuclides (from Hofmann 2003). The tracer ratios treated in this PhD Thesis are shown in red.

Parent nuclide	Daughter nuclide	Half life (yr)	Tracer ratio
^{87}Rb	^{87}Sr	48.8×10^9	$^{87}Sr/^{86}Sr$
^{147}Sm	^{143}Nd	106×10^9	$^{143}Nd/^{144}Nd$
^{176}Lu	^{176}Hf	35.7×10^9	$^{176}Hf/^{177}Hf$
^{187}Re	^{187}Os	45.6×10^9	$^{187}Os/^{188}Os$
^{40}K	^{40}Ar	1.25×10^9	$^{40}Ar/^{36}Ar$
^{232}Th	^{208}Pb	14.01×10^9	$^{208}Pb/^{204}Pb$
^{238}U	^{206}Pb	4.46×10^9	$^{206}Pb/^{204}Pb$
^{235}U	^{207}Pb	0.74×10^9	$^{207}Pb/^{204}Pb$

Rubidium is an alkali metal with two naturally occurring isotopes, ^{85}Rb and ^{87}Rb, whose abundances are 73% and 27%, respectively. ^{87}Rb is radioactive, and decays to the stable isotope ^{87}Sr by β decay. During partial melting of a typical four-phase upper-mantle assemblage (olivine, clinopyroxene, orthopyroxene, spinel/garnet/plagioclase), both Rb and Sr behave as incompatible elements but Rb is more incompatible than Sr. Therefore, a partial melt will evolve with higher Rb/Sr ratio than the original source, whereas a residual mantle will evolve with lower Rb/Sr ratio than the original source. Whatever the

type of mantle source, ^{87}Sr increases continously as ^{87}Rb constantly decays. The temporal evolution of a suite of hypothetical geological systems is illustrated in the **isochron diagram** in **Fig. 5**.

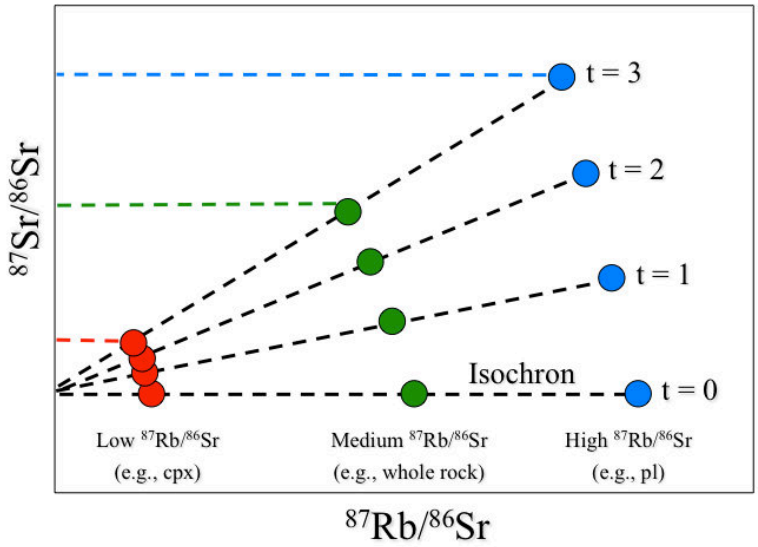

Fig. 5 – Rb-Sr isochron diagram for a suite of co-magmatic igneous materials. The conceptual model of isochron diagram was invented by Nicolaysen 1961. Acronyms cpx and pl stand for clinopyroxene and plagioclase, respectively.

Let us assume three co-magmatic systems (two minerals and one whole-rock) having the same $^{87}Sr/^{86}Sr$ ratio at the time of the solidification of the rock and different $^{87}Rb/^{86}Sr$ ratios. After each system has turned into a closed system at t=0 (e.g., fast-cooling crystallization after a volcanic eruption), the relative isotopic compositions will change with time and the slope of the isochron will become steeper as ^{87}Rb decay decreases the $^{87}Rb/^{86}Sr$ ratio and increases $^{87}Sr/^{86}Sr$ ratio. Hence, the isotope value $^{87}Sr/^{86}Sr$ in a system is a function of the time-integrated parent-daughter Rb/Sr ratio. The $^{87}Sr/^{86}Sr$ ratio of the Earth is continously increasing since its formation. The present-day average terrestrial Sr-isotope composition is defined as Bulk Silicate Earth (**BSE**) and is equal to 0.70445. Values higher than this estimate indicate derivation from sources with higher $^{87}Rb/^{86}Sr$ (i.e., enriched sources), while values lower than BSE indicate derivation from sources with lower $^{87}Rb/^{86}Sr$ (i.e., depleted sources) (**Fig. 6**).

Samarium and neodymium belong to the rare-earth elements (REE) group. Sm has seven naturally occurring isotopes, of which only three are radioactive (^{147}Sm, ^{148}Sm and ^{149}Sm). Among these, the half-life of ^{147}Sm is short enough to generate measurable differences in the abundance of the daughter isotope ^{143}Nd produced by α decay. In a classic mantle assemblage, both Sm and Nd are very incompatible element. As seen in

the Rb-Sr isotope system, the parent isotope (Rb) is **more** incompatible than the daughter isotope (Sr), but in the case of Sm-Nd isotope system the parent isotope (Sm) is **less** incompatible than the daughter isotope (Nd). Therefore, a residual mantle will have a time-integrated Sm/Nd ratio higher than the original primitive source as well as higher than a partial melt derived from that source. The average composition of the Earth in terms of $^{143}Nd/^{144}Nd$ is given by the **ChUR** (Chondritic Uniform Reservoir) estimate, which is equal to 0.51264. As seen for Sr-isotope systematics, values higher than ChUR are considered depleted, whereas values lower than ChUR are enriched (**Fig. 6**).

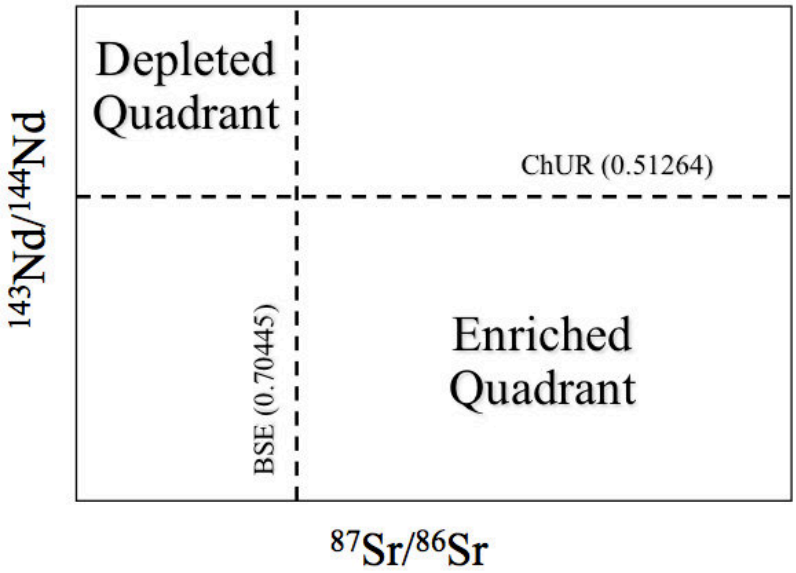

Fig. 6 - $^{87}Sr/^{86}Sr$ vs. $^{143}Nd/^{144}Nd$ showing the Depleted and Enriched Quadrants

Several petrological and geochemical studies carried out on oceanic basalts over the past decades have allowed for the identification of distinct reservoirs in the Earth's mantle (Zindler and Hart 1986; Hofmann 1997). At least three different end-members have been identified so that the geochemical characteristics of ocean basalts can be somehow explained by the mixing of these components. The first fundamental end-member of mantle composition is the **DMM** (Depleted Morb Mantle), which is considered the supposed source of the basalts erupted at plate boundaries along mid-ocean ridges, of which the process of extraction of partial melt have lead to its distinct depleted nature. Typical $^{87}Sr/^{86}Sr$ ratios of DMM range from 0.702 to 0.704 (i.e., lower than BSE), while $^{143}Nd/^{144}Nd$ ratios range from 0.5134 to 0.5128 (i.e., higher than ChUR). Depleted mantle regions that have interacted with crust-derived lithologies are named *Enriched* in terms of Sr-Nd isotope systematic, thus the second end-member of mantle compositions is

represented by Enriched Mantle (EM) components. These are usually divided into two types (**EMI** and **EMII**), which show geochemical affinities with continental/oceanic crust and sediment, and, hence, the recycling of crustal material through subduction has been inferred as the main process in the evolution of these reservoirs. Recycling of crustal lithologies has the typical effect to raise $^{87}Sr/^{86}Sr$ and lower $^{143}Nd/^{144}Nd$ of the contaminated mantle source.

Finally, the U-Th-Pb is also an important isotope system since there are three different decay chains producing isotopes of Pb (**Table 2**). ^{206}Pb and ^{207}Pb are usually known as "*Uranogenic Pb*" because they derive from the decay of U isotopes (^{238}U and ^{235}U, respectively), while ^{208}Pb is called "*Thorogenic Pb*" since it derives from ^{232}Th. The three Pb daughter isotopes are commonly normalized to the stable isotope ^{204}Pb. As seen for Rb-Sr and Sm-Nd systematics, Pb isotope ratios of an igneous rock is dependent of the amount of the parent isotope. The ratio $^{238}U/^{204}Pb$ is also known as **μ**, hence, rocks with high $^{206}Pb/^{204}Pb$ ratios (up to 21-22) are called High-μ (**HIMU**). This is because these types of rocks imply derivation from mantle sources with high $^{238}U/^{204}Pb$ ratio since ^{206}Pb derives from ^{238}U. Despite several mid-ocean ridge and ocean island basalts (MORB and OIB) contain quite variable and overlapping ranges of radiogenic Pb, suggesting the presence of a widespread HIMU-type source component, the most radiogenic Pb isotopes values, which require necessarily high U/Pb and Th/Pb ratios in their relative sources, are found in OIB. As such, these have been labeled as HIMU-type OIB (Hofmann 1997 and reference therein). Recently, Stracke et al. 2005 have suggested that the highly radiogenic Pb isotope signatures in MORB and OIB originate from melting of two distinct sources: 1) the HIMU component, which occurs in a limited number of oceanic localities, the Cook-Austral islands in the South Pacific Ocean and St. Helena in the Atlantic Ocean; 2) a component, different than HIMU, characterized by slightly less radiogenic Pb but notably more radiogenic Sr isotope signatures and closely resembling the isotopic composition of the mantle component termed FOZO (i.e., FOcal Zone) postulated by Hart et al. 1992). The FOZO component is defined as an isotopically distinct, more common and ubiquitous end-member in the MORB and OIB sources. Stracke 2012 used the term PREMA (i.e., PREvalent MAntle; Zindler and Hart 1986) instead of FOZO referring to a range of isotope composition that extends to the end of the global MORB isotopic array (**Fig. 7**). It is worth pointing out that these end-member compositions (e.g. EMI, EMII, HIMU, PREMA-FOZO) cannot be considered as distinct or separate reservoirs in the Earth's mantle but could rather represent heterogeneous regions that

might have inherited their distinctive isotope signatures due to relatively long-lasting periods of metasomatic processes (e.g. recycling of crustal materials). Indeed, a "mantle component" or "mantle domain" can be defined as a part of the mantle that is isotopically distinct from other parts of the mantle, regardless about its size, physical properties, mineralogy, genetic origin, or location in the mantle.

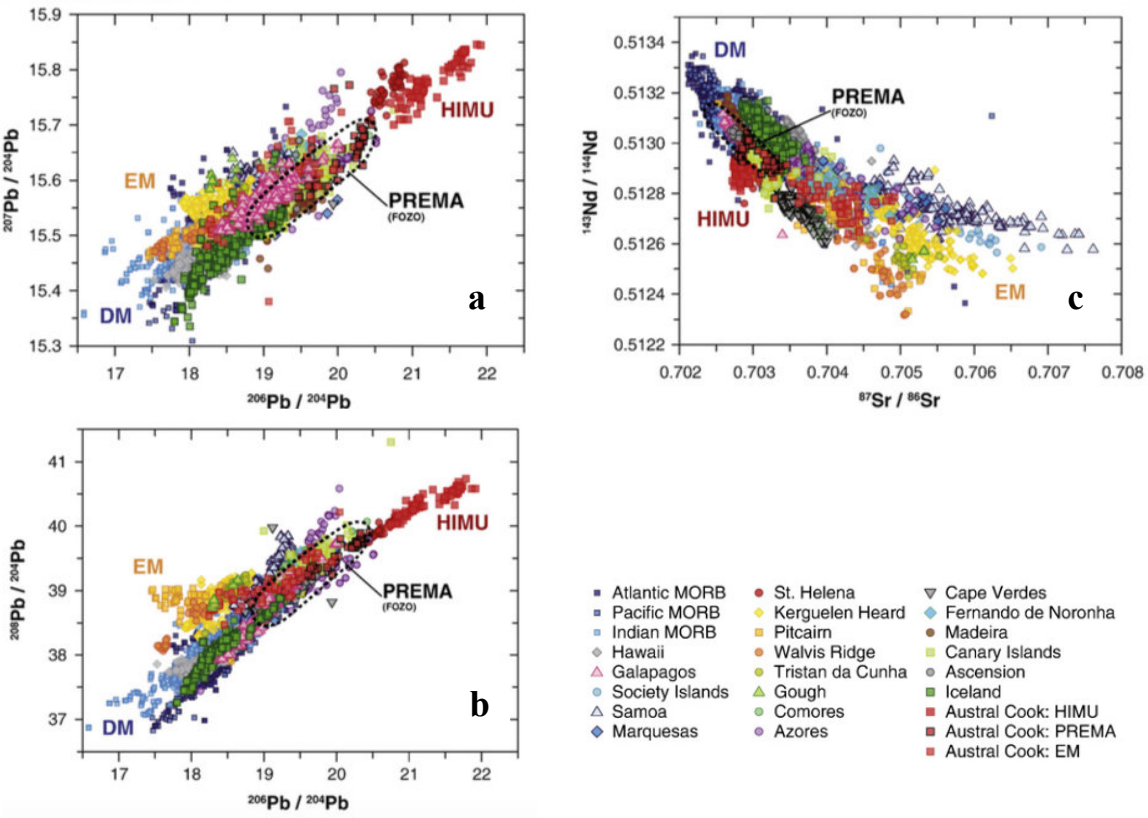

Fig. 7 - Isotopic variability in global mid ocean ridge (MORB) and ocean island basalts (OIB). a) $^{207}Pb/^{204}Pb$ vs. $^{206}Pb/^{204}Pb$; b) $^{208}Pb/^{204}Pb$ vs. $^{206}Pb/^{204}Pb$; c) $^{87}Sr/^{86}Sr$ vs. $^{143}Nd/^{144}Nd$. The range of compositions indicated for "PREMA" ("FOZO") is approximate and may extend to both more depleted and enriched compositions. The data compilation is provided in the supplementary materials (Supplementary Table 1) given in Stracke 2012.

REFERENCES

- **Aiuppa A., Burton M., Caltabiano T., Giudice G., Gurrieri S., Liuzzo M., Mure' F., and Salerno G. (2010)** – Unusually large magmatic CO2 gas emissions prior to a basaltic paroxysm – Geophysical Research Letters, vol. 37, L17303.
- **Aiuppa A., Fischer T. P., Plank T., and Bani P. (2019)** – CO2 flux emissions from the Earth's most actively degassing volcanoes, 2005-2015 – Scientific Report 9:5442
- **Allègre C. J., Hart S. R. and Minster J. F. (1983)** - Chemical structure and evolution of the mantle and continents determined by inversion of Nd and the Sr isotope data, I. Theoretical methods. *Earth. Planet. Sci. Lett.,* 66, 177–190.
- **Ballentine C.J. and Burnard P. G. (2002)** – Production, release and transport of noble gases in the continental crust. In: Porcelli D., Ballentine C.J., Wieler R. (Eds.), Noble gases in geochemistry and cosmochemistry: Rev. Min. Geoch., 47, pp. 481-538.
- **Ballentine C.J., Burgess R. and Marty B. (2002)** – Tracing fluid origin, transport and interaction in the crust. In: Porcelli D., Ballentine C.J., Wieler R. (Eds.), Noble gases in geochemistry and cosmochemistry: Rev. Min. Geoch., 47, pp. 539-614.
- **Ballentine C.J., Mazurek M., and Gautschi A. (1994)** - Thermal constrains on crustal rare gas release and migration: Evidence from Alpine fluid inclusions – Geochimica et Cosmochimica Acta, vol.58, n. 20, pp. 4333-4348.
- **Ballentine C.J., O'Nions R.K., Oxburgh E.R., Horvath F., and Deak J. (1991)** – Rare gas constrains on hydrocarbon accumulation, crustal degassing and groundwater flow in the Pannonian Basin – Earth and Planetary Science Letters, 105, pp. 229-246
- **Barberio M. D., Barbieri M., Billi A., Doglioni C. and Petitta M. (2017)** – Hydrogeochemical changes before and during the 2016 Amatrice-Norcia seismic sequence (Central Italy) – Scientific Reports, 7, 11735

- **Barfod D. N., Ballentine C. J., Halliday A. N., and Fitton J. G. (1999)** - Noble gases in the Cameroon line and the He, Ne and Ar isotopic compositions of high-μ (HIMU) mantle. J Geophys Res 104:29509-29527
- **Bräuer K., Kämpf H., Niedermann S., & Strauch G. (2018)** - Monitoring of helium and carbon isotopes in the western Eger Rift area (Czech Republic): Relationships with the 2014 seismic activity and indications for recent (2000-2016) magmatic unrest – Chem. Geology 482, pp.131-145.
- **Burnard PG, Graham DW, Turner G (1997)** - Vesicle-specific noble gas analyses of "popping rock": Implications for primordial noble gases in Earth. Science 276:568-571
- **Burnard PG, Farley KA, and Turner G. (1998)** - Multiple fluid pulses in a Samoan harzburgite. Chem Geol 147:99-114
- **Burton M., Sawyer G., and Granieri D. (2013)** – Deep carbon emissions from volcanoes – Carbon In Earth in Reviews in Mineralogy & Geochemistry, vol. 75, pp. 323-354, Hazen R. M., Jones A. P., and Baross J. A. (Editors)
- **Buttitta D., Caracausi A., Chiaraluce L., Favara R., Morticelli M. G., and Sulli A. (2020)** – Continental degassing of helium in an active tectonic setting (northern Italy): the role of seismicity – Scientific Report 10:162
- **Capasso, G., Carapezza M. L., Federico C., Inguaggiato S. and Rizzo A. (2005)** - Geochemical variations in fluids from Stromboli volcano (Italy): early evidences of magma ascent during 2002–2003 eruption, *Bulletin of Volcanology*, doi:10.1007/s00445-005- 0427-5.
- **Caracausi A., Favara R., Giammanco S., Italiano F., Paonita A., Pecoraino G., Rizzo A., and Nuccio P. M. (2003a)** - Mount Etna: Geochemical signals of magma ascent and unusually extensive plumbing system - Geophys. Res. Lett., 30(2), 1057, doi:10.1029/2002GL015463.

- **Caracausi A., Italiano F., Martinelli G., Paonita A. and Rizzo A. L. (2005)** – Long-term geochemical monitoring and extensive/compressive phenomena: case study of the Umbria Region (Central Apennines, Italy) – Ann. of Geoph., vol. 48, N. 1, pp. 43-53
- **Caracausi A., Italiano F., Paonita A., Rizzo A., and Nuccio P. M. (2003b)** - Evidence of deep magma degassing and ascent by geochemistry of peripheral gas emissions at Mount Etna (Italy): Assessment of the magmatic reservoir pressure - J. Geophys. Res., 108(B10), 2463, doi:10.1029/ 2002JB002095.
- **Caracausi A. and Paternoster M. (2015)** – Radiogenic helium degassing and rock fracturing: A case study of the southern Apennines active tectonic region – Journal of Geophysical Research, Solid Earth 120, pp. 2200-2211
- **Caracausi A., Paternoster M., Nuccio P. M (2015)** – Mantle CO_2 degassing at Mount Vulture volcano (Italy): relationships between CO_2 outgassing of volcanoes and the time of their last eruption – Earth and Planetary Science Letters, vol. 411, pp. 268-280.
- **Caracausi A. and Sulli A. (2019)** - Outgassing of mantle volatiles in compressional tectonic regime away from volcanism: The role of continental delamination. Geochemistry, Geophysics, Geosystems, 20, 2007–2020.
- **Carapezza M. L. and Federico C. (2000)** - The contribution of fluid geochemistry to the volcano monitoring of Stromboli, *JVGR*, *95*, 227–245.
- **Chiaraluce L., Chiarabba C., Collettini C., Piccinini D. and Cocco M. (2007)** – Architecture and mechanics of an active low-angle normal fault: Alto Tiberina Fault, northern Apennines, Italy – Journal of Geophysical Research, vol. 112, B10310
- **Chiaraluce L., Amato A., Carannante S., Castelli V., Cattaneo M., Cocco M., Collettini C., D'Alema E., Di Stefano R., Latorre D., Marzorati S., Mirabella F., Monachesi G., Piccinini D., Nardi A., Piersanti A., Stramondo S. and Valoroso L. (2014b)** – The Alto Tiberina Near Fault Observatory (northern Apennines, Italy) – Annals of Geophysics, 57, 3, S0327.

- **Chiaraluce L., Collettini C., Cattaneo M. and Monachesi G. (2014a) – The shallow boreholes at The AltotiBerina near fault Observatory (TABOO; northern Apennines of Italy)** – Scientific Drilling, 17, 31-35.
- **Chiodini G., Baldini A., Barberi F., Carapezza M. L., Cardellini C., Frondini F., Granieri D., and Ranaldi M. (2007)** – Carbon dioxide degassing at Latera (Italy): Evidence of geothermal reservoir and evaluation of its potential energy – Journal of Geophysical Research, vol. 112, B12204
- **Chiodini G., Caliro S., Cardellini C., Frondini F., Inguaggiato S. and Matteucci F. (2011)** – Geochemical evidence for and characterization of CO_2 rich gas source in the epicentral area of the Abruzzo 2009 earthquakes – Earth and Planetary Science Letters 304, pp. 389-398.
- **Chiodini G**., **Cardellini C., Amato A., Boschi E., Caliro S., Frondini F. and Ventura G. (2004)** – Carbon dioxide Earth degassing and seismogenesis in central and southern Italy – Geophysical Research Letters, vol. 31, L07615.
- **Chiodini G., Frondini F., Cardellini C., Parello F., & Peruzzi L. (2000)** – Rate of diffuse carbon dioxide Earth degassing estimated from carbon balance of regional aquifers: The case of central Apennines, Italy – Journal of Geophysical Research vol.105, NO.B4, pp.8423-8434
- **Class C., Goldstein S. L., Stute M., Kurz M. D. and Schlosser P. (2005)** - Grand Comore Island: A well-constrained "low $^3He/^4He$" mantle plume, Earth and Planetary Science Letters 233, pp. 391-409.
- **Correale A., Martelli M., Paonita A., Rizzo A., Brusca L., and Scribano V. (2012)** - New evidence of mantle heterogeneity beneath the Hyblean Plateau (southeast Sicily, Italy) as inferred from noble gases and geochemistry of ultramafic xenoliths. Lithos 132, 70–81.

- **Correale A., Rizzo A., Barry P. H., Lu J., and Zheng J. (2016)** - Refertilization of lithospheric mantle beneath the Yangtze craton in south-east China: evidence from noble gases geochemistry. *Gondwana Res*. 38, 289–303.
- **Craig H. and Lupton J. E. (1976)** - Primordial neon, helium, and hydrogen in oceanic basalts - Earth Planet Sci Lett 31:369-385
- **Di Muro A., Metrich N., Allard P., Aiuppa A., M., Galle B., and Staudacher T. (2016)** – Magma degassing at Piton de la Fournaise volcano - In: Bachelery, P., Lénat, J. F., Di Muro, A. and Michon, L. (Eds.), Active Volcanoes of the Southwest Indian Ocean: Piton de la Fournaise and Karthala, Springer-Verlag, pp. 203-221
- **Dixon E. T., Honda M., McDougall I., Campbell I. H., and Sigurdsson I. (2000)** - Preservation of near-solar neon isotopic ratios in Icelandic basalts. Earth Planet Sci Lett 180:309-324
- **Elliot T., Ballentine C. J., O'Nions R.K., and. Ricchiuto T. (1993)** - Carbon, Helium, Neon and Argon isotopes in a Po basin natural gas field - Chemical Geology, 106,429-440.
- **Farley K.A. & Craig H. (1994) -** Atmospheric argon contamination of ocean island basalt olivine phenocrysts. Geochem. Cosmochim. Acta, 58, 2509-2517
- **Farley K.A., Poreda R.J., Onstott T.C. (1994)** - Noble gases in deformed xenoliths from an ocean island: charcterization of a metasomatic fluid. *In* Matsuda J (ed) Noble Gas Geochemistry and Cosmochemistry. Terra Scientific, Tokyo, p 159-178
- **Federico C., Brusca L., Carapezza M. L., Cigolini C., Inguaggiato S., Rizzo A. and Rouwet D. (2008)** - Geochemical evidences of the incoming 2002–2003 Stromboli eruption: variations in CO_2 and Rn emissions and helium and carbon isotopes before 28th December 2002 - AGU Book, Learning from Stromboli.

- **Frondini F., Cardellini C., Caliro S., Beddini G., Rosiello A., and Chiodini G. (2018)** – Measuring and interpreting CO2 fluxes at regional scale: the case of the Apennines, Italy – Journal of the Geological Society, 176 (2): 408
- **Graham D. W., Jenkins W. J., Schilling J-G, Thompson G., Kurz M. D. and Humphris E. (1992a)** – Helium isotope geochemistry of mid-ocean ridge basalts from the South Atlantic, Earth and Planetary Science Letters 100, pp. 133-147
- **Graham D. W., Humphris E., Jenkins W. J., and Kurz M. D. (1992b)** - Helium isotope geochemistry of some volcanic rocks from St. Helena - Earth Planetary Science Letters 110:121-131
- **Graham D.W (2002)** – Noble Gases Isotope Geochemistry of Mid-Ocean Ridge and Ocean Island Basalts: Characterization of mantle Source Reservoirs. In Noble Gases in Geochemistry and Cosmochemistry, vol., 47, Rev. in Min. and Geochem., Min. Soc. of Am., Porcelli D., C.J. Ballentine. R. Wieler Editors
- **Hanyu T., Dunai T. J., Davies G. R., Kaneoka I., Nohda S., and Uto K. (2001)** - Noble gas study of the Reunion hotspot: evidence for distinct less-degassed mantle sources - Earth Planet Sci Lett 193:83-98
- **Hart S.R., Hauri E.H., Oschmann L. A. and Whitehead J.A. (1992)** - Mantle plumes and entrainment—isotopic evidence. Science 256, 517–520.
- **Heinicke J., Italiano F., Lapenna V., Martinelli G. and Nuccio P. M. (2000)** – Coseismic geochemical variations in some gas emissions of Umbria Region (Central Italy) – Phys. Chem. Earth, vol. 25, No. 3, pp.289-293
- **Heinicke J., Martinelli G. and Telesca L. (2011)** – Geodynamically induced variations in the emissions of CO_2 gas at San Faustino (Central Apennines, Italy) – Geofluids, doi: 10.1111/j.1468-8123.2011.00345.x
- **Hilton D. R. and Porcelli D. (2003)** – Noble gases as mantle tracers. In Treatise on Geochemistry: Meteorites, Comets and Planets, Vol. 2, pp. 277-318, Andrea M. Davis

(Volume Editor) and H. D. Holland and K. K. Turekian (Executive Editors).

- **Hofmann A.W. (1997)** - Mantle geochemistry: the message from oceanic volcanism. Nature 385:219-229
- **Hofmann A.W. (2003)** – Sampling mantle heterogeneity through Oceanic Basalts: Isotopes and Trace Elements. In Treatise on Geochemistry: Meteorites, Comets and Planets, Vol. 2, pp. 61-101, Andrea M. Davis (Volume Editor) and H. D. Holland and K. K. Turekian (Executive Editors).
- **Honda M., McDougall I., and Patterson D. (1993a)** - Solar noble gases in the Earth: the systematics of helium-neon isotopes in mantle derived samples. Lithos 30:257-265
- **Honda M., McDougall I., Patterson D. B., Doulgeris A., and Clague D. A. (1991)** - Possible solar noble-gas component in Hawaiian basalts. Nature 349:149-151
- **Honda M., McDougall I., Patterson D. B., Doulgeris A., and Clague D. A. (1993b)** - Noble gases in submarine pillow basalt glasses from Loihi and Kilauea, Hawaii: a solar component in the Earth. Geochim Cosmochim Acta 57:859-874
- **Honda M., Kurita K., Hamano Y., ans Ozima M. (1982)** - Experimental studies of He and Ar degassing during rock fracturing. *Earth Planet. Sci. Lett.* 59, 429–436.
- **Honda M., Reynolds J., Roedder E., and Epstein S. (1987)** - Noble gases in diamonds: occurrences of solar like helium and neon. J Geophys Res 92:12507-12521.
- **Hiyagon H., Ozima M., Marty B., Zashu S., and Sakai H. (1992)** - Noble gases in submarine glasses from mid- oceanic ridges and Loihi Seamount: constraints on the early history of the Earth - Geochim Cosmochim Acta 56:1301-1316
- **Italiano F., Caracausi A., Favara R., Innocenzi P. and Martinelli G. (2005)** - Geochemical monitoring of cold waters during seismicity: implications for earthquake-induced modification in shallow aquifers. Terr. Atmos. Ocean. Sci. 16 (4), 709–729.

- **Italiano F., Martinelli G., Bonfanti P., and Caracausi A. (2009)** – Long-term (1997-2007) geochemical monitoring of gases from the Umbria-Marche region – Tectonophysics, 476, pp.282-296
- **Italiano F., Martinelli G., and Nuccio P. M. (2001)** – Anomalies mantle-derived helium during the 1997-1998 seismic swarm of Umbria-Marche, Italy, Geophysical Research Letters, vol. 28, n. 5, pp. 839-842
- **Italiano F., Martinelli G. and Rizzo A.L. (2004)** – Geochemical evidence of seismogenic-induced anomalies in the dissolved gases of thermal waters: A case study of Umbria (Central Apennines, Italy) both during and after the 1997-1998 seismic swarm – G-cubed, vol. 5, number 11.
- **Kennedy B. M., Hiyagon H., and Reynolds J. H. (1990)** - Crustal neon: A striking uniformity - Earth Planet Sci Lett 98:277-286
- **Lee J. Y., Marti K., Severinghaus J. P., Kawamura K., Yoo H. S., Lee J. B. and Kim J. S. (2006)** – A redetermination of the isotopic abundances of atmospheric Ar – Geochimica et Cosmochimica Acta, 70, pp. 4507-4512
- **Mamyrin B.A. and Tolstikhin I.N. (1984)** - Helium isotopes in nature, Developments in Geochemistry, Elsevier Science Ltd., Fyfe W. S. (Eds.)
- **Marty B., Jambon A. and Sano Y. (1989)** - Helium isotopes and CO_2 in volcanic gases of Japan, *Chemical Geology,* 76, 25–40.
- **Marty B. and Humbert F (1997)** - Nitrogen and argon isotopes in oceanic basalts. Earth and Planetary Science Letters 152, pp. 101-112
- **Miller, S. A., C. Collettini, L. Chiaraluce, M. Cocco, M. Barchi, and B. J. P. Kaus (2004)** - Aftershocks driven by a high pressure CO_2 source at depth, Nature, 427, 724–727.
- **Moreira M**. **(2013)** – Noble gas constrains on the origin and evolution of Earth's volatiles, Geochemical Perspectives, Vol. 2, n. 2, pp. 229-403.

- **Moreira M. and Allègre C. J. (1998)** - Helium-neon systematics and the structure of the mantle - Chem Geol 147:53-59
- **Moreira M., and Allègre C. J. (2002)** - Rare gas systematics on Mid Atlantic Ridge (37-40°N). Earth Planet Sci Lett 198:401-416
- **Moreira M, Doucelance R, Kurz M.D., Dupré B., and Allègre C.J. (1999)** - Helium and lead isotope geochemistry of the Azores Archipelago – Earth and Planetary Science Letters 169:489-205
- **Moreira M., Gautheron C., Breddam K., Curtice J., Kurz M. D. (2001) -** Solar neon in the Icelandic mantle: new evidence for an undegassed lower mantle - Earth Planet Sci Lett 185:15-23
- **Moreira M., Staudacher T., Sarda P., Schilling J-G, Allègre C. J. (1995)** - A primitive plume neon component in MORB: the Shona ridge anomaly, South Atlantic (51-52°S) - Earth Planet Sci Lett 133:367-377
- **Moreira M., Kunz J., and Allègre C. J. (1998)** - Rare gas systematics in popping rock: isotopic and elemental compositions in the upper mantle. Science 279:1178-1181
- **Moreira M., Valbracht P. J., Staudacher T., Allègre C. J. (1996)** - Rare gas systematics in Red Sea ridge basalts. Geophys Res Lett 23:2453-2456
- **Mörner N. and Etiope G. (2002)** - Carbon degassing from the lithosphere, Global and Planetary Changes, 33, pp. 185-203.
- **Mukhopadhyay S. (2012)** - Deep mantle neon and xenon preserve a record of early planetary differentiation and heterogeneous volatile accretion - Nature 486, pp. 101–104
- **Nicolaysen L. O. (1961)** - Graphic interpretation of discordant age measurements on metamorphic rocks. Ann. NY Acad. Sci. 91, 198–206.
- **Niedermann S. and Bach W. (1998)** - Anomalously nucleogenic neon in North Chile Ridge basalt glasses, suggesting a previously degassed mantle source. Earth Planet Sci Lett 160:447-462

- **Niedermann S., Bach W., and Erzinger J. (1997)** - Noble gas evidence for a lower mantle component in MORBs from the southern East Pacific Rise: decoupling of helium and neon isotope systematics. Geochim et Cosmochim Acta 61:2697-2715
- **O'Nions R. K. and Ballentine C. J. (1993**) - Rare gas studies of basin scale fluid movement - Philosophical transactions of the Royal Society of London, A344, 141-156.
- **Pearson D. G., Canil D., and Shirley S. B. (2003)** - Mantle samples included in volcanic rocks: xenoliths and diamonds. In Treatise on Geochemistry: Meteorites, Comets and Planets, Vol. 1, pp. 171-275, Andrea M. Davis (Volume Editor) and H. D. Holland and K. K. Turekian (Executive Editors).
- **Porcelli C.J, Ballentine C. J. and Wieler R. (2002)** – An Overview of Noble Gas Geochemistry and Cosmochemistry. In Noble Gases in Geochemistry and Cosmochemistry, vol., 47, Rev. in Min. and Geochem., Min. Soc. of Am., Porcelli D., C.J. Ballentine. R. Wieler Editors.
- **Porcelli D and Pepin R.O. (2000)** - Rare gas constraints on early Earth history - *In* Canup RM, Righter K (eds) Origin of the Earth and Moon. The University of Arizona Press, Tucson, p 435-458
- **Poreda R. J. and Farley K. A. (1992)** - Rare gases in Samoan xenoliths - Earth Planet Sci Lett 113:129-144
- **Rizzo A., Caracausi A., Favara R., Martelli M., Paonita A., Paternoster M., Nuccio P. M. and Rosciglione A. (2006)** - New insights into magma dynamics during last two eruptions of Mount Etna as inferred by geochemical monitoring from 2002 to 2005 - Geochem. Geophys. Geosyst., vol. 7, N. 6.
- **Rizzo A., Federico C., Inguaggiato S., Sollami A., Tantillo M., Vita F., Bellomo S., Longo M., Grassa F., and Liuzzo M. (2015)** - The 2014 effusive eruption at Stromboli

volcano (Italy): Inferences from soil CO_2 flux and $^3He/^4He$ ratio in thermal waters, Geophysical Research Letters 42, pp. 2235–2243.

- **Rizzo A., Grassa F., Inguaggiato S., Liotta M., Longo M., Madonia P., Brusca L., Capasso G., Morici S., Rouwet D. and Vita F. (2009)** – Geochemical evaluation of observed changes in volcanic activity during the 2007 eruption at Stromboli (Italy) – Journal of Volcanology and Geothermal Research 182, pp. 246-254
- **Rizzo A., Pelorosso B., Coltorti M., Ntaflos T., Bonadiman C., Matusiak-Malek M., Italiano F., and Bergonzoni G (2018)** – Geochemistry of noble gases and CO_2 in fluid inclusions from lithospheric mantle beneath Wilcza Gora (Lower Silesia, southwest Poland) – Frontiers in Earth Science 6:215.
- **Sano Y., Kagoshima T., Takahata N., Nishio Y., Roulleau E., Pinti D. L., Fisher T. P., 2015** – Ten-year helium anomaly prior to 2014 Ontake eruption - Sci. Rep., Nature.
- **Sarda P, Moreira M, Staudacher T, Schilling J-G, Allègre CJ (2000)** - Rare gas systematics on the southernmost Mid-Atlantic Ridge: constraints on the lower mantle and the Dupal source. J Geophys Res 105:5973-5996
- **Sarda P**., **Staudacher T., Allègre C.J., (1988)** - Neon isotopes in submarine basalts. Earth Planet. Sci. Lett., 91, 73-88
- **Scholz C. H., Sykes L. R., and Aggarwal Y. P. (1973)** - Earthquake prediction: A physical basis - Science, 181, 803–810.
- **Shaw A. M., Hilton D. R., Macpherson C. G., and Sinton J. M. (2001)** - Nucleogenic neon in high $^3He/^4He$ lavas from the Manus back-arc basin: a new perspective on He-Ne decoupling. Earth Planet Sci Lett 194:53-66
- **Shukolyukov Yu A., Sharif-Zade V. B., and Sh Ashkinadze G (1973)** - Neon isotopes in natural gases – *Geochemistry International* 4: 346-354.
- **Staudacher T., Sarda P., and Allègre C. J. (1990)** - Noble gas systematics of Réunion Island - Chem Geol 89:1-17

- **Stracke A., Hofmann A. W., Hart S. R. (2005**) - FOZO, HIMU and the rest of the mantle zoo, Geochemistry, Geophysics, Geosystems 6, Q05007.
- **Stracke A. (2012)** – Earth's heterogeneous mantle: A product of convection-driven interaction between crust and mantle, Chemical Geology 330-331, pp. 274-299
- **Sumino H., Yamamoto J., Kumagai H. (2005)** – Noble gas studies of mantle-derived xenoliths: Mantle metasomatism revealed by noble gas isotope – A revew. Japanese Magazine of Mineralogical and Petrological Sciences, 34, vol. 4, pp.173-185
- **Tamburello G., Pondrelli S., Chiodini G. and Rouwet D. (2018)** – Global-scale control of extensional tectonics on CO_2 earth degassing - Nature Comm. 9
- **Torgersen T. and O'Donnell J. (1991**) - The degassing flux from the solid earth: Release by fracturing - *Geophys*. *Res*. *Lett*. **18**, 951–954,
- **Trieloff M., Kunz J., Clague D.A., Harrison D. and Allegre C.J. (2000) -** The nature of pristine noble gases in mantle plumes. Science, 288, 1036-1038
- **Wetherill G.W. (1954)** -Variations in the isotopic abundances of neon and argon extracted from radioactive minerals. Phys Rev 96:679-683
- **Valbracht P. J., Staudacher T. J., Malahoff A., and Allègre C. J. (1997)** - Noble gas systematics of deep rift zone glasses from Loihi Seamount, Hawaii - Earth Planet Sci Lett 150:399-411
- **Valbracht P. J., Honda M., Matsumoto T., Mattielli N., McDougall I., Ragettli R., and Weis D. (1996)** - Helium, neon and argon isotope systematics in Kerguelen ultramafic xenoliths: implications for mantle source signatures - Earth Planet Sci Lett 138:29-38
- **Vlastelic I. and Pietruszka A. J. (2016)** – A review of the recent geochemical evolution of Piton de la Fournaise volcano (1927-2010) - In: Bachelery, P., Lénat, J. F., Di Muro, A. and Michon, L. (Eds.), Active Volcanoes of the Southwest Indian Ocean: Piton de la

Fournaise and Karthala, Springer-Verlag, pp. 185-201

- **Yatsevich I. and Honda M. (1997)** - Production of nucleogenic neon in the Earth from natural radioactive decay - J Geophys Res 102:10291-10298
- **Zindler A. and Hart S. (1986)** - Chemical geodynamics. – Ann. Rev. Earth Planet. Sci. 14: 493 – 571.

CHAPTER II

Development of a new system for total in-vacuum extraction of noble gas dissolved in water isolated in copper tubes

1. INTRODUCTION

It is well know in the literature that noble gases are among the most powerful source tracers of natural processes, and, for this reason, useful and valuable tools in the framework of in geochemical monitoring of active volcanic systems. In particular, the $^{3}He/^{4}He$ isotopic ratio is considered the most efficient geochemical tracer whose variations can be straightforwardly ascribed to magmatic/crustal dynamics and therefore is of primary importance in volcanic and seismic forecasting. The most critical aspect of the geochemical monitoring in volcanic and near-fault areas is to acquire continuous data recording. However, the larger limit is the lack of methodologies and field-based instrumentations allowing the acquisition of high frequency data, which would strongly contribute to a multidisciplinary approach to the understanding of seismic and volcanic systems. At present day, it is not possible to measure noble gas isotopes directly on the field, and only a few data per month can be achieved through discrete sampling.

A new laboratory-based method for total in-vacuum extraction of noble gases dissolved in water (mainly He, Ne and Ar) sampled with copper tubes has been developed at the Istituto Nazionale di Geofisica e Vulcanologia (Sezione di Palermo). The application of this new approach would allow for the acquisition of geochemical data at hourly and daily frequency, enabling future evaluation of natural dynamics in the short term and direct comparison of these measurements with geophysical and geodetic parameters.

However, if the relationships between isotopic variations of helium and natural dynamics are known to medium-long time scales, little or nothing is known about the behavior of noble gases in the short-term timescales (day-to-day). The ability to obtain high-frequency data (thus reducing the sampling window) would thus open up a new field of study with considerable potential both in speculative-theoretical and monitoring terms.

2. TECHNICAL FEATURES OF THE EXTRACTION SYSTEM

The development of a new extraction system for noble gases dissolved in water samples collected in copper samplers stems from the need to optimize a method already in use in the Noble Gas Laboratory at the INGV of Palermo. So far, the extraction of noble gases was achieved by introducing the copper tubes in 30-cm long flexible metal hoses connected to the Ultra-High Vacuum (UHV) line of the Mass Spectrometer (**Fig. 1**). Althought this approach offers simplicity of execution, it can give rise to some technical issues at the same time. In order to extract the noble gases from water, the copper tube (which is pre-cut with pipe-cutter prior to introduction) is manually broken by bending repeatedly the UHV flexible. This can, in the long run, damage the flexible itself thus compromising the vacuum operations (**Fig. 2**).

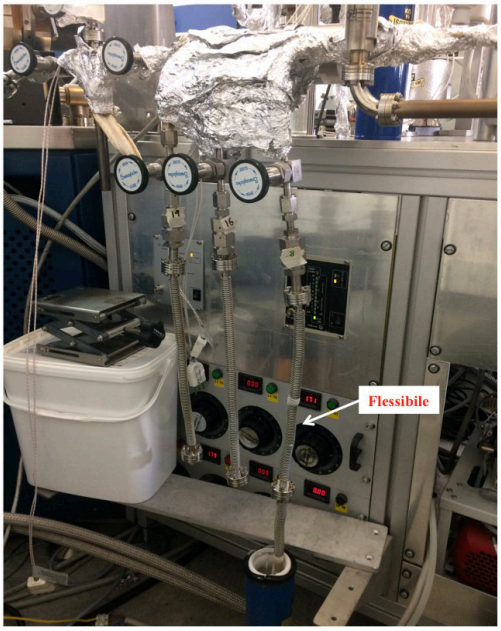

Fig. 1 – Flexibles connected to the UHV line of the Mass Spectrometer

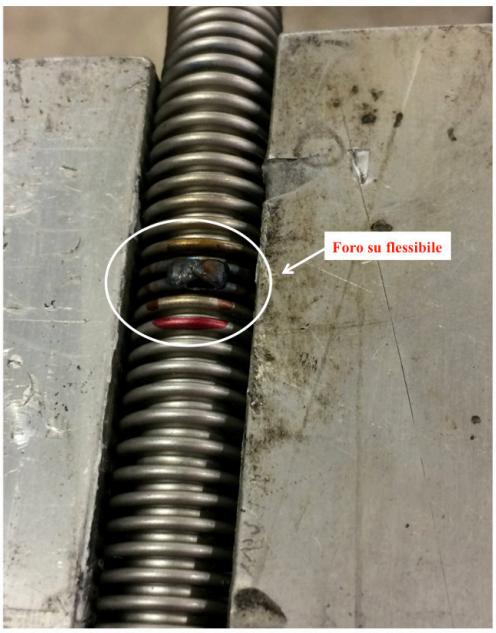

Fig. 2 – Example of damaged flexible

The idea of manufacturing a new in-vacuum extraction system for noble gases arose by observing the different types of Cu-tube cutting systems (from automated to manual systems) commonly used in the industrial sector in copper pipe cutting operations.

The object of our study is inspired by an instrument usually employed for engraving and cutting round tubes made of light alloy and copper. It consists of a manual tool that uses

the combination of two motions to make a sharp and complete cut across the entire circumference of the tube.
The tube has a circular cross-section and is laid on two parallel-axis rollers so that it can rotate on itself without changing its position. At the same time, a rotating and sharpened disc exerts pressure transversely to the axis of the tube. The combination of these two motions, in relation to the properties of the material to be cut, allows to produce a clear separation of the tube into two parts.

The most important aspect to be developed is to place the cutting system into a vacuum chamber in order to connect it directly to the pumping system. The realization of this system requires a preliminary design phase (**Fig. 3**) related to both the construction geometry and the choice of materials to be used.

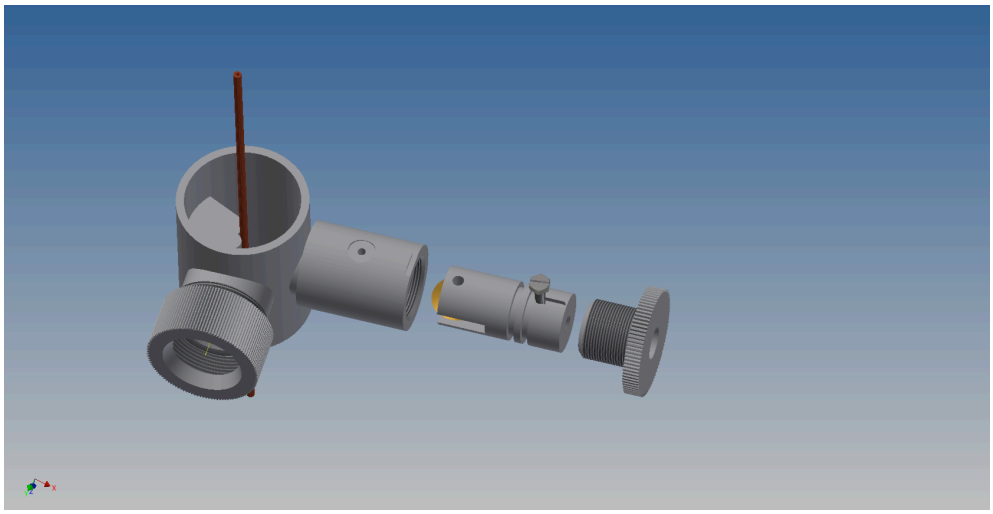

Fig. 3 – 3D design of the extraction system

The extraction system consists of a main cylinder-shape body and other secondary components (**Fig. 4**). The body has been obtained by turning and milling a AISI 316 L stainless steel cylinder and it is composed of two grooves placed 90° degrees to each other and arranged transversally to its axis. These grooves house the component characterized by the rotating cutting disk on one side and a circular inspection window on the other, which allows cutting operations to be monitored. Both sections are made of 316 L stainless steel and equipped with O-rings capable of ensuring vacuum tightness.

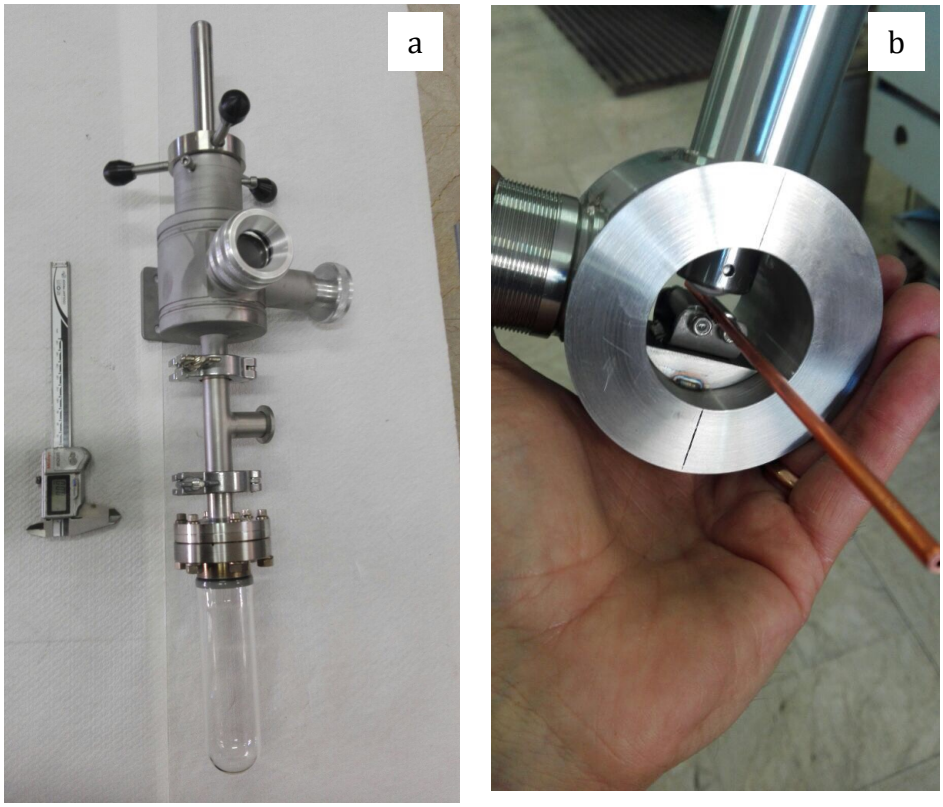

Fig. 4a-b – Components of the extraction system

The assemblage of the different components is made by means of a TIG welding procedure, consisting of an electric arc with an infusible tungsten electrode and inert gas (Argon) used as shielding gas to create a controlled atmosphere. The cylindrical central body houses the rotating support which allows to fix the copper tube in order to imparting rotation by exerting force on small knobs. The component that holds the copper tube tight is removable so as to facilitate the assembly, cleaning and disassembly operations and it is equipped with vacuum O-rings too (Fig. 3 a-b-c-d). In the botton part of the system, a two-way connection made with PN flanges is connected to the vacuum pumpings of the line and to a glass bulb that serves to collect the detached copper segment and thus to verify the successful of the operation (Fig. 3 abcd). Finally, the cutting system is mounted on a special steel support that allows it to be connected to the analytical bench.

3. SAMPLING SYSTEM AND PRE-ANALYSIS PROTOCOL

The sampling system is represented by the commercially available automatic sampler called S.P.A.R.T.A.H. (**S**yringe **P**ump **A**pparatus for the **R**etrieval and **T**emporal **A**nalysis of **H**elium; Barry et al. 2009) consisting of a syringe-pump device equipped with high-power stepper motor that is connected to a 1.65mm-diameter copper tube that directly captures the fluids of a well or thermal spring by preserving them from atmospheric contamination (**Fig.5 a-b**).

The application of this equipment allows for the continuous record of fluids in both volcanic and seismically active areas with the aim to acquire high-frequency, short-term data of noble gases at hourly to daily frequency. Fluid samples are continously and smoothly drawn into the Cu tubings for periods up to 6 months in a single deployment and are time-stamped by user-defined pumping setup parameters. The syringe-pump unit is capable of withdrawal rates ranging from 0.0001 ml/h up to 220 ml/min. Thus, all potential geochemical anomalies, regardless of duration, can be captured, and matched against the timing of external transient natural events such as volcanic eruptions or earthquakes.

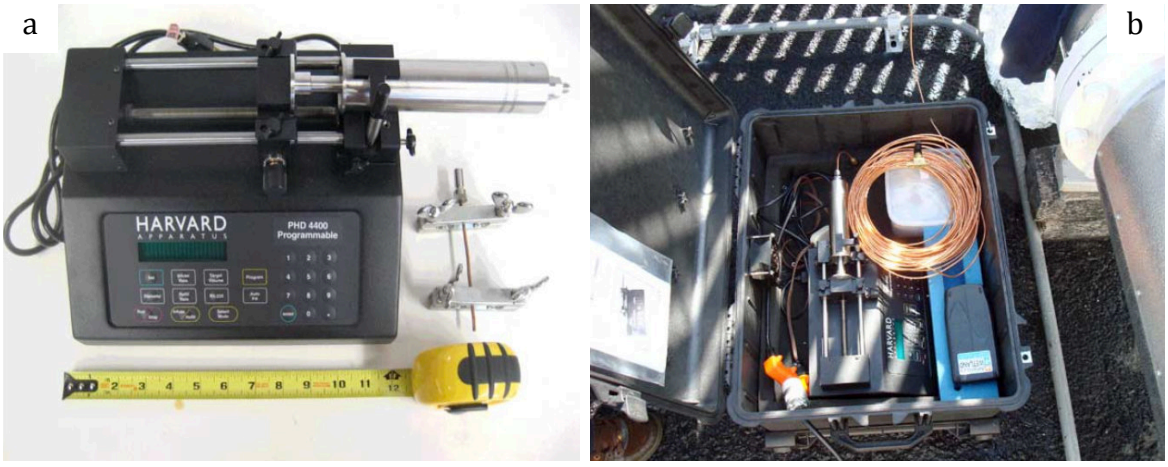

Fig. 5 – a) SPARTAH model PHD 4400 Hpsi manufactured by Harvard Apparatus (see Barry et al. 2009) **b)** Example of SPARTAH installation

The determination of the isotopic signature and concentrations of noble gases in natural waters involves several crucial steps from sampling to laboratory analysis. As noble gases are highly volatile it is extremely critical to avoid any gas exchange between the atmosphere and water during sampling, transport and storage. A laboratory protocol for the extraction and purification of noble gases dissolved in water has been developed at the Instituto Nazionale di Geofisica e Vulcanologia of Palermo.

After return to the laboratory, the copper tube containing the sampled fluid is segmented and numbered into defined intervals by means of clamps (**Fig. 6a**). Each interval represents a single water sample. Then, the external tips of the copper segments are sealed by hot-welding (**Fig. 6b**) in order to avoid water leakage inside the extraction line during the vacuum operations. Once the tube exits are welded, the clamps can be removed. Successively, the copper tubes are pre-cut with a pipe-cutter before being washed with acetone and weighted and then introduced into the extraction system. The weighing of the sample is performed both before and after the isotopic analyses as it is strictly necessary to know the amount of water stored in the copper segment in order to calculate the abundances of the dissolved noble gases in relation to the volume of the sampled fluid.

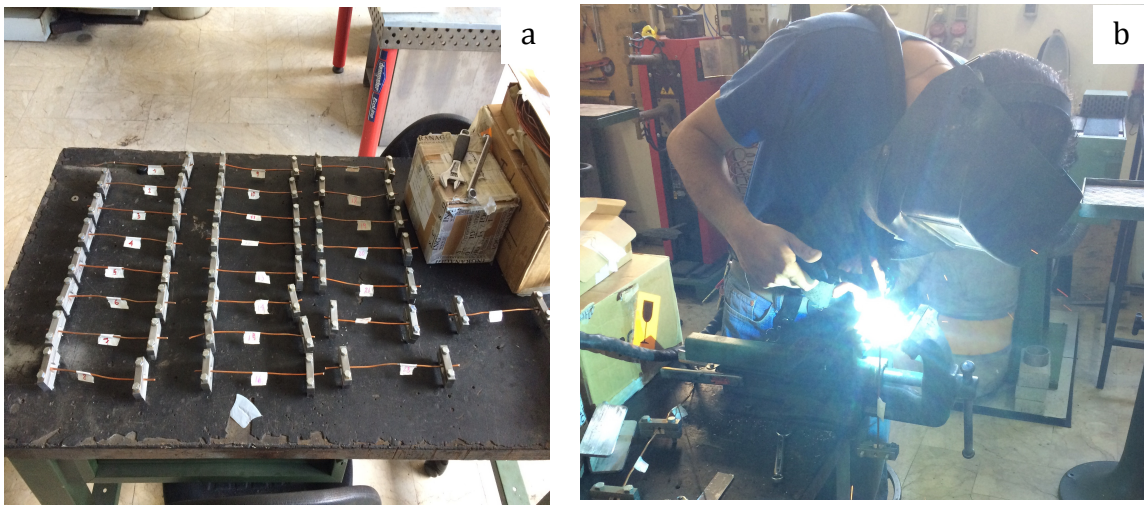

Fig. 6 - Images showing the steps for sample preparation. **a)** clamping and sample numbering and **b)** hot welding of the copper tubes

4. DESCRITPION OF THE EXTRACTION AND PURIFICATION LINES

4.1 Extraction line

The extraction line aims to extract the gaseous phase dissolved in the water sample stored in the copper tube. It consists of the aforementioned glass bulb acting as cryiogenic trap and connected to the cutting system by custom-made isolation valves. During the extraction phase, the line is kept at high- or ultra-high-vacuum ($P<10^{-5}$ mbar).

This vacuum is maintained through a primary (rotary) pumping system necessary to create the first vacuum phase from atmospheric pressure after loading the system with a new sample, and another pumping system consisting of both a diaphragm pump and a turbomolecular pump needed to reach pressures required for the extraction process ($<10^{-3}$ mbar). The extraction line is equipped with accurate diaphragm vacuum gauge that allows both to control the vacuum of the line and to monitor the gas extraction phase from the water. This step is crucial to verify that the loaded copper tube containing the water from which the gases are to be extracted has been well sealed and that the gas phase is completely extracted, thus avoiding any chemical and/or isotopic fractionation.

Once the complete isolation of the pumping system has been verified, the copper tube is cut in two parts through the rotating cutting disk and a 15-20 minute time interval is required for the total extraction of the dissolved gas phase and the re-equilibration in the extraction line. At this point, the glass bulb is immersed in liquid nitrogen (-196 ° C) for 15 minutes in order to condense all the water vapor and any possible CO_2, CH_4 component present in the gaseous mixture. Then, the extraction system is connected to the second segment of the line in which there is an additional steel trap immersed in liquid nitrogen to remove any residual water vapor and condensable gases. After a further additional 10-15 minutes, it is necessary to ensure that the total pressure of the gas extracted from the water is compatible with the volume of water sample as well as the expected pressure P of the dissolved gas phase. At this point, the extracted gas can be expanded into the noble gas purification line for the removal of the residual gaseous species.

4.2 Purification line

The purification line, which is connected to the extraction line by means of metal valves, aims at eliminating from the gas mixture all those unwanted species that can hamper the analysis of noble gases. It is composed of:

a) a vacuum gauge in the range 10^{-3} - 10^{-10} mbar that permits to monitor the vacuum in the entire line. Under normal conditions, the line runs generally at a pressure of 10^{-9} mbar, which is essential for evaluating the cleaning conditions of the line and excluding any type of contamination.

b) Three GP50-type getters pumps running simultaneously and operating for selective adsorption through a particular Zr-Al alloy which has a different reactivity as a function of temperature. Specifically, the first getters pump runs at temperatures around 300-350°C to remove all the reactive species (N_2, O_2, CO_2, CH_4 and H_2O), whereas the other two are held at room temperature to adsorb H_2 as well as to minimize the release of H_2 from the steel of the purificaton line.

c) Two activated charcoal traps held in liquid nitrogen boiling temperature (T = -196 ° C) to adsorb the Ar and separate it from He and Ne.

d) a turbo-molecular pump and an ion pumping system to restore UHV conditions.

e) a pipette at known volume for the introduction of the standard sample that is contained in a special UHV-flanged cylinder.

g) an activated-charcoal cryogenic trap (cold head) kept cooled through a He compressor up to temperatures of -263°C. At this temperature, the activated charcoal is capable to adsorb Ne and He. The cryogenic trap is equipped with a resistance and a thermo regulator that allows the release of He (T = -223 ° C) and Ne (T = -183 ° C) separately.

Once the gas has been extracted from the copper tube, it is introduced into the purification line as follows:

1) In the first step, the activated charcoal traps are isolated from the rest of the line for about 15 minutes. The sample is then subjected only to the action of the getters held at different temperatures. In a 10-15 minute time interval, all reactive species are adsorbed except the noble gases.

2) In the second step, the activated charcoal traps are immersed in liquid nitrogen for 10-15 minutes in order to condense all the noble gases, except He and Ne. Ultimately, the purified gas fraction made of residual He and Ne are adsorbed in the cryogenic trap at -263 ° C and then separated from each other for isotopic analysis. He is measured by Helix SFT-GVI mass spectrometer which allows the simultaneous measurement of ^{3}He and ^{4}He, while ^{20}Ne is analysed by Helix MC plus-Thermo Scientific mass spectrometer.

However, it should be noted that in the case of water-dissolved gas samples, the isotopic measurements of ^{21}Ne and ^{22}Ne are not carried out.

5. FIELD DEPLOYMENT AND RESULTS

The SPARTAH apparatus has been installed for periods of 2 months (October-November 2017) at *Parrano*, sited in the Umbria Apennines (central Italy; **Fig 7a**). The Parrano thermal spring is located in the western side of the tectonic discontinuity of the Tiber Valley characterized by Pliocene calcareous-siliceous marls that uncomformably overlie a succession of low-permeability marine Miocene turbidite sandstone and marls. The spring of Parrano discharges thermal waters (26.5 °C) with an outflow rate of 10 l/s.

The SPARTAH has been placed in a drainage gallery (**Fig. 7b**) carved in the so-called Devil's Den that opens up in the steep walls of a calcareous gorge. Thermal waters were sampled by introducing a 15m-long copper coil directly into a borehole to a depth of 3 meters from the wellhead, using a withdrawal-pumping rate at 0.02 cm^3/h.

Successful operation and proper functioning of the SPARTAH device has been verified following instrument retrieval after field installation. The device has successfully sampled well fluids for the entire duration of the deployments with no hiatus existing in the time record.

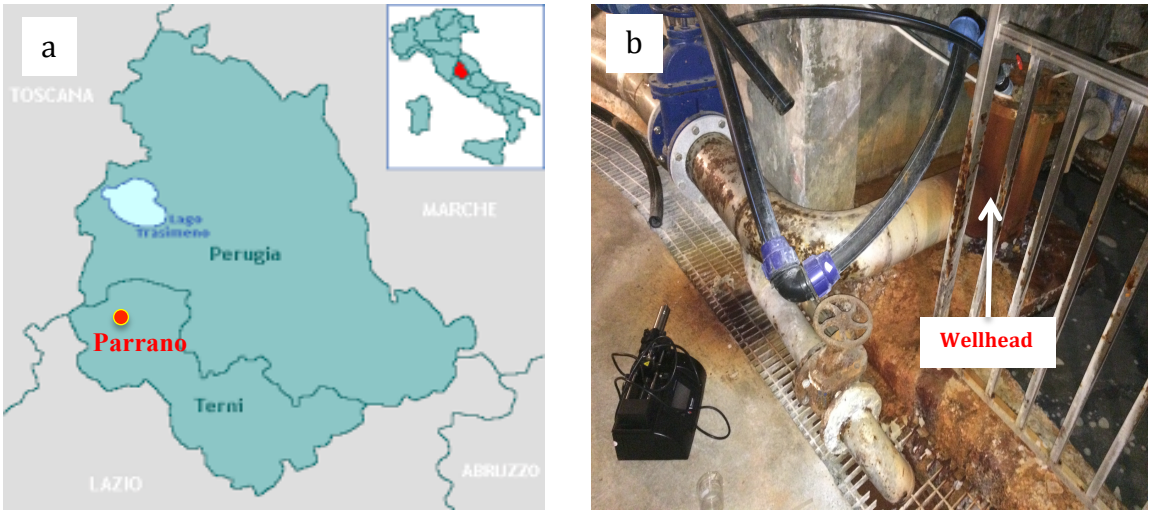

Fig. 7 - a) Geographical location of Parrano in Umbra region**; b)** SPARTAH installation in the drainage gallery

The $^{3}He/^{4}He$ ratios of the thermal waters, collected both with copper tubes and glass bottles, range from 0.028 up to 0.092 Ra (where Ra is the He isotopic ratio in atmosphere equal to 1.4×10^{-6}; **Table 1**) thus showing a characteristic radiogenic (crustal-derived) isotope signature. These values are notably indistinguishable to those measured in glass bottles as previously reported for this Apennine sector (Italiano et al. 2009).

The $^{4}He/^{20}Ne$ ratios range from 6.9 to 18.6, with He and Ne concentrations in the range of $1.6 - 3.8 \times 10^{-3}$ cc/L STP and $1.1 - 4.3 \times 10^{-4}$ cc/L STP, respectively.

The results show that Rc/Ra values (mean= 0.068) display some isotopic fluctuations over the entire deployment period characterized by two negative peaks beyond 2σ uncertainty (**Fig. 8**). Moreover, He and Ne concentrations remain constant over their respective average values (**Fig. 9**). These results must be considered preliminary.

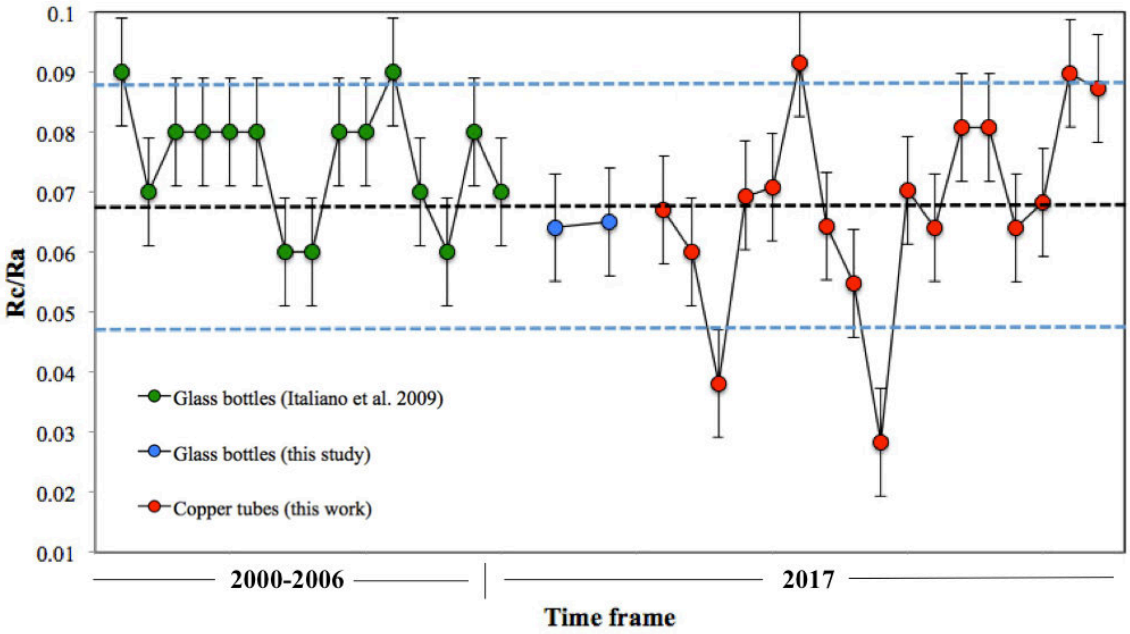

Fig. 8 – Comparison of time series of the helium isotope ratios (as Rc/Ra) of thermal waters sampled at Parrano with both glass bottles and copper tubes

Table 1. Analytical results of the extraction system .$^{3}He/^{4}He$ ratios are expressed as Rc/Ra units, where Rc/Ra is the R/Ra value corrected for atmospheric contamination (Ra is the atmospheric ratio (equal to 1.4×10^{-6} [*Ozima and Podosek, 2002*]). He and Ne concentrations are expressed in ccSTP/l $\times 10^{-3}$ and ccSTP/l $\times 10^{-4}$. The ^{4}He and ^{20}Ne signals expressed in Volt and fAmp, respectively.
(P= Parrano; G= Glass bottles).

Sample	Rc/Ra	He cc/L	Ne cc/L	He/Ne	^{4}He signal	^{20}Ne signal
P1	0.067	3.03	4.38	6.91	13.005	509.453
P2	0.060	2.48	2.85	9.96	12.428	337.541
P3	0.038	3.52	2.52	14.01	15.745	304.177
P4	0.069	2.74	1.90	14.37	12.231	230.345
P5	0.071	3.14	2.04	15.44	13.781	241.588
P6	0.092	1.59	1.56	10.17	7.239	192.681
P7	0.064	2.34	2.02	11.62	11.083	257.993
P8	0.055	2.55	2.14	11.92	11.824	268.389
P9	0.028	1.78	1.82	9.77	8.423	233.371
P10	0.070	2.21	1.47	15.03	9.668	174.094
P11	0.064	3.88	3.42	11.35	17.409	413.374
P12	0.081	2.02	1.33	15.18	9.568	170.585
P13	0.081	1.97	1.30	15.14	8.820	157.610
P14	0.064	2.57	1.38	18.63	11.930	173.307
P15	0.068	2.53	1.85	13.66	11.088	219.688
P16	0.090	1.67	1.16	14.36	7.756	146.100
P17	0.087	1.73	1.50	11.53	7.736	181.482
G1	0.064	-	-	-	-	-
G2	0.065	-	-	-	-	-
Mean	*0.067*	*2.48×10^{-3}*	*2.04×10^{-4}*	*12.88*	*11.16*	*247.75*
Stdev	*0.016*	*6.64×10^{-4}*	*8.46×10^{-5}*	*2.84*	*2.86*	*97.42*

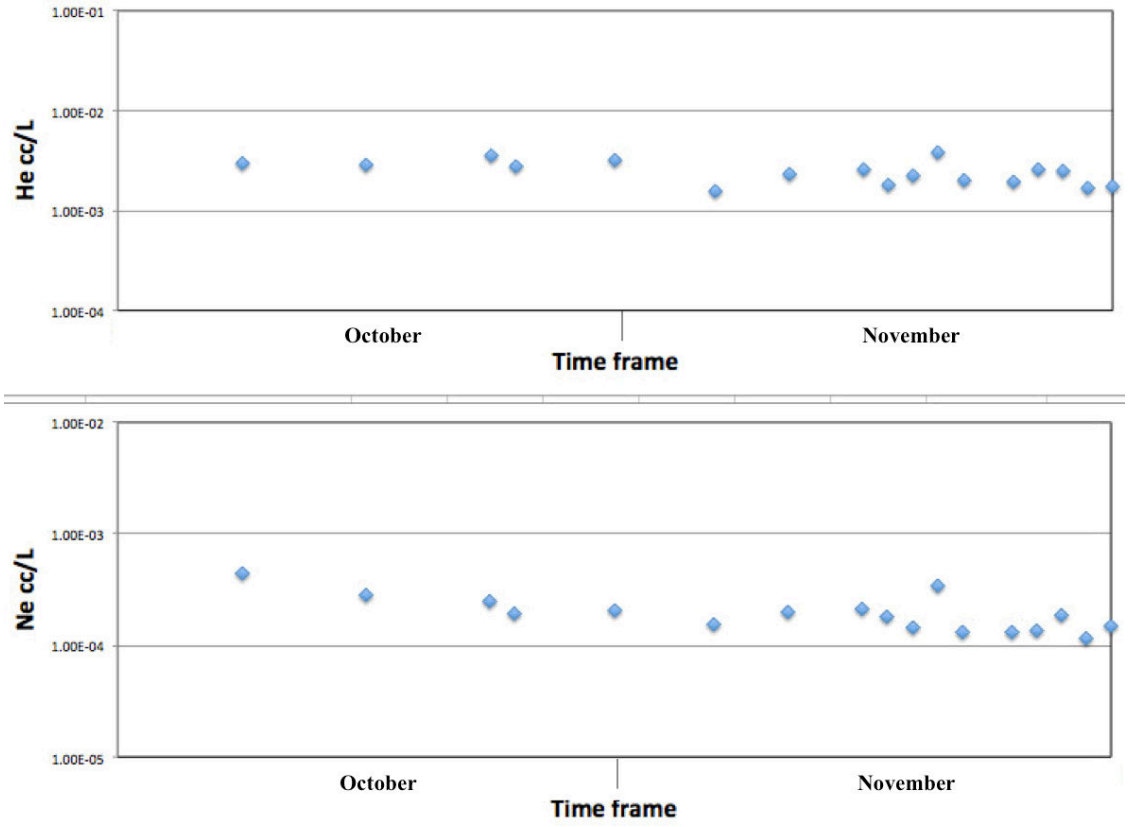

Fig. 9 – Time series of He and Ne abundances

The site of Parrano has been selected since it is well recognized in scientific literature as well as the chemistry of these waters is very sensitive to geochemical perturbations due to the regional seismicity. Additionally, this site is very well equipped (e.g. power supply), because it is located in a thermal bath, furnishing the proper condition for long-lasting application in the field. The thermal waters have periodically been sampled and analyzed for validating the reliability and results obtained by the application of the SPARTAH apparatus.

REFERENCES

- **Barry P., Hilton D., Tyron M., Brown K. and Kulongoski J. (2009)** - A new syringe pump apparatus for the retrieval and temporal analysis of helium in groundwaters and geothermal fluids, *G3 cubed Technical Brief*, vol. 10. N. 5,
- **Italiano F., Martinelli G., Bonfanti P. and Caracausi A. (2009)** – Long-term (1997-2007) geochemical monitoring of gases from the Umbria-Marche region – Tectonophysics, 476, pp.282-296

CHAPTER III

The role of gas-water interaction in controlling the chemistry of volatiles emitted in a seismic region: The central Apennines case (Italy)

1. INTRODUCTION

Much attention has been devoted in the past few decades on the natural degassing occurring far from volcanic systems, such as the Earth's regions affected by continental rifting and active tectonics (i.e., Barnes et al. 1978; Irwin and Barnes 1980; Chiodini et al. 2000; Kämpf et al. 2013; Bräuer et al. 2013, 2018). Indeed, seismically- and tectonically-active regions are today worldwide renowned for being sites of extensive emissions of deep fluids (i.e., Chiodini et al., 2004; Italiano et al. 2009; Caracausi and Paternoster 2015; Brune et al. 2017; Tamburello et al. 2018) as they can substantially contribute to the present-day global carbon output through the degassing of significant amount of CO_2 to the atmosphere. It is well documented that tectonic discontinuities act as preferential channels for deep fluids within continental crust from levels at depth (e.g., Kennedy et al. 1997, Kennedy and Van Soest 2007; Caracausi et al. 2013, 2015) as well as from the seismogenic zone in the crust (Chiodini et al. 2004; Di Luccio et al. 2018).

The capability of modern Earth science to combine in multidisciplinary approach geological, geochemical and geophysical observations is of great importance to expand our scientific knowledge on the relationship between fluid circulation, crustal degassing and seismicity at regional scale. Understanding the fluid-fault coupling process is therefore crucial as high-pressure fluids could play a significant role in controlling the nucleation and recurrence of earthquake ruptures due to pore-pressure variations in faulting strength (Sibson, 2000). Moreover, it has been proposed that the coseismic release of crustal-trapped over-pressurized fluids may represent one of the main triggering mechanisms of the aftershocks of large earthquakes (Miller et al. 2004). In a study of central-southern Apennines, Chiodini et al. (2004) discussed a relation between carbon dioxide degassing and seismogenesis in Italy. These authors observed a remarkably drop in CO_2 flux coincident with a narrow band where the seismicity is mostly concentrated, and have concluded that Apennines earthquakes are induced by over-pressurized CO_2 reservoirs due to the accumulation of gas trapped in the crust. Furthermore, on the basis of an examination of a large mainshock and aftershock data set Di Luccio et al. (2010) and Chiarabba et al. (2018) have argued that high fluid pressure within the crustal rocks may have facilitated the reactivation of pre-existing faults, and thus playing a critical role in the triggering of large ruptures associated with the 2009 L'Aquila and 2016-2017 Amatrice-Norcia seismic sequences, respectively. The occurrence of seismogenic processes can affect the release of volatiles over a seismic area and may cause either modification in the fluid phase as a consequence of changes in the

physical parameters (e.g., permeability, changes in the water table and groundwater circulation etc.) [Petitta et al. 2018, and reference therein] or variations in the gas flow-rate (e.g., Heinicke et al. 2006) and in the chemical and isotopic composition of the dissolved gases (e.g., Italiano et al. 2004, 2005). However, the primary composition of uprising volatiles can also be modified upon migration to the surface as a result of secondary chemical processes at shallow levels (e.g., mixing processes, fractionation mechanisms due to gas-water interaction, mineral precipitation, etc.). Hence, the spatio-temporal variations of the physical-chemical conditions may modify the gas chemistry furnishing powerful tools to recognize the earthquake-related signals that fluids transport to the surface. In this respect, the long-term geochemical monitoring allows to the identification of such processes and is of crucial importance to constrain any potential seismicity-induced anomalies of the emitted fluids. Therefore, the acquisition of the **background level** in a seismic area during quiescent periods is a fundamental requirement to investigate the behaviour of geochemical anomalies as a consequence of the development of seismogenic processes and recognize the geochemical variations due to the seismogenetic processes. In fact, this approach allows creating models that are fundamental for deciphering and interpreting geochemical variations in the fluids discharged in seismic regions.

Here we report the investigation of the chemical and isotopic (helium and carbon) compositions of gases emitted from high fluxes gaseous manifestations in central Apennines (Italy). This area represents a natural laboratory for exploring the possible relationship between fluid circulation, degassing and regional-scale seismicity for different reasons:

a) The Umbria Apennine is one of the Earth's most seismically active regions and characterized by high seismicity rate (e.g., Castello et al. 2005; Chiaraluce et al. 2007)
b) It is strongly affected, even in absence of seismicity, by widespread degassing of CO_2 (e.g., Chiodini et al. 2004) and characterized by fluid over-pressure at depth (Miller et al. 2004); the existence of deep high-pressure processes is evidenced by over-pressurized CO_2 reservoirs encountered at about 85% of lithostatic load within two deep boreholes drilled in the study area at Pieve S. Stefano and San Donato sites at depths of 3.7 km and 4.8 km, respectively (Bicocchi et al. 2013);
c) Several investigations have highlighted how this sector of the Apennines is particularly sensitive to seismogenic-induced geochemical anomalies (Caracausi

et al. 2005; Heinicke et al. 2000, 2011; Italiano et al. 2001, 2004, 2005, 2009; Quattrocchi et al. 2000; Barberio et al. 2017);

d) It is characterized by the presence of active faults. The Umbria Apennine is affected by a ≈ 100km-long alignment of NW-SE- and NE-SW-trending active normal fault (UFS=Umbria Fault System; Collettini & Barchi 2004), where the strongest historical and instrumental earthquakes have occurred (Boschi et al. 1997, 1998). The interpretation of the deep seismic reflection profiles from CROP03-NVR (Crosta Profonda Project Near Vertical Reflection [Pialli et al., 1998; Mirabella et al. 2011]) has shown the existence of an active extensional fault system dominated by a regional NW-trending low-angle normal fault (dip 15°-25°) named Alto Tiberina Fault (ATF) with associated SW-dipping high-angle antithetic structures (e.g. the Gubbio fault) [Boncio et al. 1998; Pucci et al. 2003; Chiaraluce et al. 2007];

e) It is monitored with multidisciplinary observing system. With the aim of investigating the seismogenic potential of the Alto Tiberina Fault, the area has been instrumented through the deployment of a near-fault observatory known as TABOO (The AltotiBerina near fault ObservatOry), a multidisciplinary research infrastructure managed by the Italian National Institute of Geophysics and Volcanology (INGV). The observatory consists of a dense geophysical network equipped with multi-sensor stations (seismometers, GPS, geochemical and electromagnetic sensors) located in the central-northern Apennines (Chiaraluce et al. 2014a-b).

This study highlights the pristine sources of the emitted fluids and how the secondary chemical processes control their composition. The main goal of this investigation is to emphasize the physicochemical processes governing the concentrations and isotope signature of natural emissions in seismic regions. Moreover, this study represents the first ever hydro-geochemical model of water-gas interaction developed in a seismic region aimed at unraveling the relationships between crustal degassing, fluid flow-induced seismicity, tectonics and water-gas interaction at regional scale.

2. THE STUDY AREA

2.1 Geological and hydrogeological background

The Apennines represents the accretionary prism resulted from the collision between the westward –directed Adriatic micro-plate and the European continental margin (Alvarez, 1972; Buiter et al. 1998; Doglioni et al. 1999). The Umbria region is geologically part of the Umbria-Marche Apennines (UMA) fold-and-thrust orogenic belt. The present-day geo-structural setting of the area is characterized by two main sectors resulted from the coeval superposition of two major tectonic phases. The external eastern sector (Adriatic domain) is marked by compressional structures (arc-shaped folds and thrusts) of Early Miocene-Early Pliocene age, while the internal western sector (Tyrrhenian domain) is affected by extensional tectonics characterized by several Pliocene-Quaternary graben and half-graben systems bounded by NW-SE trending normal faults (Lavecchia et al. 1994; Collettini and Barchi 2002, 2004). The study area is located in a transitional zone between the outer compressional Adriatic domain and the inner Tyrrhenian domain where extensional tectonic and crustal thinning processes are still active.

The stratigraphy and lithological units of the studied area consists, from the bottom to the top, of an Hercynian crystalline basement made of phyllitic rocks of Carboniferous age topped by Permian to Middle Triassic clastic and meta-sedimentary rocks of the Verrucano Group (Barchi et al. 2012). Then, the Upper Triassic dolomitic-evaporitic sequences and a lower Liassic platform limestone (the Calcare Massiccio formation) are overlain by a calcareous and marly multilayer of pelagic origin (Upper Lias-Eocene). Finally, the sedimentary column culminates with Neogene synorogenic deposists represented by the flyschic/turbiditic sequence of the Marnoso-Arenacea Formation attributable to the Oligocene to Upper Pliocene age (Ponziani et al. 1995; Barchi et al. 2012).

Hydrogeological investigations in central Italy have been extensively reported by numerous authors (Mastrolillo et al. 2009 and reference therein). The hydrogeology of the study area is largely reflected by the geological evolution of the central Apennines and is essentially characterized by two different systems of aquifer separated by aquicludes consisting mainly of marly and clayey layers. Specifically, a lower aquifer system, hosted by Jurassic-Lower Miocene limestone complexes of the carbonate lithological units and Triassic-Lower Liassic dolomitic and evaporitic complexes (the latter also known as the Burano anhydrites), and a multiple shallower aquifer systems

hosted by Pliocene-Quaternary deposits represented by marly and arenaceous-flysh sequences, volcanic rocks, alluvional terrains and travertine (Boni et al. 1986).

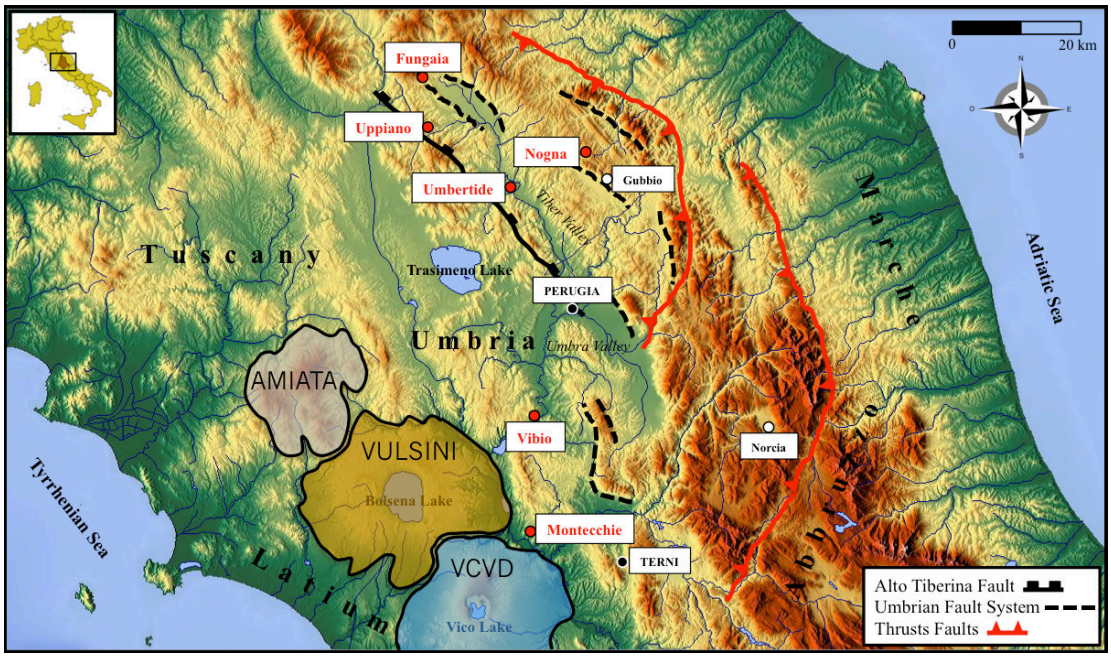

Fig. 1 – Topographical map of central Italy showing the geographical locations of the degassing manifestations sampled for this work (red circles) with the main tectonic features (Barchi et al. 2012). The peri-Tyrrhenian volcanic districts of Mt.Amiata, Vulsini and Vicano-Cimino (VCVD), located in close proximity of the Umbria region, are also reported.

2.2 Seismic activity in the Umbria region

Seismic activity is generally clustered in the northernmost sector of the study area. The seismicity does not occur across the arc-shaped fold structures resulted from the Neogenic compressional phase but concentrates along a NW-SE-trending 20-30-km wide zone (Chiaraluce et al. 2004; Chiarabba et al. 2005). At least, five major seismic events have affected the area during the past three decades (**Fig. 2**). The first worth-mentioning seismic event is represented by the **1984 Gubbio-Valfabbrica** seismic sequence with a Mw 5.6 mainshock located at a depth of 7 km and aftershock distributed on SW-dipping rupture planes (Haessler et al. 1988; Collettini et al. 2003). Then, a relatively long period of seismic quiescence was interrupted by the long-lasting 1997-1998 Umbria-Marche multiple shock seismic crisis characterized by five main earthquakes with magnitude larger than 4.0 and a cascade of thousands of minor shocks (Amato et al. 1998). The

seismic sequence started on May 12th 1997 with the Mw 4.5 **Massa Martana** mainshock (Di Luccio et al. 1998; Di Giovanbattista & Tyupkin 2000). From September 26th 1997 to March 26th 1998, a series of strong earthquakes (Mw 5.7, 6.0 and 5.6) occurred in the vicinity of the **Colfiorito** village (Amato et al. 1998; Barba and Basili 2000; Cello et al. 2000). After a decrease in the seismic activity, another earthquake hit the area on April-May 1998 with the Mw 5.1 **Gualdo Tadino** mainshock (Ciaccio et al. 2005). The most recent seismic events recorded in the Umbria Apennine and surroundings Italian regions are the two strong earthquakes that struck the town of **Norcia** on 26th (Mw 5.9) and 30th October 2016 (Mw 6.5), respectively, that followed the Mw 6.0 Accumoli and Campotosto earthquakes occurred on 24th August in the Abruzzo region. These events occurred seven years after the 6th April 2009 Mw 6.3 L'Aquila earthquake (Bindi et al. 2009). The Mw 6.5 Norcia mainshock was the largest recorded seismic event in Italy since the 1980 Mw 6.9 Irpinia earthquake in southern Apennines (Bernard and Zollo 1989).

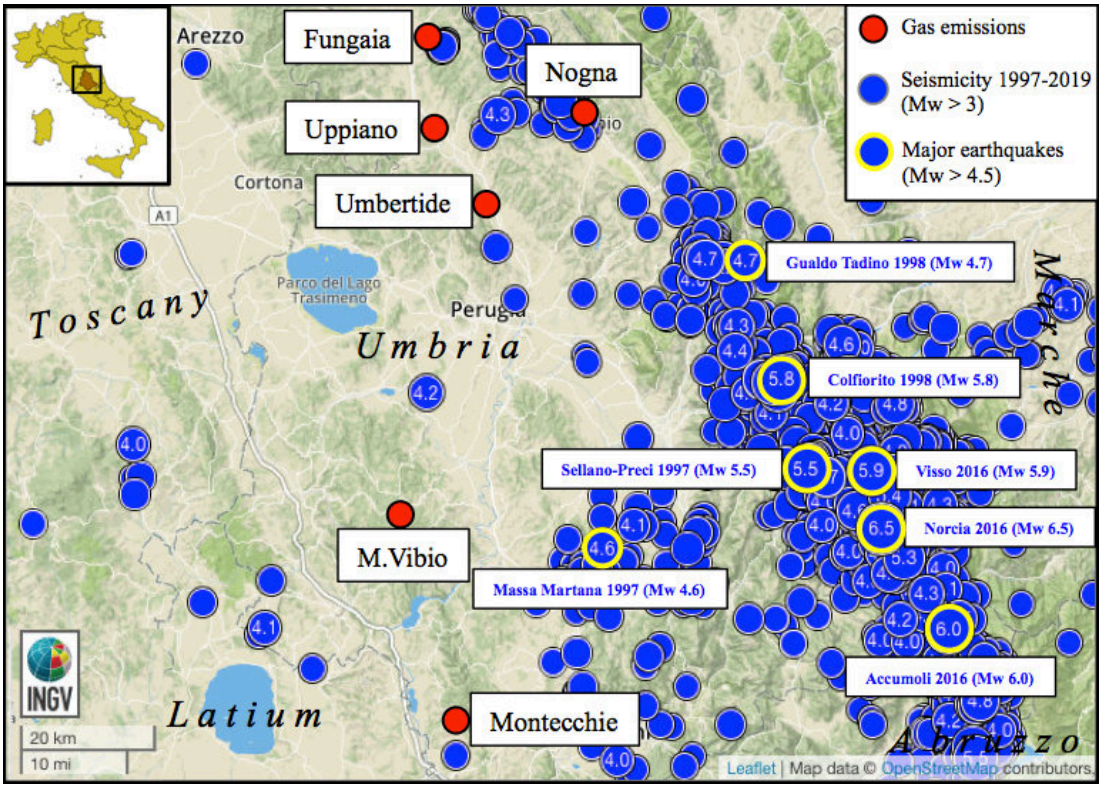

Fig. 2 – Geographical location of the studied gas emissions with repsect to the spatial distribution of seismicity in central Apennines in the period 1997-2019. Web source: http://cnt.rm.ingv.it

3. METHODOLOGY

3.1 Sampling and analytical methods

Fig. 1 shows the location of the six selected high flux gas manifestations sampled for this study together with the main structural features of the investigated area. The gas emissions are distributed across the whole Umbria region. The northernmost sampling locations (namely, Umbertide, Uppiano and Nogna) fall along the Tiber river Valley (**Fig. 3a-b**) within the framework of the interdisciplinary research network of TABOO (The AltotiBerina near fault ObservatOry; Chiaraluce et al. 2014b), while the southernmost sampling sites (Montecastello di Vibio and Montecchie) are sited close to the Vicano-Cimino Volcanic District (VCVD) located in the northern sector of Latium region (Figure x). A total number of six samplings for each degassing site were performed over a quiet seismic period between July 2017 to September 2018, which allowed us to acquire the **baseline data** for chemical and isotopic composition of the gases that characterize the investigated area. This activity is part of the geochemical monitoring performed periodically by the Instituto Nazionale di Geofisica e Vulcanologia (INGV - Sezione di Palermo) for seismic surveillance in the Umbria region. The samplings sites (**Fig. 4**) are here summarized as follows:

The ***Fungaia*** gas emission is sited near the village of Pieve S. Stefano located in Tuscany region in close proximity to the border with Umbria. The ***Umbertide*** gas vent is sited 20 km north off Perugia town along the Tiber river Valley. It derives from an old drilling for hydrocarbon exploration up to a depth of about 5 km. The venting gas is located in an elongate depression within Pliocene-Quaternary deposits and it is considered the strongest CO_2 gas manifestation of the Umbria region with a flow rate of around 3 m^3/s. The ***Uppiano*** bubbling pool is located within Miocene-Pliocene sediments in the province of the town of Città di Castello. The ***Nogna*** is a water-well managed by the Umbria Acque s.p.a. sited 15 km nort-west of the town of Gubbio. It is geologically placed between the external front of the Tuscan Nappe and the east-verging UMA (Barchi et al. 2012). The ***Montecastello di Vibio*** gas emission (hereafter referred as M.Vibio) is located within Miocene-Pliocene sediments and characterized by a CO_2 flow rate of about 1 m^3/s. The ***Montecchie*** gas manifestation is characterized by several aligned rainwater-filled pools featured with diffuse gas bubbling.

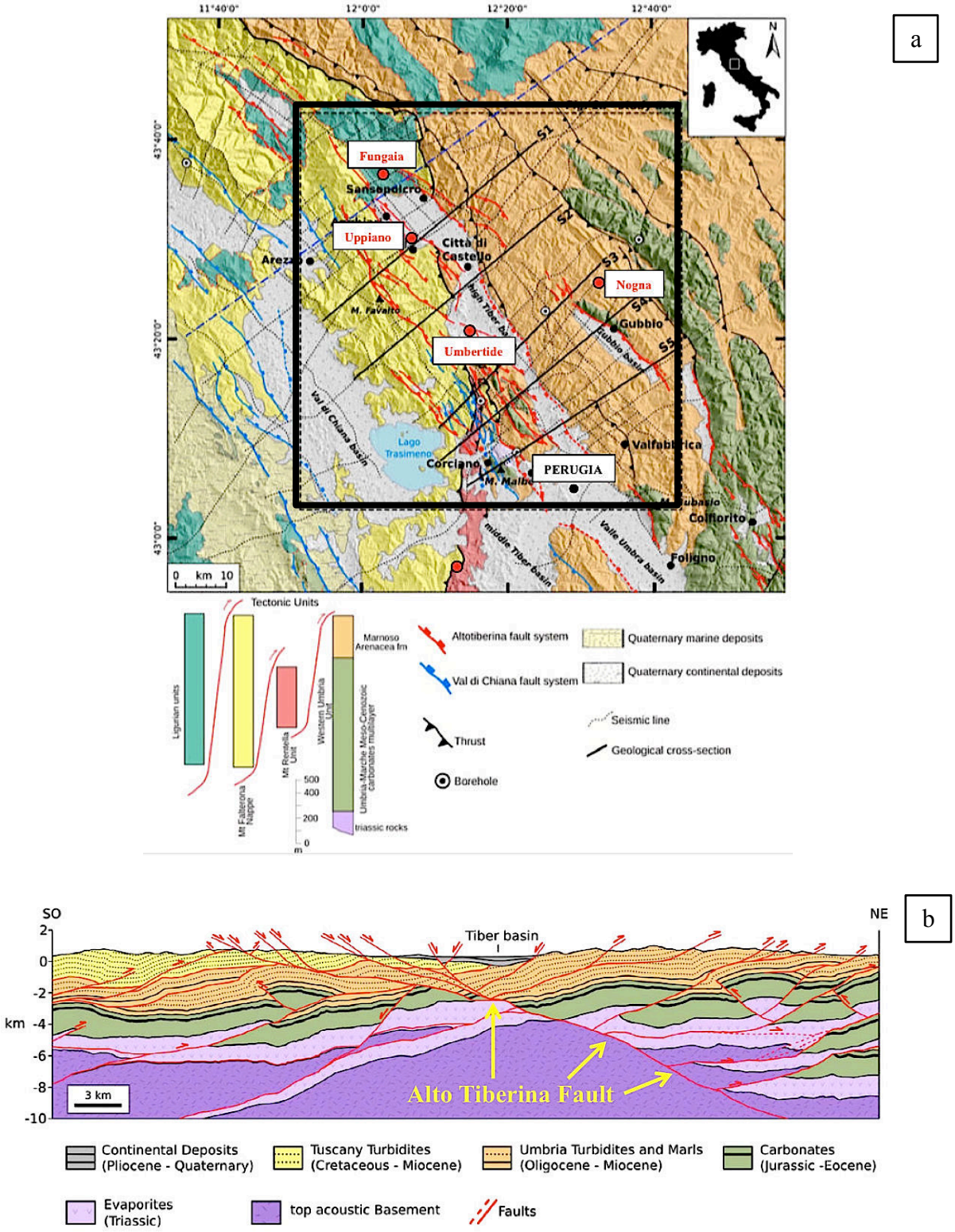

Fig. 3 – a) Geostructural map showing the norternmost samples within the TABOO area, outcroppings terrains, main thrust and normal fault systems, and trace of the geological cross-sections (from Mirabella et al. 2011).
b) S1 geological cross-section (S2, S3, S4 and S5 cross-sections can be found in Mirabella et al. 2011)

Fig. 4 – The six gaseous manifestations sampled for this work. A) Fungaia; B) Uppiano; C) Umbertide; D) Nogna; E) Montecastello di Vibio; F) Montecchie

The venting gases were collected by using a funnel, whose size changed depending on the site conditions. The sampling system adopted for collecting the gaseous manifestations consists of three different components (a funnel, a sampler and a syringe) connected by silicone tubes through a three-way pyrex valve (**Fig. 5**). The choice of employing a funnel is given by the fact that it is able to channel the released gas towards a water-filled container. The free gases were sampled following a cleaning procedure which allows to purge the glass bottle of air. The released gas is conveyed to the silicon tube through the funnel. The gas is slowly withdrawn by the syringe and then pushed hardly to the glass sampler for several times producing water bubbling in the container (the induced bubbling serves to test out the effective functioning of the sampling system).

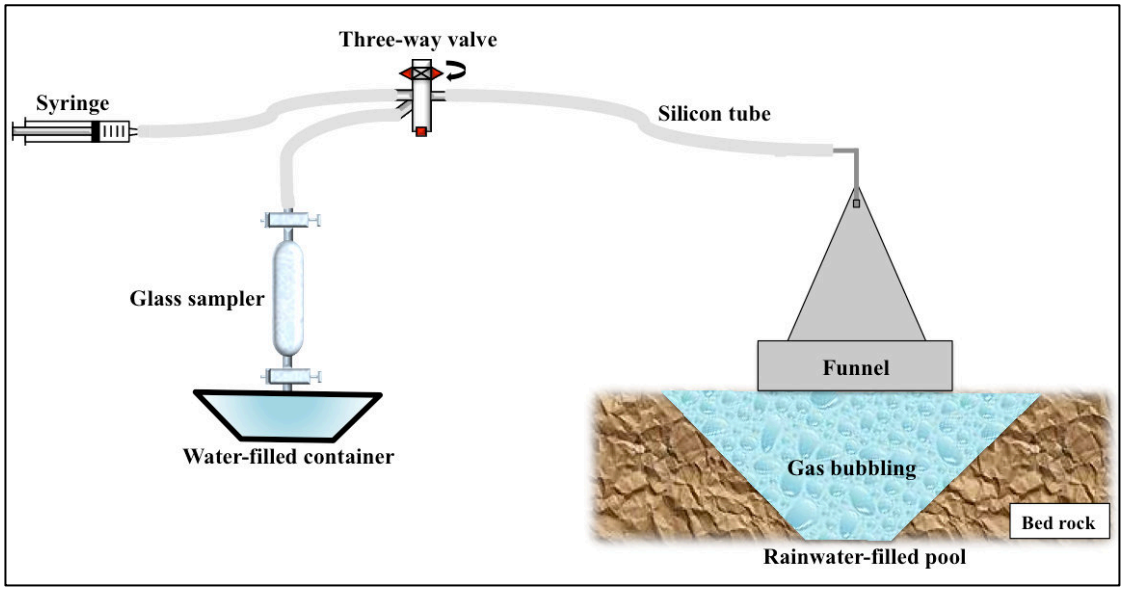

Fig. 5 – Schematic illustration showing the sampling system used for collecting the gaseous manifestations.

The gas samples have been collected in high flux gas emission and this allows reducing air contamination during the sampling procedures. All the analyses have been performed in the laboratories of the INGV-Palermo in two weeks from the sampling. The concentrations of CO_2, CH_4, O_2 and N_2 were analysed by an Agilent 7890B gas chromatograph with Ar as carrier and equipped with a 4-m Carbosieve S II and PoraPlot–U columns. A TCD detector was used to measure the concentrations of He, O_2, N_2 and CO_2 and a FID detector for CO and CH_4. The analytical errors were 10% for He and 5% for O_2, N_2, CO, CH_4 and CO_2. The carbon isotopic composition of CO_2 ($\delta^{13}C_{CO2}$) was determined using a **Thermo Delta XP IRMS** coupled with a Thermo Scientific™ TRACE™ Ultra Gas Chromatograph, e a 30 m Q-plot column (i.e. of 0.32 mm). The resulting $\delta^{13}C_{CO2}$ values are expressed in ‰ notation with respect to the international V-PDB (Vienna Pee Dee Belemnite) standard and analytical uncertainties of ±0.15‰.

^{3}He, ^{4}He and ^{20}Ne and the $^{4}He/^{20}Ne$ ratios were determined by separately admitting He and Ne into a split flight tube mass spectrometer (GVI-Helix SFT, for He analysis) and into a multi-collector mass spectrometer (Thermo-Helix MC plus, for Ne analysis), after purification procedures. The reproducibility was <0.1% for ^{4}He and ^{20}Ne. However, the estimation of He and Ne concentration is within 10% uncertainty respect to GC measurements.

4. RESULTS

4.1 Chemical composition of the gases

The chemical composition of the collected gases is reported in **Table 1**. Carbon dioxide is overall the main component in all of the gas manifestations (78-97 vol.%; **Fig. 6a**), except for the site of Nogna that is CH_4-dominated (>90 vol. %, table 1).

Helium and nitrogen (hereafter He and N_2 respectively) concentrations are significantly variable (from 6.9 to 494 ppm and from1.2 to 20.8 vol%, respectively; **Table 1** and **Fig. 6b**). The highest He and N_2 contents are found at the site of Uppiano, where they are one order of magnitude higher than the other gas emissions (**Fig. 6a-b**).

The sites of M.Vibio and Montecchie both display the highest CO_2 contents (94-97 vol.%) among the sampled gases, paralleled by the lowest He concentrations (6.9-12.9 ppm). The Fungaia and Umbertide gas emissions show CO_2 contents ranging from 90 to 94 vol.% and intermediate He concentrations between 31.8 and 45.5 ppm. Finally, Nogna shows He contents (35-62 ppm) quite comparable to those found at Fungaia and Umbertide sites.

Argon contents are variable and range between 9.5 to 866 ppm. Oxygen is extremely low (0.002-0.6 vol. The low Ar and O_2 concentrations in all the analyzed gases indicated that these gases are affected by low air contamination.

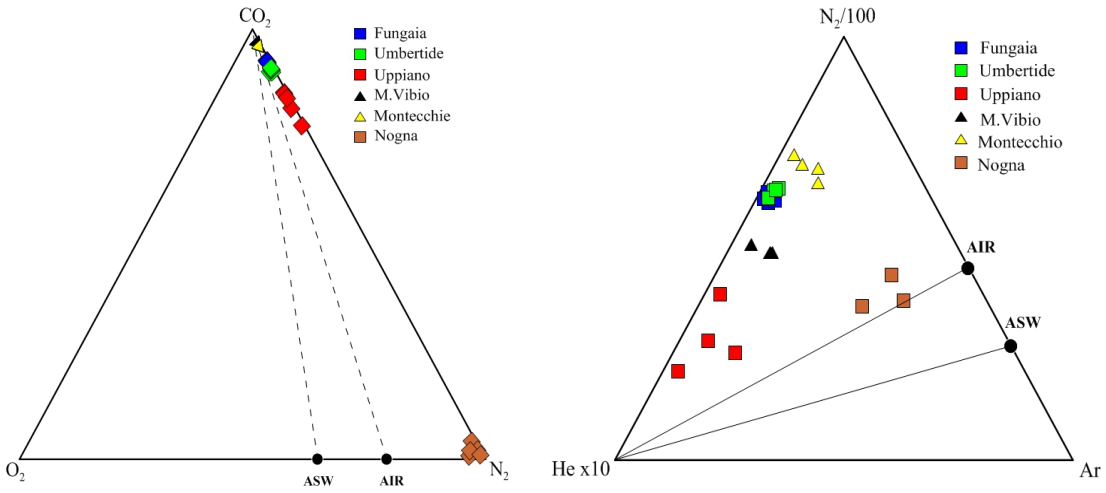

Fig. 6. Chemical composition of the Umbrian gas emissions. **a)** CO_2-N_2-O_2 triangular plot highlights that all the samples fall along the CO_2-N_2 side of the diagram. Nogna samples (light brown squares) fall in the N_2 corner due to the fact that this gas manifestation is dominated by CH_4. **b)** Ternary diagram showing the relative abundance of N_2, Ar and He. The compositions of air and air-saturated water (ASW) at 25°C are plotted for reference as black circles.

Table 1. Chemical composition of the gases sampled in Umbria. CO_2, CH_4, N_2 and O_2 concentrations expressed in vol %,: He, Ne, Ar in ppm. n.d.= not determined

Sample	Date	CO_2	CH_4	N_2	O_2	He	Ne	Ar
Fungaia								
1	19/07/17	94.07	0.1869	5.03	0.034	32.64	0.054	28.64
2	27/09/17	93.72	0.1870	5.23	0.042	32.59	0.09	n.d.
3	22/11/17	93.20	0.1870	5.16	0.004	32.41	0.016	n.d.
4	19/12/17	93.16	0.1882	5.11	n.d.	33.04	0.008	15.89
5	18/02/18	93.11	0.2016	5.42	0.073	32.99	0.008	16.97
6	29/09/18	92.80	0.1835	5.17	0.052	31.82	0.094	39.87
Mean		*93.34*	*0.19*	*5.19*	*0.04*	*32.58*	*0.05*	*25.34*
Stdev		*0.46*	*0.01*	*0.13*	*0.03*	*0.44*	*0.04*	*11.27*
Umbertide								
1	19/07/17	91.02	0.2280	6.97	0.695	40.48	0.05	34.58
2	27/09/17	91.28	0.2284	7.46	0.160	45.50	0.08	n.d.
3	22/11/17	90.94	0.2280	6.88	0.013	40.77	0.011	n.d.
4	19/12/17	90.93	0.2340	7.04	0.008	44.23	0.023	31.35
5	18/02/18	90.96	0.2269	6.88	0.023	37.92	0.015	43.08
6	28/09/18	91.13	0.2236	6.67	0.018	37.89	0.035	38.17
Mean		*91.04*	*0.23*	*6.98*	*0.15*	*41.13*	*0.04*	*36.80*
Stdev		*0.14*	*0.003*	*0.26*	*0.27*	*3.15*	*0.03*	*5.03*
Uppiano								
1	19/07/17	82.36	4.38	20.86	0.045	335.62	0.183	208.79
2	27/09/17	82.63	4.38	11.83	0.036	324.51	0.122	n.d.
3	22/11/17	82.68	4.36	12.07	0.100	324.88	0.15	n.d.
4	19/12/17	80.99	4.61	11.97	n.d.	494.02	0.133	218.77
5	18/02/18	78.09	4.97	14.82	0.270	385.32	0.429	373.07
6	29/09/18	80.00	4.67	12.78	0.088	348.29	1.193	760.53
Mean		*81.13*	*4.56*	*14.06*	*0.11*	*368.77*	*0.37*	*390.29*
Stdev		*1.83*	*0.24*	*3.51*	*0.09*	*65.37*	*0.42*	*258.03*
Nogna								
1	18/07/17	0.49	93.44	7.2	0.024	62.87	0.389	760.11
2	27/09/17	0.23	91.99	7.43	0.200	n.d.	n.d.	n.d.
3	22/11/17	0.31	91.76	6.81	0.006	n.d.	n.d.	n.d.
4	19/12/17	n.d.	n.d.	n.d.	n.d.	n.d.	n.d.	n.d.
5	16/02/18	0.33	90.63	7.45	0.140	35.57	0.346	696.51
6	27/09/18	0.23	91.5	6.93	0.062	39.50	0.329	866.82
Mean		*0.32*	*91.86*	*7.16*	*0.09*	*45.98*	*0.35*	*774.48*
Stdev		*0.11*	*1.02*	*0.29*	*0.08*	*14.76*	*0.03*	*86.06*
M. Vibio								
1	19/07/17	96.81	0.2381	1.23	0.048	11.46	0.026	25.22
2	27/09/17	97.68	0.2375	1.26	0.027	11.63	0.021	n.d.
3	22/11/17	95.89	0.2481	1.28	0.033	11.47	0.017	n.d.
4	20/12/17	95.83	0.2482	1.24	0.002	11.91	0.005	11.20
5	18/02/18	94.96	0.2397	1.28	0.039	11.74	0.013	n.d.
6	29/09/18	96.45	0.2397	1.23	0.033	11.32	0.018	26.09
Mean		*96.27*	*0.24*	*1.25*	*0.03*	*11.59*	*0.02*	*20.88*
Stdev		*0.93*	*0.005*	*0.02*	*0.02*	*0.21*	*0.04*	*8.36*
Montecchie								
1	20/07/17	95.86	0.2638	2.07	0.032	8.15	0.045	38.69
2	27/09/17	96.80	0.2651	2.17	0.018	8.42	0.014	n.d.
3	22/11/17	94.76	0.2638	2.12	0.005	8.16	0.037	n.d.
4	19/12/17	95.30	0.2639	2.12	0.007	8.18	0.014	19.37
5	18/02/18	95.24	0.2606	2.05	0.005	7.83	0.009	9.54
6	29/09/18	95.68	0.2540	1.99	n.d.	6.95	0.018	29.90
Mean		*95.61*	*0.26*	*2.09*	*0.013*	*7.95*	*0.02*	*19.60*
Stdev		*0.70*	*0.004*	*0.06*	*0.011*	*0.52*	*0.01*	*12.66*

Table 2. Isotopic composition of the gases sampled in Umbria. Carbon isotope ratios ($^{13}C/^{12}C$) are expressed as δ‰ units vs. V-PDB. All the measured $^{3}He/^{4}He$ ratios are expressed as R/Ra units and normalized to the atmospheric ratio (Ra= 1.38 □10^{-6} [*Ozima and Podosek, 2002*]). Rc/Ra is the R/Ra value corrected for atmospheric contamination. n.d.= not determined

Sample	Date	δ ^{13}C-CO_2	R/Ra	Rc/Ra	$^{40}Ar/^{36}Ar$	$^{20}Ne/^{36}Ar$
Fungaia						
1	19/07/17	-4.8	0.026	0.026	350.9	0.67
2	27/09/17	-4.9	0.030	0.026	n.d.	n.d.
3	22/11/17	-4.6	0.025	0.025	n.d.	n.d.
4	19/12/17	-4.4	0.020	0.023	387.4	0.20
5	18/02/18	-4.9	0.020	0.020	371.4	0.18
6	29/09/18	-4.3	0.020	0.021	337.9	0.80
Mean		*-4.6*	*0.023*	*0.023*	*365.60*	*0.46*
Stdev		*0.3*	*0.004*	*0.002*	*21.85*	*0.31*
Umbertide						
1	19/07/17	-3.8	0.023	0.022	339.8	0.49
2	27/09/17	-3.9	0.024	0.024	n.d.	n.d.
3	22/11/17	-3.6	0.025	0.025	n.d.	n.d.
4	19/12/17	-3.7	0.020	0.022	342.9	0.25
5	18/02/18	-3.9	0.020	0.022	320.4	0.11
6	28/09/18	-3.6	0.020	0.016	347.0	0.33
Mean		*-3.7*	*0.022*	*0.021*	*337.55*	*0.30*
Stdev		*0.1*	*0.002*	*0.003*	*14.31*	*0.16*
Uppiano						
1	19/07/17	-3.4	0.020	0.019	352.1	0.31
2	27/09/17	-2.9	0.023	0.023	n.d.	n.d.
3	22/11/17	-3.2	0.026	0.026	n.d.	n.d.
4	19/12/17	-3.4	0.020	0.017	351.0	0.21
5	18/02/18	-3.2	0.020	0.020	328.5	0.38
6	29/09/18	n.d.	0.020	0.017	310.6	0.49
Mean		*-3.2*	*0.02*	*0.02*	*335.61*	*0.35*
Stdev		*0.2*	*0.002*	*0.003*	*19.87*	*0.12*
Nogna						
1	18/07/17	-12.1	0.015	0.013	299.19	0.15
2	27/09/17	-14.3	n.d.	n.d.	n.d.	n.d.
3	22/11/17	-9.7	n.d.	n.d.	n.d.	n.d.
4	19/12/17	n.d.	n.d.	n.d.	n.d.	n.d.
5	16/02/18	n.d.	0.02	0.014	299.07	0.15
6	27/09/18	-12.9	n.d.	n.d.	306.62	0.12
Mean		*-12.3*	*0.017*	*0.013*	*301.63*	*0.14*
Stdev		*1.9*	*0.003*	*0.0007*	*4.32*	*0.02*
M. Vibio						
1	19/07/17	n.d.	0.120	0.124	311.9	0.32
2	27/09/17	-1.30	0.110	0.110	n.d.	n.d.
3	22/11/17	-0.90	0.130	0.134	n.d.	n.d.
4	20/12/17	-0.67	0.110	0.112	349.8	0.16
5	18/02/18	-1.10	0.120	0.122	n.d.	n.d.
6	29/09/18	-0.91	0.110	0.106	325.2	0.23
Mean		*-1.0*	*0.116*	*0.118*	*328.98*	*0.24*
Stdev		*0.2*	*0.008*	*0.01*	*19.23*	*0.08*
Montecchie						
1	20/07/17	-1.05	0.636	0.635	308.1	0.36
2	27/09/17	-1.1	0.653	0.643	n.d.	n.d.
3	22/11/17	-1.0	0.695	0.693	n.d.	n.d.
4	19/12/17	-0.6	0.660	0.657	320.2	0.23
5	18/02/18	-0.8	0.690	0.687	325.5	0.33
6	29/09/18	-0.74	0.620	0.623	310.2	0.19
Mean		*-0.9*	*0.659*	*0.658*	*316.05*	*0.28*
Stdev		*0.2*	*0.029*	*0.027*	*8.23*	*0.07*

4.2 Helium Isotopes

He is a reliable geochemical tracer for discriminating the crustal and mantle components in the gas sources due to the different origin of its two isotopes (^{3}He has a primordial origin, whereas ^{4}He is produced in the crust by radioactive α-decay of ^{235,238}U and ^{232}Th [Ballentine & Burnard 2002]). The sampled fluids have ^{3}He/^{4}He ratios from 0.01 to 0.69 Ra (**Table 2**) with corresponding He/Ne ratios in the range of 102-4130 (**Table 1**). These ^{4}He/^{20}Ne ratios are much higher than the same ratio in atmosphere (He/Ne= 0.318; Ozima & Podosek 2002) supporting that atmospheric He component in the sampled fluids is negligible. A progressive decrease in terms of ^{3}He/^{4}He values is observed from south to north in the Umbria region. The ^{3}He/^{4}He ratios in the fluids collected in the northern sector of the study area are in a narrow range (0.01-0.02 Ra) that coincides with the He isotopic ratios in crustal fluids dominated by radiogenic ^{4}He due to U and Th decay in the crust (Ballentine and Burnard 2002). In contrast higher ^{3}He/^{4}He ratios (0.11-0.69 Ra) have been measured in the fluids emitted in the southern sector of the investigated area and they show a slight presence of the primordial mantle ^{3}He.

These data indicate a geographical variability of the He isotopic signature in the outgassing volatiles and also the occurring of a mantle-derived component in the fluids Emitted at the Vi and Mo sites.

It is worthy of note that the He isotopic signature at Mo site fits with the ratio in the fluids from the Roman Co-magmatic Province (RCP) (e.g., Martelli et al. 2004; Cinti et al., 2014), whose gas emissions are in 30 km.

Furthermore, it is possible to compute the percentage of the different He sources by using three components mixing equations and both the ^{3}He/^{4}He and ^{4}He/^{20}Ne ratios of the crustal, mantle and atmospheric end members. Assuming a Sub-Continental Lithospheric Mantle (SCLM) with a ^{3}He/^{4}He ratio of 6.32 ± 0.39 Ra (Gautheron et al. 2005), the mantle contribution affecting the M.Vibio (0.11-0.13 Ra) and Montecchie (0.62-0.69 Ra) gases range from 1.8% to 10.2%, respectively. The ^{3}He/^{4}He values, uncorrected for atmospheric contamination, are reported versus ^{4}He/^{20}Ne ratios in **Fig.7** together with the helium isotope composition of gas discharges emitted from different volcanic districts located alongside the peri-Tyrrhenian margin of the Italian peninsula extending from southern Tuscany to the Campanian region.

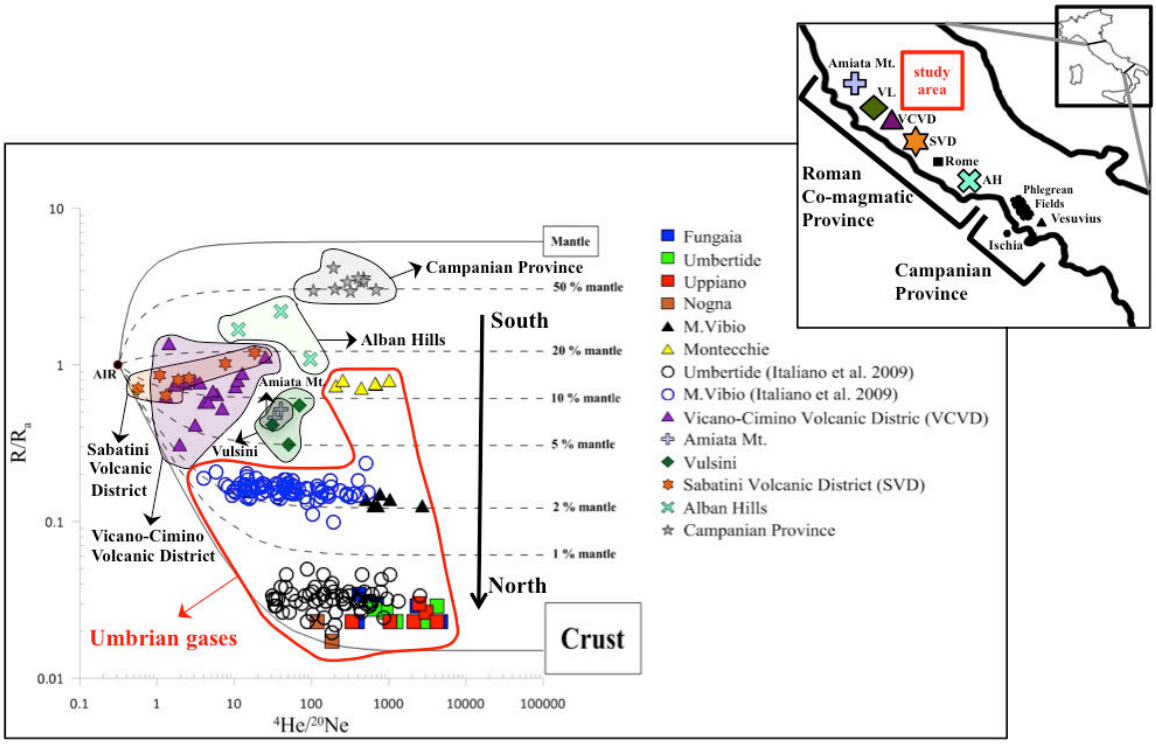

Fig. 7 - R/Ra vs. $^{4}He/^{20}Ne$ ratios of the Umbria gas emissions reported with those from the Italian volcanic provinces. The data define a northward decrease of $^{3}He/^{4}He$ values. The dashed lines show different mixing trends with various addition of a mantle component. Furthermore, as far as concern Umbertide and Montecastello di Vibio gases, $^{3}He/^{4}He$ values are in good agreement with those reported by Italiano et al. (2009). Vicano-Cimino Volcanic District (VCVD; Cinti et al. 2014); Amiata Mt. (Minissale 2004); Vulsini includes data from Latera and Torre Alfina (Minissale 2004); Sabatini Volcanic District (SVD; Cinti et al. 2017); Alban Hills (AH; Carapezza & Tarchini 2007; Minissale 2004); Campanian Province includes data from Phlegrean Fields (Vaselli et al. 2011) and Ischia Island (Inguaggiato et al. 2000). The volcanic sectors of Vulsini, Vicano-Cimino, Sabatini and Alban Hills are reported in the literature under the name of Roman Co-magmatic Province (RCP; Martelli 2004).

4.3 Argon Isotopes

The Ar isotope composition is reported in **Table 2**. The $^{40}Ar/^{36}Ar$ ratios show a small range from values close to atmosphere (298.56 ± 0.31; Lee et al. 2006) up to $^{40}Ar/^{36}Ar$ = 387. As the inventory of Ar in the atmosphere is dominated by ^{36}Ar, the correlation between $^{40}Ar/^{36}Ar$ versus the reciprocal of $1/^{36}Ar$ was used to assess the presence of trends of air contribution in the collected gas samples. Higher values of $^{40}Ar/^{36}Ar$ vs. $1/^{36}Ar$ indicate an addition of crustal-derived ^{40}Ar and lower atmospheric contribution, while lower values reflect higher air contamination and lower production of radiogenic ^{40}Ar. By and large, three apparent trends can be observed in the studied gas emissions (**Fig. 8a**). The first trend is defined by Uppiano and Nogna samples, the second is defined by Fungaia and Umbertide sites, and finally the third is given by M.Vibio and Montecchie gases. For a given $^{40}Ar/^{36}Ar$ ratio, a slightly higher atmospheric Ar

contribution is generally observed in the northernmost samples (Fungaia, Umbertide, Uppiano and Nogna) compared to those collected in the southern sector of the region (M.Vibio and Montecchie). The closest $^{40}Ar/^{36}Ar$ ratios to the air value were measured in the Nogna gases, where also the lowest $^{4}He/^{20}Ne$ were found. On the contrary, the highest $^{40}Ar/^{36}Ar$ ratios are found at the site of Fungaia suggesting the presence of crustal-derived Ar. For this reason we used the helium isotopes as a discriminating tool in order to constrain the excess of Ar in the northernmost gas samples (**Fig. 8b**).

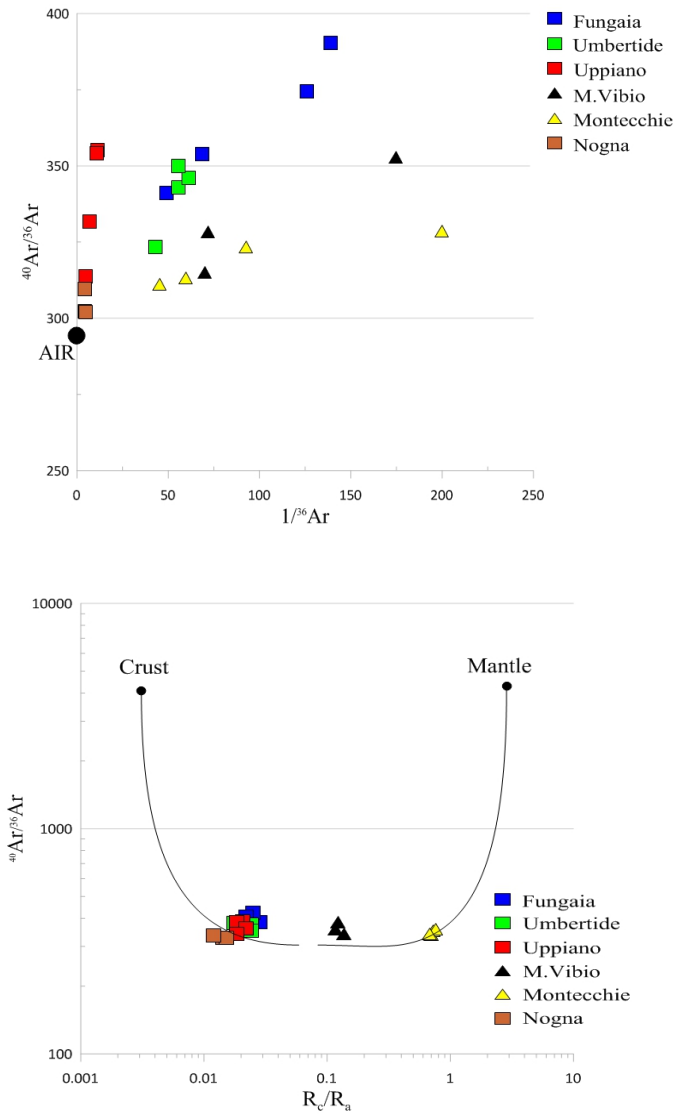

Fig. 8 – (a) $^{40}Ar/^{36}Ar$ versus $1/^{36}Ar$ and **(b)** binary plot that correlates the argon isotope ratio $^{40}Ar/^{36}Ar$ with the helium isotope ratio $^{3}He/^{4}He$ reported as Rc/Ra (Prinzhofer 2013). The air value is shown as black circle.

4.4 Carbon Isotopes

The isotope signature of carbon ranges from -14.3 to -0.6‰ for $\delta^{13}C$-CO_2 vs. V-PDB (**Table 2**). We observe that the $\delta^{13}C_{CO2}$ of the sampled gases tends to be more negative from south to north along with a gradual enrichment of the less soluble volatiles (He and N_2) with respect to CO_2 abundance. Accordingly, the highest (i.e., the less negative) $\delta^{13}C$ values (-0.6 to -1.3‰), related to the ^3He-rich compositions and highest CO_2 contents, are found in the gas emissions collected in the southern sector of the region (M.Vibio and Montecchie). Conversely, the lowest (i.e., the more negative) $\delta^{13}C$ values (-2.9 to -14.3‰), associated to crustal-type $^3He/^4He$ signature and lower CO_2 abundance, are found in the gas emissions sampled in the northern sector of the study area (Fungaia, Umbertide, Uppiano and Nogna). Plotting $\delta^{13}C$-CO_2 vs. CO_2 vol.% (**Fig. 9**) reveals that the sampled gases (expect for the CH_4-dominated emission of Nogna) fall within an area covering the whole range of sedimentary carbon (Hoefs 2015). This area is defined by a mixing between a magmatic end-member and a shallow sedimentary component. Due to the geographical vicinity to the gas samples collected in southern Umbria, the Vicano-Cimino Volcanic District (see **Fig.1**) has been chosen as being the representative non-fractionated magmatic gas end-member.

The theoretical mixing lines between the magmatic end-member (VCVD) and the shallow sources are calculated from the following equation:

$$(\lambda_{CO_2}\delta^{13}C)_{mix} = x(\lambda_{CO_2}\delta^{13}C)_{sed} + (1-x)(\lambda_{CO_2}\delta^{13}C)_{deep} \quad \text{Eq. (1)}$$

The mixing line between the VCVD end-member and air component is computed from the following equation:

$$(\lambda_{CO_2}\delta^{13}C)_{mix} = x(\lambda_{CO_2}\delta^{13}C)_{air} + (1-x)(\lambda_{CO_2}\delta^{13}C)_{deep} \quad \text{Eq. (2)}$$

where λ and $\delta^{13}C$ indicate the fractions and carbon isotope composition of CO_2 in the mixture (mix) and in the sedimentary organic (sed) and magmatic end-member (deep) components; and x depicts the fraction of soil CO_2 in the mixture (ranging from 0 to 1). As shown in the binary plot, the collected gas samples fit with the theoretical mixing curves defined by the range of sedimentary carbon ($\delta^{13}C$ ranging from -40 to -15‰ [Hoefs 2015]). However, a quite scattering distribution of the data points is observed in

Fungaia and Umbertide gas samples, suggesting the presence of additional processes other than mixing involving the uprising CO_2–rich gas phase. Finally, Nogna samples are distributed within and close a mixing area defined by an atmospheric component and two different CO_2 concentrations (1% and 10%).

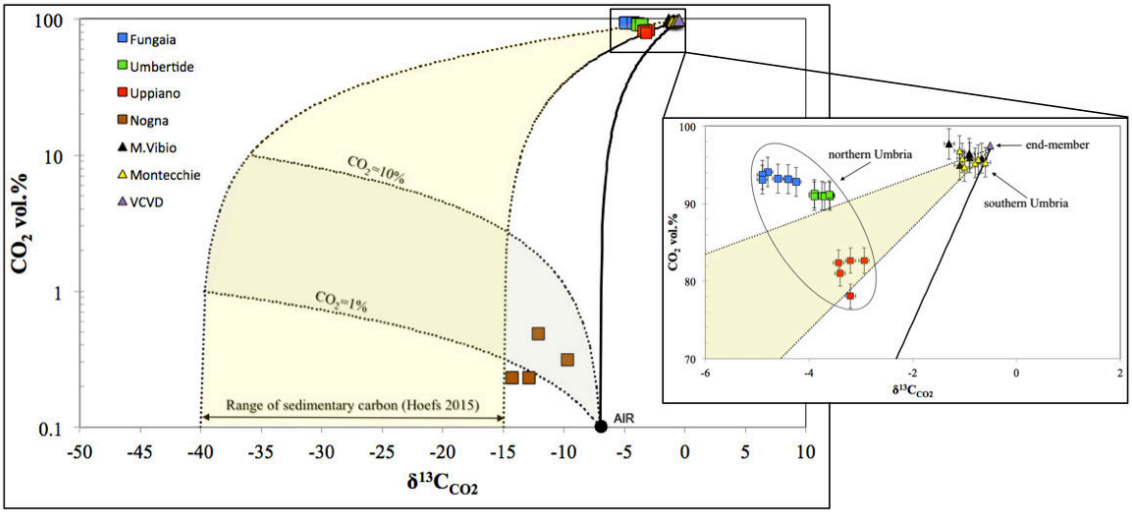

Fig. 9 - $\delta^{13}C$ vs CO_2 vol.% binary plot. Inset zoom shows the variation of $\delta^{13}C$ from south to north Umbria. The mixing line between the VCVD end-member and air component is shown for reference and calculated from Eq.2.

5. DISCUSSION

5.1 Chemical processes affecting the gas composition

The occurrence of secondary chemical processes involved upon ascent toward the surface may lead to modifications of the pristine chemical and isotopic composition of deep rising gases (Capasso et al. 1997; Federico et al. 2002; Caracausi et al. 2003).

Either mixing processes involving two or more gas sources or solubility-controlled fractionation mechanisms due to water-gas interaction can be invoked in order to explain the observed variability of the chemistry of the collected gases. The identification and investigation of chemical processes able to affect the gas geochemistry of the studied gas emissions can be achievable by coupling the elemental abundances of the main components (i.e., He, N_2) to carbon stable isotopes ($\delta^{13}C$-CO_2). As seen in **Fig. 9**, a mixing between a magmatic end-member and a sedimentary gas source is considered to explain the northward negativization of the $\delta^{13}C$-CO_2 of the gas emissions characterizing the Umbria region. However, from **Fig. 10a-b** it is evident a chemical trend showing that the gas samples with the highest He and N_2 contents are associated to the lowest CO_2 abundance suggesting the occurrence of processes that would cause a CO_2 removal due to partial dissolution in water. This is particularly seen at the Uppiano degassing site. Any proposed chemical model accounting for the geochemistry of the collected gases has to be consistent with the chemical composition of the Uppiano gas samples which show enhanced He and N_2 contents (up to 494 ppm and 20.8 vol.%, respectively) and CO_2 depletion (< 80 vol. %) compared to the other degassing sites.

Fig. 11a-b reveals that the gas emissions fall along either mixing or fractionation curves suggesting that the chemistry of the gaseous manifestations in the Umbria region can be best explained by a combination of two different processes: a mixing between the deep magmatic end-member (VCVD) and a shallow component (**model 1**) or chemical fractionation due to partial dissolution in water (**model 2**).

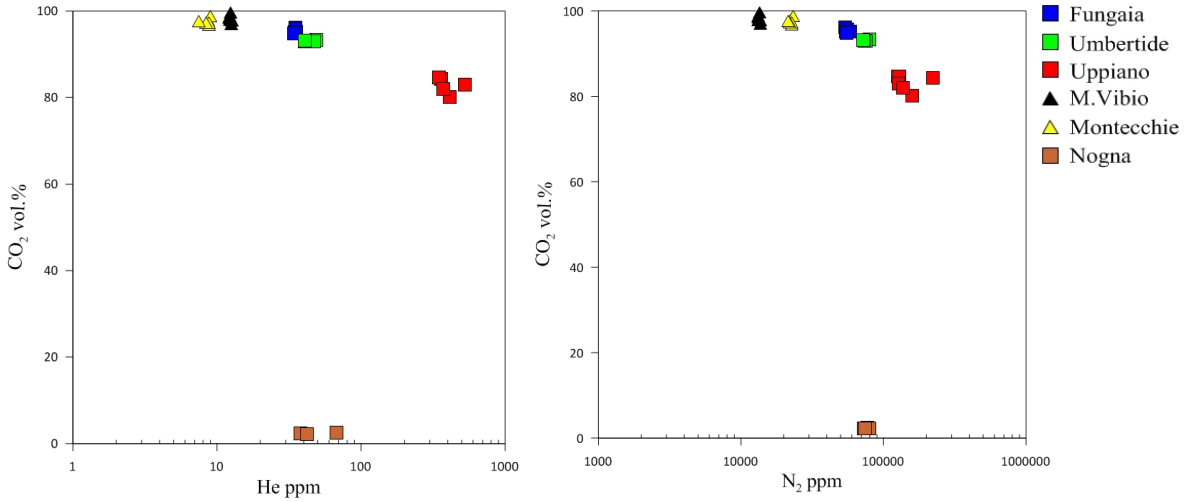

Fig. 10 – **(a)** He-CO_2 and **(b)** N_2-CO_2 binary plots showing an enrichment of He and N_2 in the gas samples observed along with a decrease in CO_2 contents.

The He/CO_2 and N_2/CO_2 ratios ($3.08E^{-06}$ and $1.74E^{-02}$ average values, respectively [Minissale et al. 1997; Minissale 2004]) and the $\delta^{13}C$-CO_2 isotopic composition ($\delta^{13}C$-CO_2 = -0.51‰ average value, [Minissale et al. 1997; Minissale 2004]) from the Vicano-Cimino Volcanic District have been chosen as being the representative non-fractionated gas end-member values. The $\delta^{13}C$ of gaseous CO_2 increases with decreasing of He/CO_2 and N_2/CO_2 in the gas phase, approaching that of the carbon isotopic composition of the deep magmatic end-member. Indeed, M.Vibio and Montecchie are considered to be the gas samples that have experienced the least CO_2 loss with respect to the magmatic end-member. The mixing lines between the VCVD end-member and the shallow-sedimentary gas sources are calculated from the following equations for He and N_2 respectively:

$$(\lambda_{CO_2}\delta^{13}C)_{mix} = x(\lambda_{CO_2}\delta^{13}C)_{sed} + (1-x)(\lambda_{CO_2}\delta^{13}C)_{deep} \quad \text{Eq. (3)}$$

$$\left(\lambda_{CO_2} He/CO_2\right)_{mix} = x(\lambda_{CO_2} He/CO_2)_{soil} + (1-x)(\lambda_{CO_2} He/CO_2)_{deep} \quad \text{Eq. (4)}$$

$$\left(\lambda_{CO_2} N_2/CO_2\right)_{mix} = x(\lambda_{CO_2} N_2/CO_2)_{soil} + (1-x)(\lambda_{CO_2} N_2/CO_2)_{deep} \quad \text{Eq. (5)}$$

where λ and $\delta^{13}C$ indicate the fractions and carbon isotope composition of CO_2 in the mixture (mix) and in the sedimentary organic (sed) and magmatic end-member (deep) components; and x depicts the fraction of soil CO_2 in the mixture (ranging from 0 to 1).

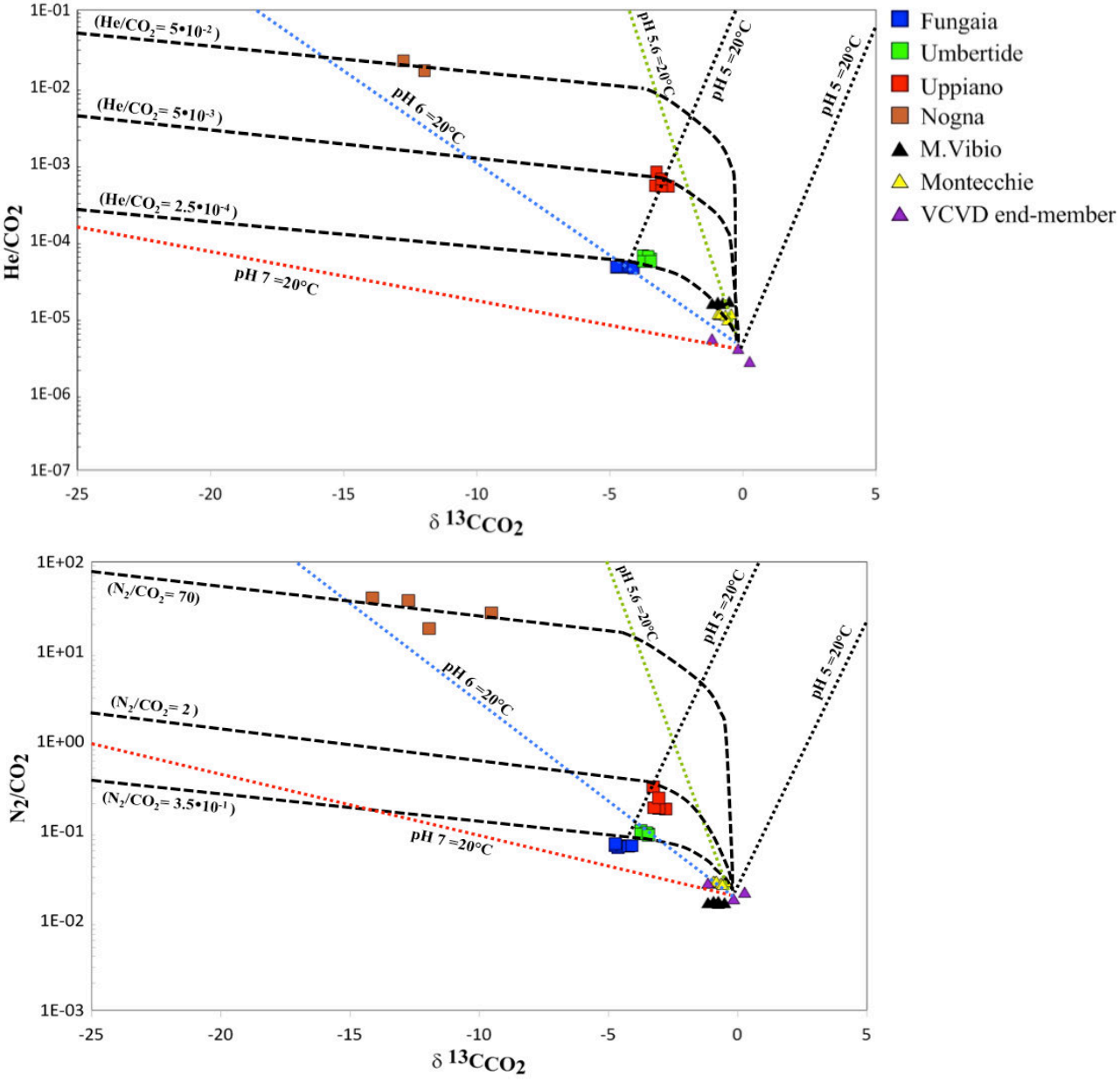

Fig. 11 – (a) He/CO_2 and **(b)** N_2/CO_2 molar ratios vs. $\delta^{13}C_{(CO2)g}$ in the Umbria gas manifestations. The theoretical mixing curves (black dashed curves) between the magmatic end-member (defined by the Vicano-Cimino Volcanic District (Minissale et al. 1997; Minissale 2004) and three shallow-sedimentary components ($\delta^{13}C_{(CO2)g}$ = -25‰, and C_{CO2} = 10%, 2%, and 0.01%) are shown. The mixing lines are computed from Eq.3,4,5. The theoretical Rayleigh-type fractionation lines (coulored dashed lines) computed from Eq.9,10,11,12 are reported along with pH and temperature values used in the calculations (Table 3).

The total dissolved inorganic carbon (TDIC) and concentrations of dissolved carbon species (H_2CO_3, HCO_3^- and CO_3^{2-}) were computed by using the following equations:

$$\left[H_2CO_3\right]=\frac{\left\{H^+\right\}\times\left[HCO_3^-\right]}{K_1} \quad \text{Eq. (6)} \quad \text{and} \quad \left[CO_3^{2-}\right]=\frac{K_2\times\left[HCO_3^-\right]}{\left\{H^+\right\}} \quad \text{Eq. (7)}$$

where K_1 and K_2 define the first and the second dissociation constants of carbonic acid (equal to $4.47\text{x}10^{-7}$ and $4.69\text{x}10^{-11}$ at 25°C, respectively), and $\{H^+\}$=pH. The abundances of the dissolved carbon species (H_2CO_3, CO_3^{2-}, HCO_3^-) are expressed in mg/L. The total fractionation factor 10^3 ln $a_{TDC-CO_{2g}}$ (the fractionation factor A-B is equal to the difference between the isotopic composition of the species A and B; Hoefs 2015) is computed by summing up the enrichment factors (ε) of each dissolved carbon species with respect to CO_{2g}, weighted for their relative abundances and divided by the total dissolved inorganic carbon (TDIC), as follows:

$$\alpha_{TDC-CO_{2g}}=\frac{\varepsilon_{TDC-CO_{2g}}}{1000}+1=\left(\frac{\varepsilon_{HCO_{3^-}-CO_{2g}}\left[HCO_{3^-}\right]+\varepsilon_{CO_3^{2-}-CO_{2g}}\left[CO_3^{2-}\right]+\varepsilon_{H_2CO_3-CO_{2g}}\left[H_2CO_3\right]}{\left[HCO_3^-\right]+\left[CO_3^{2-}\right]+\left[H_2CO_3\right]}\right)\times10^{-3}+1 \quad \text{Eq. (8)}$$

Due to the different Henry's solubility constants in water of He (K_{He} = 141048 atm mol^{-1}) and N_2 (K_{N2}=78545 atm mol^{-1}) compared to CO_2 (K_{CO2}= 1217 atm mol^{-1}) at 20°C (Capasso and Inguaggiato 1998), a gradual enrichment of the less soluble volatile species (i.e., He and N_2) is expected to occur in the residual gas phase as gaseous CO_2 dissolves progressively in water. A Rayleigh-type condensation process needs to be considered in order to explain the chemical changes experienced by the gas phase upon interaction with water according to the following equations:

$$\left(He/CO_2\right)_r=\left(He/CO_2\right)_i\cdot F^{\frac{K_{CO_2}}{K_{He}}} \quad \text{Eq. (9)} \qquad \delta^{13}C_{(CO_2)_r}=\left(\delta^{13}C_{(CO_2)_i}+1000\right)\cdot F^{\alpha-1}-1000 \quad \text{Eq. (10)}$$

$$\left(N_2/CO_2\right)_r=\left(N_2/CO_2\right)_i\cdot F^{\frac{K_{CO_2}}{K_{N_2}}} \quad \text{Eq. (11)} \qquad \delta^{13}C_{(CO_2)_r}=\left(\delta^{13}C_{(CO_2)_i}+1000\right)\cdot F^{\alpha-1}-1000 \quad \text{Eq.(12)}$$

where F represents the fraction of residual gas after partial dissolution in water (ranging from 0 to 1); $(He/CO_2)_i$ and $(He/CO_2)_r$ are the molar ratios in the initial and residual gas phase for each F value considered, respectively; K_{CO2}/K_{He} and K_{CO2}/K_{N2} are the ratios of

Henry's solubility constants for CO_2, He and N_2, respectively; $\delta^{13}C_{CO2i}$ and $\delta^{13}C_{CO2r}$ stand for the initial and residual carbon isotopic composition of CO_2. The Rayleigh fractionation theoretical curves were computed by combining Eqs. (9) and (10) for He and CO_2, and Eqs. (11) and (12) for N_2 and CO_2; α depicts the fractionation factor between dissolved carbon species and gaseous CO_2 for different pH and T=20° C (**Table 3**).

Table 3. Fractionation (**α**) and enrichment (**ε**) factors are reported together with pH and temperature values used in the calculations (see text). TDC= total dissolved carbon; T= temperature in degrees Celsius

$\alpha_{TDC-CO_{2g}}$	$\varepsilon_{TDC-CO_{2g}}$	pH	T°C
0.99946	-0.54	5	20
1.00044	0.44	5.6	20
1.00177	1.77	6	20
1.00622	6.22	7	20

Furthermore, a fractionation process at pH 5 departing from the end-member Fungaia must be invoked to explain the enrichment in He and N_2 at the Uppiano degassing site

It is worth noting that, although these values (Vibio and Montecchie) are very close to those that characterize the gas emissions from the geothermal field of the Vicano-Cimino Volcanic District ($\delta^{13}C$ ~ -0.5 ‰ average value; Minissale et al. 1997, 2004), the Vesuvius volcano ($\delta^{13}C$ ~ 0 ‰ average value; Chiodini et al. 2001), as well as the largest non-volcanic degassing area of Mefite d'Ansanto in the southern Apennines ($\delta^{13}C$ ~ 0.4 ‰; Chiodini et al. 2010), they are not consistent with those reported for mantle CO_2 typically showing $\delta^{13}C$ of about -5 ‰ (Hoefs 2015). These findings suggest a different end-member value than generally accepted for magmatic $\delta^{13}C$-CO_2 in this area.

5.2 He-Ne-Ar relationships

The atmosphere-derived contamination trends in **Fig.8a** have been observed in a number of crustal fluid studies (Ballentine et al. 1991; Ballentine & O'Nions 1994; Battani et al. 2000; Wen et al. 2017) and may arise either from air component which had previously dissolved in groundwater or entrained as formation water during sediment deposition. The $^{20}Ne/^{36}Ar$ ratios in the gas samples are variable (**Fig.12**) and show values intermediate between air-equilibrated water ($^{20}Ne/^{36}Ar_{asw}$= 0.12-0.19; Weiss 1970, 1971) and air ($^{20}Ne/^{36}Ar_{air}$= 0.52), although two gas samples from Fungaia have values higher than atmosphere (0.67 and 0.80, respectively). Notwithstanding, any possibility of the samples being contaminated by air either during sampling in the field or laboratory analysis or by air trapped in sediments can be ruled out as the measured $^{4}He/^{20}Ne$ ratios are far greater than air (**see Table 1**). Highly fractionated $^{20}Ne/^{36}Ar$ ratios (> 1-1.5), usually associated with low ^{36}Ar concentrations, have also been reported by previous investigations on natural gases (Ballentine et al. 1991; Battani et al. 2000) and waters (Castro et al. 1998) in continental environments. According to Bosch and Mazor (1988) and Ballentine et al. 1991, partitioning of Ne and Ar into the gas phase, assuming a single-stage equilibration model, may result in highly fractionated values with elevated Ne/Ar ratios when a very small gas-water volume ratio is considered. These enhanced $^{20}Ne/^{36}Ar$ ratios may even extend to values up to 0.6, which is very close to the highest values measured in the Umbrian gases. In such a case, this consideration can also be applied to Rayleigh fractionation of a simple gas-water system.

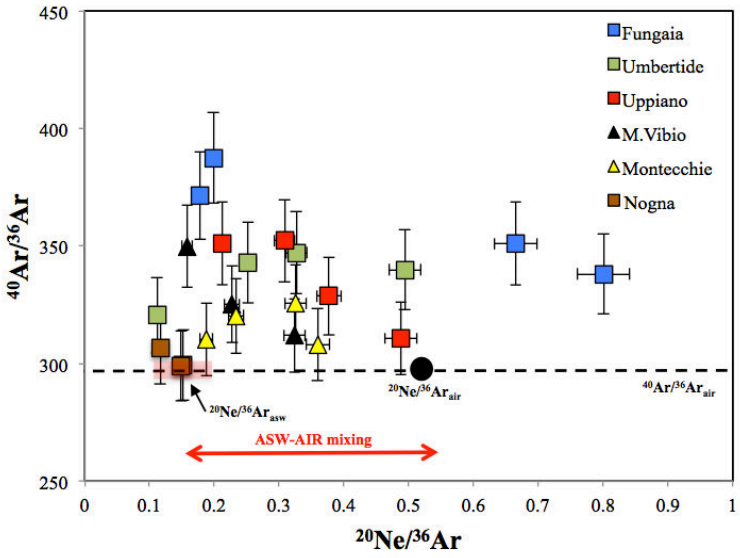

Fig. 12 – $^{40}Ar/^{36}Ar$ versus $^{20}Ne/^{36}Ar$ in the Umbrian gases. Dotted band defines the ASW domain for temperature range from 0° to 25°C according to Weiss (1970, 1971). The air line for Ar isotope ratio is also reported in the diagram.

Thus, following Ballentine et al. 1991, the $^{4}He/^{40}Ar^{*}$ and $^{20}Ne/^{36}Ar$ isotope ratios of the gas samples have been normalised to predicted end-member values to obtain a *fractionation factor F* with the aim to assess the relative magnitude of fractionation between differently-sourced rare gas components. The fractionation factor F serves to quantify the extent of deviation for both rare gas isotope pairs (crustal and atmosphere-derived) with respect to reference expected ratios. Therefore, any deviations from the end-member ratio must reflect the chemical-physical processes that the studied gaseous manifestations have undergone in the system. For reasons of clarity, $^{40}Ar^{*}$ refers to the radiogenic component of ^{40}Ar which is calculated by:

$$^{40}Ar^{*} = {}^{36}Ar\left[\frac{^{40}Ar}{^{36}Ar} - 298.56\right] \quad \text{Eq. (13)},$$

where ^{36}Ar and $^{40}Ar/^{36}Ar$ are respectively the concentration and ratio in parts-per-million measured in the sample and 298.56 is the value of the $^{40}Ar/^{36}Ar$ ratio in the atmosphere. In **Fig.13**, $\mathbf{F(^{4}He/^{40}Ar^{*})_{rad}}$ and $\mathbf{F(^{20}Ne/^{36}Ar)_{asw}}$ values for Umbrian gases are plotted together with the values of gas samples from the Pakistan Indus Basin and the Pannonian Basin (in order to highlight any possible differences between our study area and other well-studied sedimentary basins on Earth.

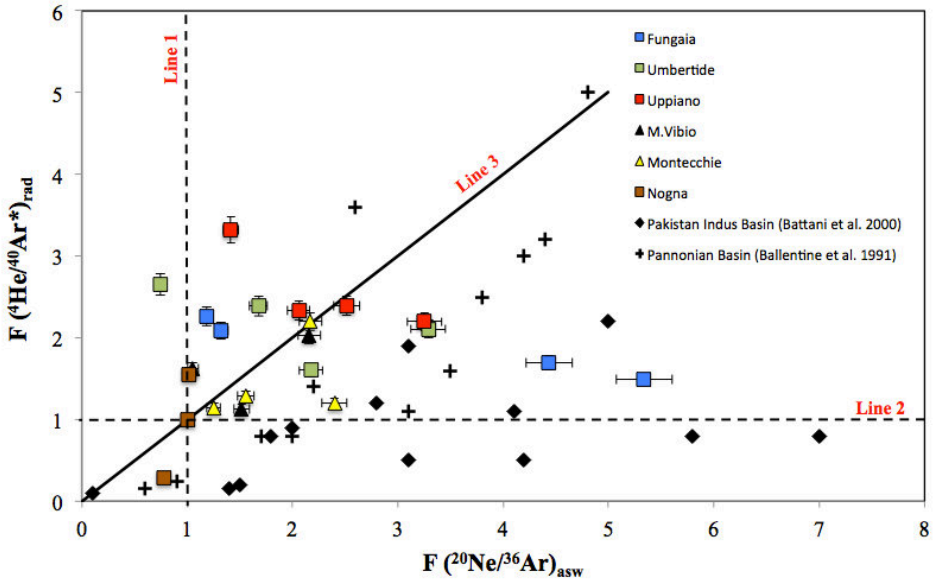

Fig. 13 – The extent of fractionation of the rare gas components defined by the fractionation factors $F(^{4}He/^{40}Ar^{*})_{rad}$ and $F(^{20}Ne/^{36}Ar)_{asw}$ obtained by dividing the measured ratios by reference end-member values. The figure shows a comparison between gases sampled in the Umbria region with those collected in two other different crustal environments such as the Pakistan Indus Basin (Battani et al. 2000) and the Pannonian Basin (Ballentine et al. 1991). Dashed lines labelled **Line 1** and **Line 2** show that when F=1 any elemental deviation from the reference ratio has occurred, while **Line 3** represents the trend of equal fractionation.

Ballentine et al. 1991 and Battani et al. 2000 report the $^{20}Ne/^{36}Ar$ ratios being divided to the reference value of 0.192 for the $^{20}Ne/^{36}Ar$ ratio of air-saturated water at 25°C (Ozima and Podosek 2002) and the $^{4}He/^{40}Ar^{*}$ values to the present-day average radiogenic production ratio for crustal rocks of 4.9.

Unlike the end-member values used for the Pannonian and Pakistan Indus Basins, the $^{20}Ne/^{36}Ar$ and $^{4}He/^{40}Ar^{*}$ ratios of the Umbrian gas samples have been normalized to the values of Nogna, respectively 0.15 and 4.28. The gas manifestation of Nogna has been chosen as reference site due to the fact that it is the only location among the sampled gas emissions that contains water in the borehole and characterized both by very little bubbling and high water/gas ratio.

In general, the Pannonian Basin gas samples fall on a linear array showing a markedly co-variation in terms of magnitude of fractionation for both isotope pairs. Ballentine et al. 1991 argue that the observed coherent covariance suggest that the crustal- and atmosphere-derived rare gases must have been mixed before fractionation processes had occurred. On the contrary, the Pakistan Indus Basin exhibits an overall much larger dispersion of the data points characterized by a first group of samples showing a general coherent trend of fractionation for both $^{4}He/^{40}Ar^{*}$ and $^{20}Ne/^{36}Ar$ ratios, followed by second group with Ne/Ar being far more fractionated than He/Ar. Battani et al. 2000 conclude that these data could represent aged geological system which have undergone fractionation of their $^{4}He/^{40}Ar^{*}$ and $^{20}Ne/^{36}Ar$ ratios, suggesting the presence of a multi-step process where gas phase had contact with air-equilibrated water, which, in turn, had previously been in contact with oil in geological past times.

As far as concern the Umbrian gases, we observe that, for a given $^{4}He/^{40}Ar^{*}$ ratio, the gas samples collected in winter months fall around the line of equal fractionation (**Line 3**) while the gas collected in summertime show $^{20}Ne/^{36}Ar$ ratios more fractionated. This could be due to the fact that during summer periods the gas phase mixes with water that had already been fractionated.

In contrast to atmosphere-derived gases, crustally-produced radiogenic noble gases can also be resolved as their concentrations are proportional to the abundances of U, Th and K radioelements in the crust. Specifically, aside from Ne isotopes whose crustal production is entirely controlled by nucleogenic processes, the present-day radiogenic ^{4}He is governed by the α-decay ^{235,238}U and ^{232}Th, while ^{40}Ar is produced from ^{40}K by electron capture.

In order to investigate the contribution of He and Ar produced in the crust have been calculated for each gas sample. The present-day ^{4}He crustal output produced in 1 g of rock per year is given by:

$$\mathbf{^{4}He\ atoms\ g^{-1}\ yr^{-1}} = (3.115\text{x}10^{6} + 1.272\text{x}10^{5})\ [\text{U}] + 7.710\text{x}10^{5}\ [\text{Th}] \qquad \text{Eq. (14)},$$

On the other hand, the ^{40}Ar crustal production can be expressed as

$$\mathbf{^{40}Ar\ atoms\ g^{-1}\ yr^{-1}} = 102.2\ [\text{K}] \qquad \text{Eq. (15)},$$

where [U], [Th] and [K] are the concentrations of ^{235,238}U, ^{232}Th and ^{40}K in weight fraction or parts-per-million (ppm).

Thus, combining the term for He radiogenic production (Eq. 14) with that for the Ar (Eq. 15), the total crustal production ratio can be obtained as follows (Ballentine & Burnard 2002):

$$\mathbf{^{4}He/^{40}Ar^{*}} = \{(3.115\text{x}10^{6} + 1.272\text{x}10^{5})\ [^{235,238}\text{U}] + 7.710\text{x}10^{5}\ [^{232}\text{Th}]\}\ /\ 102.2\ [^{40}\text{K}]$$

Eq. (16)

Table 4 - Reservoir, lithology and average values of U, Th K_2O (expressed in ppm) from Boraso (2008) and Coltorti et al (2011)

Reservoir	Lithology	U	Th	K_2O	^{4}Hr/^{40}Ar* (This study)
Sedimentary cover	Limestone, marly limestone, evaporates, mudstones	1.68	1.86	42000	16.03
Italian Upper Crust	Amphibolite, micaschist, phyllite, granite, marble	1.54	7.9	19700	5.51
Italian Lower Crust	Gabbro, diorite, granulite	0.3	3.53	12000	3.01

The calculated $^{4}He/^{40}Ar^{*}$ ratios, ranging from values as low as 1.26 up to as high as 14.21, indicate that the Umbrian gas samples fall within a band between a typical Italian continental crust and the sedimentary cover (**Fig. 14**). The lithologies of the reservoir together with the average values of U, Th and K_2O used for the calculation are listed in **Table 4**.

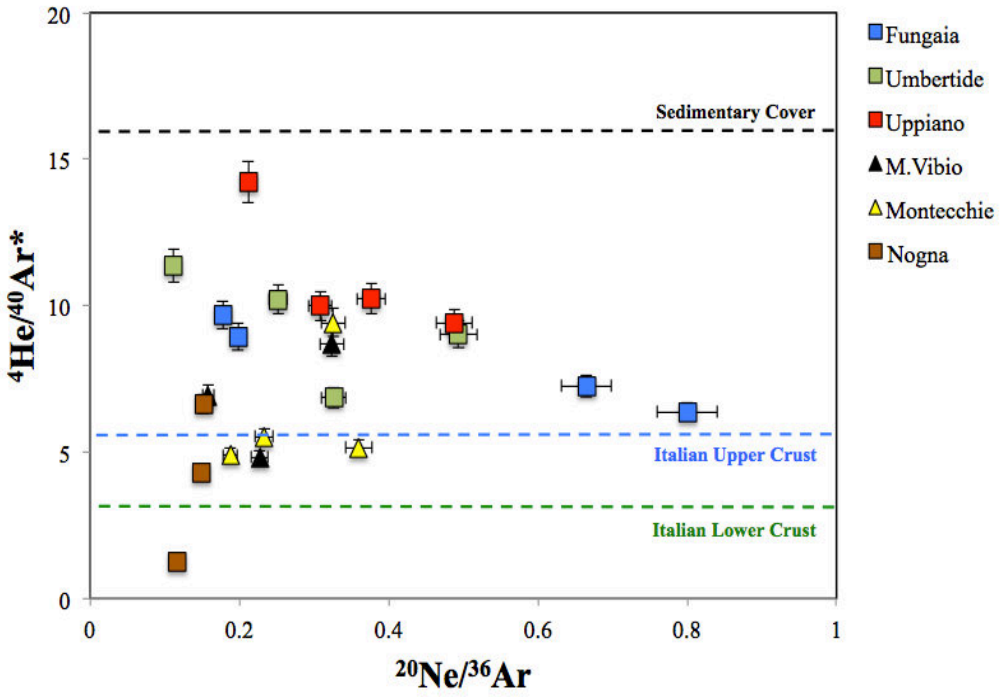

Fig. 14 – Binary diagram showing $^{4}He/^{40}Ar^{*}$ vs. $^{20}Ne/^{36}Ar$

CONCLUSIONS

The geochemical investigation of gaseous emissions discharged in a seismic region can provide useful insights on the interaction processes of uprising volatiles with subsurface waters encountered during their ascent to the surface. The variable compositions of the gaseous manifestations emitted across the Umbria region can be best interpreted as a result of the combination of two different chemical processes which are not mutually exclusive: 1) a mixing between a magmatic end-member (VCVD) and a shallow-sedimentary sources, and 2) solubility-controlled fractionation mechanisms taking place upon interaction with shallow subsurface waters.

I have proposed a geochemical model of fluid circulation and secondary chemical processes (i.e., mixing and gas-water interaction) developed in a earthquake-prone area acting under quiescence condition of high intensity seismic activity that could serve as baseline for future geochemical monitoring of a vulnerable and high-risk area as the central Apennines.

Hence, the investigation of natural gas emissions in seismic areas under quiescence conditions is essential to:

1. Define a **background model** of fluid circulation and of the control of secondary chemical processes on gas geochemistry at shallow levels and their relationship with the seismo-tectonic setting of the area;
2. To evaluate the extent of potential **geochemical changes** that could be correlated to the acquired baseline dataset for seismic surveillance.

This approach could be useful to interpreting future geochemical variations in the fluids that move across the crust transferring to the surface some messages about the relationship between fluids and rock deformation.

REFERENCES

- **Alwarez W. (1972)** - Rotation of the Corsica-Sardinia microplate. *Nature,* 248, 309-314.
- **Amato A., Azzara R., Chiarabba C., Cimini G. B., Cocco M., Di Bona L., Margheriti S., Mazza F., Mele F., Selvaggi A., Basili A. and Boschi E. (1998)** – The 1997 Umbria-Marche, Italy, earthquake sequence: a first look at the main shocks and aftershocks – Geophysical Research Letters, vol. 25, No.15, pp. 2861-2864
- **Ballentine C.J., O'Nions R.K., Oxburgh E.R., Horvath F., and Deak J. (1991)** – Rare gas constrains on hydrocarbon accumulation, crustal degassing and groundwater flow in the Pannonian Basin – Earth and Planetary Science Letters, 105, pp. 229-246
- **Ballentine C.J. and O'Nions R.K. (1994)** – The use of natural He, Ne and Ar isotopes to study hydrocarbon-related fluid provenance, migration and mass balance in sedimentary basins – From Parnell J. (ed.), 1994, Geofluids: Origin, Migration and Evolution of Fluids in Sedimentary Basins, Geol. Soc. Sp. Publ. No. 78, pp. 347-361
- **Ballentine C.J. and Burnard P. G. (2002)** – Production, release and transport of noble gases in the continental crust. In: Porcelli D., Ballentine C.J., Wieler R. (Eds.), Noble Gases in Geochemistry and Cosmochemistry: Rev. Mineral. Geochem., 47, pp. 481-538.
- **Barba S. and Basili R. (2000)** – Analysis of seismological and geological observations for moderate-size earthquake: the Colfiorito Fault System (Central Apennines, Italy) – Geophysical International Journal, 141, pp. 241-252
- **Barberio M. D., Barbieri M., Billi A., Doglioni C. and Petitta M. (2017)** – Hydrogeochemical changes before and during the 2016 Amatrice-Norcia seismic sequence (Central Italy) – Scientific Reports, 7, 11735
- **Barchi M., Alvarez W. & Shimabukuro D. H. (2012)** – The Umbria-Marche Apennines as a Double Orogen: Observations and hypotheses – Ital. J. Geosci. (Boll. Soc. Geol. It.), Vol. 131, No. 2, pp. 258-271.

- **Barnes, I., Irwin, W.P., White, D.E. (1978)** - Global distribution of carbon-dioxide discharges, and major zones of seismicity, scale 1:40,000,000. Wat. Res. Invest. WRI 78-39
- **Battani A., Sarda P. and Prinzhofer A. (2000)** – Basin scale natural gas source, migration and trapping traced by noble gases and major elements: the Pakistan Indus basin – Earth and Planetary Science Letters 181, pp. 229-249
- **Bernard P. and Zollo A. (1989)** – The Irpinia (Italy) 1980 Earthquake: Detailed Analysis of a Complex Normal Faulting – Journal of Geophysical Research, vol. 94, No. B2, pp. 1631-1647.
- **Bicocchi, G., Tassi, F., Bonini, M., Capecchiacci, F., Ruggieri, G., Buccianti, A., Burgassi, P., Vaselli, O. (2013):** The high pCO_2 Caprese Reservoir (Northern Apennines, Italy): relationships between present- and paleo-fluid geochemistry and structural setting. *Chem. Geol.*, **351**, 40-56, doi: 10.1016/j.chemgeo.2013.05.001.
- **Bindi D., Pacor F., Luzi L., Massa M. and Ameri G. (2009)** – The Mw 6.3, 2009 L'Aquila earthquake: source, path and site effects from spectral analysis of strong motion data – Geophysical Journal International, 179, pp. 1573-1579
- **Boncio P., Brozzetti F., Ponziani F., Barchi M., Lavecchia G. and Pialli G. (1998)** – Seismiciy and extensional tectonics in the northern Umbria-Marche Apennines – Memorie della Societá Geologica Italiana, 52, pp. 539-555
- **Boni C., Bono P., & Capelli G. (1986)** – Schema idrogeologico dell'Italia centrale – Mem. Soc. Geol. Ital. 35, 991-1012
- **Boraso R. (2008)** – Un approccio geochimico-geologico-geofisico per la stima delle abbondanze di Th e U nella crosta dell'Appennino Centrale, per testare I geoneutrini come strumento d'indagine per l'interno della Terra. PhD Thesis, University of Ferrara.
- **Bosch A. and Mazor E. (1988)** – Natural gas association with water and oil as depicted by atmospheric noble gases: case study from the southeastern Mediterrean Coastal Plain – *Earth and Planetary Science Letters* 87, pp. 338-346

- **Boschi, E., Guidoboni, E., Ferrari, G., Valensise, G., Gasperini, P., (1997)** - CFTI, Catalogo dei Forti Terremoti Italiani dal 461 a.C. al 1990. Istituto Nazionale di Geofisica, Storia Geofisica Ambiente, Bologna.
- **Boschi E., Guidoboni E., Ferrari G. and Valensise G. (1998)** - I terremoti dell'Appennino Umbro-Marchigiano (area sud orientale dal 99 a.C. al 1984)-ING-SGA, 267 pp., Compositori, Bologna, Italy.
- **Bräuer K., Kämpf H., Niedermann S., & Strauch G. (2013)** – Indications for the existence of different magmatic reservoirs beneath the Eifel area (Germany): A multi-isotope (C, N, He, Ne, Ar) approach - Chemical Geology 356, pp.193-208.
- **Bräuer K., Kämpf H., Niedermann S., & Strauch G. (2018)** - Monitoring of helium and carbon isotopes in the western Eger Rift area (Czech Republic): Relationships with the 2014 seismic activity and indications for recent (2000-2016) magmatic unrest – Chem. Geology 482, pp.131-145.
- **Brune S., Williams S. E. and Dietmar Müller R. (2017)** - Potential links between continental rifting, CO2 degassing and climate change through time - Nature Geoscience, vol. 10, pp.941-946
- **Buiter S.J.H., Wortel M.J. & Govers R. (1998)** – The role of subduction in the evolution of the Apennines foreland basin – Tectonophysics 296, pp. 249-268.
- **Capasso G., Favara R. & Inguaggiato S. (1997)** – Chemical features and isotopic composition of gaseous manifestations on Vulcano Island, Aeolian Islands, Italy: An interpretative model of fluid circulation – Geochimica et Cosmochimica Acta, Vol. 61, No.16, pp. 3425-3440
- **Capasso G. & Inguaggiato S. (1998)** – A simple method for the determination of dissolved gases in natural waters. AN application to thermal waters from Volcano Island – Applied Geochemistry, Vol. 13, No.5, pp. 631-648

- **Castello B., G. Selvaggi, C. Chiarabba and A.Amato (2005),** CSI Catalogo della sismicità italiana 1981-2002, vers. 1.0, INGV-CNT, Roma, www.ingv.it/CSI/.
- **Castro M.C., Jambon A., de Marsily G. and Schlosser P. (1998)** – Noble gases as natural tracers of water circulation in the Paris Basin: 1. Measurements and discussion of their origin and mechanisms of vertical transport in the basin, *Water Resources Research*, Vol. 34, No. 10, pp. 2443-2466
- **Caracausi A., Italiano F., Nuccio P.M., Paonita A. & Rizzo A. L. (2003)** – Evidence of deep magma degassing and ascent by geochemistry of peripheral gas emissions at Mt. Etna (Italy): assessment of the magmatic reservoir pressure – Journal of Geophysical Research 108 (B10): 2463
- **Caracausi A., Italiano F., Martinelli G., Paonita A. and Rizzo A. L. (2005)** – Long-term geochemical monitoring and extensive/compressive phenomena: case study of the Umbria Region (Central Apennines, Italy) – Annals of Geophysics, vol. 48, N. 1, pp. 43-53
- **Caracausi A**., **Martelli M., Nuccio P.M., Paternoster M. and Stuart F. M. (2013)** – Active degassing of mantle-derived fluid: A geochemical study along the Vulture line, southern Apennines (Italy) – Journal of Volcanology and Geothermal Research 253, pp. 65-74
- **Caracausi A. and Paternoster M. (2015)** – Radiogenic helium degassing and rock fracturing: A case study of the southern Apennines active tectonic region – Journal of Geophysical Research, Solid Earth 120, pp. 2200-2211
- **Carapezza M. L. and Tarchini L. (2007)** – Accidental gas emission from shallow pressurized aquifers at Alban Hills volcano (Rome, Italy): Geochemical evidence of magmatic degassing – Journal of Volcanology and Geothermal Research, 165, pp. 5-16
- **Cello G., Deiana G., Ferelli L., Marchegiani L., Maschio L., Mazzoli S., Michetti A., Serva L., Tondi E. and Vittori T. (2000)** – Geological constraints for earthquake

faulting studies in the Colfiorito area (central Italy) – Journal of Seismology, 4, pp. 357-364.

- **Chiarabba, C., L. Jovane and R. Di Stefano (2005)**. A new view of Italian seismicity using 20 years of instrumental recordings, Tectonophysics, 395, 251-268.
- **Chiarabba C., De Gori P., Cattaneo M., Spallarossa D. and Segou M. (2018)** – Faults geometry and the role of fluids in the 2016-2017 Central Italy seismic sequence – Geophysical Research Letters, 45, 6963-6971.
- **Chiaraluce, L., A. Amato, M. Cocco, C. Chiarabba, G. Selvaggi, M. Di Bona, D. Piccinini, A. Deschamps, L. Margheriti, F. Courboulex and M. Ripepe (2004)**. Complex Normal Faulting in the Apennines Thrust- and-Fold Belt: The 1997 Seismic Sequence in Cen- tral Italy, B. Seismol. Soc. Am., 94 (1), 99-116.
- **Chiaraluce L., Chiarabba C., Collettini C., Piccinini D. and Cocco M. (2007)** – Architecture and mechanics of an active low-angle normal fault: Alto Tiberina Fault, northern Apennines, Italy – Journal of Geophysical Research, vol. 112, B10310
- **Chiaraluce L., Collettini C., Cattaneo M. and Monachesi G. (2014a) – The shallow boreholes at The AltotiBerina near fault Observatory (TABOO; northern Apennines of Italy)** – Scientific Drilling, 17, 31-35.
- **Chiaraluce L., Amato A., Carannante S., Castelli V., Cattaneo M., Cocco M., Collettini C., D'Alema E., Di Stefano R., Latorre D., Marzorati S., Mirabella F., Monachesi G., Piccinini D., Nardi A., Piersanti A., Stramondo S. and Valoroso L. (2014b)** – The Alto Tiberina Near Fault Observatory (northern Apennines, Italy) – Annals of Geophysics, 57, 3, S0327.
- **Chiodini G., Frondini F., Cardellini C., Parello F., & Peruzzi L. (2000)** – Rate of diffuse carbon dioxide Earth degassing estimated from carbon balance of regional aquifers: The case of central Apennines, Italy – Journal of Geophysical Research vol.105, NO.B4, pp.8423-8434

- **Chiodini G., Marini L. & Russo M. (2001)** – Geochemical evidence for the existence of high-temperature hydrothermal brines at Vesuvio volcano, Italy – Geochimica et Cosmochimica Acta, 65, 2129-2147
- **Chiodini G**., **Cardellini C., Amato A., Boschi E., Caliro S., Frondini F. and Ventura G. (2004)** – Carbon dioxide Earth degassing and seismogenesis in central and southern Italy – Geophysical Research Letters, vol. 31, L07615.
- **Chiodini G., Granieri D., Avino R., Caliro S., Costa A., Minopoli C., & Vilardo G. (2010) –** Non-volcanic CO_2 Earth degassing: Case of Mefite d'Ansanto (southern Apennines), Italy – Geophysical Research Letters, vol. 37, L11303.
- **Ciaccio M. G., Barchi M. R., Chiarabba C., Mirabella F. and Stucchi E. (2005)** – Seismological, geological and geophysical constraints for the Gualdo Tadino fault, Umbria-Marche Apennines (central Italy) – Tectonophysics, 406, pp. 233-247
- **Cinti D., Tassi F., Procesi M., Bonini M., Capecchiacci F., Voltattorni N., Vaselli O. & Quattrocchi F. (2014)** – Fluid geochemistry and geothermometry in the unexploited geothermal field of the Vicano-Cimino Volcanic District (Central Italy) – Chemical Geology 371, 96-114
- **Cinti D., Tassi F., Procesi M., Brusca L., Cabassi J., Capecchiacci F., Delgado Huertas A., Galli G., Grassa F., Vaselli O. and Voltattorni N. (2017)** –Geochemistry of hydrothermal fluids from the eastern sector of the Sabatini Volcanic District (central Italy) - Applied Geochemistry, 84, pp. 187-201
- **Collettini C. and Barchi M. R. (2002)** – A low-angle normal fault in the Umbria region (Central Italy): a mechanical model for the related microseismicity – Tectonophysics 359, pp. 97-115.
- **Collettini C**., **Barchi M. R., Chiaraluce L., Mirabella F. and Pucci S. (2003)** – The Gubbio fault: can different methods give pictures of the same object? – Journal of Geodynamics 36, pp. 51-66.

- **Collettini C. and Barchi M. R. (2004)** – A comparison of structural data and seismic images for low-angle normal faults in the Northern Apennines (Central Italy): constraints on activity – In Alsop G. I., Holdsworth R. E., McCaffrey K. J. W. and Hand M. (eds) 2004. *Flow Processes in Faults and Shear Zones,* Geological Society, London, Special Publications, 224, 95-112.
- **Coltorti M., Boraso R., Mantovani F., Morsili M., Fiorentini G., Riva A., Rusciadelli G., Tassinari R., Tomei C., Di Carlo G. and Chubakov V. (2011)** – U and Th content in the Central Apennines continental crust: A contribution to the determination of the geo-neutrinos flux at LNGS, *Geochimica et Cosmochimica Acta*, 75, pp. 2271-2294
- **Di Giovambattista R. and Tyupkin Y. S. (2000)** – Spatial and temporal distribution of seismicity before the Umbria-Marche September 26, 1997 earthquakes – Journal of Seismology 4, pp. 589-598
- **Di Luccio F., Amato A., Azzara R.M., Basili A., Delladio A., Di Bona M., Gorini A., Lucente F.P., Marcucci S., Margheriti L., Milana G., Ponziani., Selvaggi G., & Zambonelli E. (1998)** - La sequenza sismica del maggio 1997 a Massa Martana (PG), in *Atti XIX Convegno Nazionale GNGTS*, 7-9 Novembre 1998, Roma, Italy, **1**, 65.
- **Di Luccio F., Ventura G., Di Giovambattista R., Piscini A., and Cinti R. (2010)** – Normal faults and thrusts reactivated by deep fluids: The 6 April 2009 Mw 6.3 L'Aquila earthquake, central Italy – J. of Geophys. Res., vol. 115, B06315.
- **Di Luccio F., Chiodini G., Caliro S., Cardellini C., Convertito V., Pino N. A., Tolomei C., & Ventura G. (2018)** – Seismic signature of active intrusions in mountain chains – Science Advance, 4., pp. 1-9.
- **Doglioni C., Gueguen E., Harabaglia P. & Mongelli F (1999)** – On the origin of W-directed subduction zones and applications to the western Mediterrean – Geol. Soc. Sp. Publ., 156, 541-561

- **Federico C., Aiuppa A., Allard P., Bellomo S., Jean-Baptiste P., Parello F. & Valenza M. (2002)** – Magma-derived gas influx and water-rock interactions in the volcanic aquifer of Mt. Vesuvius, Italy - Geochimica et Cosmochimica Acta, Vol. 66, No.6, pp. 963-981
- **Gautheron C., Moreira M., and Allègre C. J. (2005)** - He, Ne and Ar composition of the European lithospheric mantle. *Chem. Geol.* 217, 97–112.
- **Haessler H., Gaulon R., Rivera L., Console R., Frogneux M., Gasparini G., Martel L., Patau G., Siciliano M. and Cisternas A (1988)**: The Perugia (Italy) earth- quake of 29 April 1984: a microearthquake survey, *Bull. Seismol. Soc. Am.*, **78**, 1948-1964.
- **Heinicke J., Italiano F., Lapenna V., Martinelli G. and Nuccio P. M. (2000)** – Coseismic geochemical variations in some gas emissions of Umbria Region (Central Italy) – Phys. Chem. Earth, vol. 25, No. 3, pp.289-293
- **Heinicke J., Braun T., Burgassi P., Italiano F. and Martinelli G. (2006)** – Gas flow anomalies in seismogenic zones in the Upper Tiber Valley, Central Italy – Geophysical Journal International 167, pp.794-806
- **Heinicke J., Martinelli G. and Telesca L. (2011)** – Geodynamically induced variations in the emissions of CO_2 gas at San Faustino (Central Apennines, Italy) – Geofluids, doi: 10.1111/j.1468-8123.2011.00345.x
- **Hoefs J. (2015)** – Stable Isotope Geochemistry. 7th Edition. Springer International Publishing Switzerland Berlin, p. 389.
- **Inguaggiato S., Pecoraino G. and D'Amore F. (2000)** – Chemical and isotopical characterization of fluid manifestations of Ischia Island (Italy) – Journal of Volcanology and Geothermal Research, 99, pp. 151-178
- **Irwin W.P. & Barnes I. (1980)** – Tectonic relations of carbon dioxide discharges and earthquakes - Journal of Geophysical Research vol.85, NO.B6, pp.3115-3121

- **Italiano F., Martinelli G. and Nuccio P.M. (2001)** – Anomalies of mantle-derived helium during the 1997-1998 seismic swarm of Umbria-Marche, Italy – Geophysical Research Letters, vol. 28, No.5, pp.839-842
- **Italiano F., Martinelli G. and Rizzo A.L. (2004)** – Geochemical evidence of seismogenic-induced anomalies in the dissolved gases of thermal waters: A case study of Umbria (Central Apennines, Italy) both during and after the 1997-1998 seismic swarm – G-cubed, vol. 5, number 11.
- **Italiano F., Caracausi A., Favara R., Innocenzi P. and Martinelli G. (2005)** - Geochemical monitoring of cold waters during seismicity: implications for earthquake-induced modification in shallow aquifers. Terr. Atmos. Ocean. Sci. 16 (4), 709–729.
- **Italiano F., Martinelli G., Bonfanti P., and Caracausi A. (2009)** – Long-term (1997-2007) geochemical monitoring of gases from the Umbria-Marche region – Tectonophysics, 476, pp.282-296
- **Kennedy, B.M., Kharaka, Y.K., Evans, W.C., Ellwood, A., DePaolo, D.J., Thordsen, J., Ambats, G., Mariner, R.H. (1997)** - Mantle fluids in the San Andreas fault system, California. Science 278, 1278–1281.
- **Kennedy, B.M. and Van Soest, M. (2007)** - Flow of mantle fluids through the ductile lower crust: helium isotope trends. Science 318, 1433–1436.
- **Kämpf H., Bräuer K., Schumann J., Hahne K. & Strauch G. (2013) –** CO_2 discharged in a active, non-volcanic continental rift area (Czech Republic): Characterization (Delta 13C, 3He/4He) and quantification of diffuse and vent CO2 emissions – Chemical Geology, 339, 71-83.
- **Lavecchia, G., Brozzetti, F., Barchi, R.M., Keller, J., Menichetti, M., 1994.** Seismotectonic zoning in east-central Italy deduced from the analysis of the Neogene to present deformations and related stress fields. Bull. Geol. Soc. Am. 106, 1107–1120.

- **Lee J. Y., Marti K., Severinghaus J. P., Kawamura K., Yoo H. S., Lee J. B. and Kim J. S. (2006)** – A redetermination of the isotopic abundances of atmospheric Ar – Geochimica et Cosmochimica Acta, 70, pp. 4507-4512
- **Martelli, M., Nuccio, P. M., Stuart, F.M., Burgess, R., Ellam, R. M., Italiano, F., (2004)**. Helium–strontium isotope constraints on mantle evolution beneath the Roman Comagmatic Province, Italy. Earth Planet. Sci. Lett. 224, 295–308.
- **Mastrolillo L., Baldoni T., Banzato F., Boscherini A., Cascone D., Checcucci, Petitta M., & Boni C. (2009)** – Quantitative hydrogeological analysis of the carbonate domani if the Umbria Region (Central Italy) – Italian Journal of Engineering Geology and Environment 1, pp.137-155
- **Miller, S. A., C. Collettini, L. Chiaraluce, M. Cocco, M. Barchi, and B. J. P. Kaus (2004)** - Aftershocks driven by a high pressure CO_2 source at depth, Nature, 427, 724–727.
- **Minissale A., Magro O., Vaselli O., Verrucchi C. and Perticone I. (1997)** – Geochemistry of water and gas discharged from the Mt. Amiata silicic complex and surrounding areas (central Italy) – Journal of Volcanology and Geothermal Research, 79, pp. 223-251
- **Minissale A. (2004)** - Origin, transport and discharge of CO_2 in Central Italy. Earth-Sci. Rev. 66, 89–141
- **Mirabella F., Brozzetti F., Lupattelli A. and Barchi M. R. (2011)**. Tectonic evolution of a low angle extensional fault system from restored cross sections in the northern Apennines (Italy), Tectonics, 30, TC6002.
- **Ozima M. & Podosek F.A. (2002)** – Noble Gas Geochemistry. Cambridge University Press, Cambridge, UK

- **Petitta M., Mastrolillo L., Preziosi E., Banzato F., Barberio M. D., Billi A., Cambi C., De Luca G., Di Carlo G., Di Curzio D., Di Salvo C., Nanni T., Palpacelli S., Rusi S., Saroli M., Tallini M., Tazioli A., Valigi D., Vivalda., & Doglioni C. (2018)** – Water-table and discharge changes associated with the 2016-2017 seismic sequence in central Italy: hydrogeological data and a conceptual model for fractured carbonate aquifers – Hydrogeology Journal, 26, pp.1009-1026.
- **Pialli, G., M. Barchi and G. Minelli (1998)**. Results of the CROP03 deep seismic reflection profile, Memorie della Società Geologica Italiana, 52, 657 pp.
- **Ponziani F., De Franco R., Minelli G., Biella G., Federico C. and Pialli G. (1995)** – Crustal shortening and duplication of the Moho in the Northern Apennines: a view from seismic refraction data – Tectonophysics 252, 391-418
- **Prinzhofer A. (2013)** - Noble Gas in Oil and Gas Accumulations – In: *The Noble Gases as Geochemical Tracers*, Advances in Isotope Geochemistry, P. Burnard (ed.), Springer-Verlag Berlin Heidelberg
- **Pucci S., De Martini P. M., Pantosti D. and Valensise G. (2003)** – Geomorphology of the Gubbio Basin (Central Italy): understanding the active tectonics and earthquake potential – Annals of Geohpysics, vol. 46, No. 5, pp. 837-864
- **Quattrocchi F., Pik R., Pizzino L., Guerra M., Scarlato P., Angelone M., Barbieri M., Conti A., Marty B., Sacchi E., Zuppi G. M. and Lombardi S. (2000)** – Geochemical changes at the Bagni di Triponzo thermal springs during the Umbria-Marche 1997-1998 seismic sequence – Journal of Seismology 4, pp. 576-587
- **Sibson, R. H. (2000)** - Fluid involvement in normal faulting - Journal of Geodynamics, 29, 469- 499.
- **Tamburello G., Pondrelli S., Chiodini G. and** – Global-scale control of extensional tectonics on CO_2 earth degassing - Nature Comm. 9

- **Vaselli O., Tassi F., Tedesco D., Poreda J. R. and Caprai A. (2011)** – Submarine and inland gas discharged from the Campi Flegrei (southern Italy) and the Pozzuoli Bay: geochemical clues for a common hydrothermal-magmatic source – Procedia Earth and Planetary Science, 4, pp. 57-73
- **Weiss R. F. (1970) -** The solubility of nitrogen, oxygen and argon in water and seawater, *Deep Sea Res*., *17*, pp. 721–735.
- **Weiss R. F. (1971) -** Solubility of helium and neon in water and seawater, *J*. *Chem*. *Eng*. *Data*, *16*, pp. 235–241.
- **Wen T., Castro M.C., Nicot J., Hall C.M., Pinti D., Mickler P., Darvari R. and Larson T. (2017)** – Characterizing the noble gas isotopic composition of the Barnett Shale and Strawn Group and constraining the source of stray gas in the Trinity Aquifer, North-Central Texas – Environmental Science & Technology 51, pp. 6533-6541.

CHAPTER IV

Geochemistry of noble gas and radiogenic isotopes of ultramafic mantle xenoliths from La Grille volcano (Grand Comore Island, Indian Ocean)

1. INTRODUCTION

The western Indian Ocean has recently received significant interest in the scientific literature as far as concern late Cenozoic to present Comorean magmatism which have provided petrological and geochemical constraints to be placed on the genesis and magmatic evolution of the Comorean archipelago and Le Reunion volcanism (Class et al. 2005 and references therein; Vlastelic and Pietruszka 2016). In fact, here are located the two most active volcanoes in the southwest Indian Ocean: Piton de la Fournaise at La Réunion Island and Karthala on Grande Comore in the Comorian archipelago. Karthala is a magnificent volcano and, although its eruptions are less frequent than those of Piton de la Fournaise, it poses a serious threat to the population living close to its shores and around its flanks, as demonstrated by recent eruptions. Karthala, the youngest of the Comorian volcanoes, rises from the floor of the Mozambique Channel. Grande Comore rises as a volcanic doublet comprising the coalescing shields of La Grille and Karthala. There are, however, no historic eruptions from La Grille, whereas Karthala has erupted at least twenty times since records began in 1857 and three of them occurred since 2000 producing damages to the villages at Gran Comore and led to the evacuation of people.

It is a matter of debate whether the origin of the Comoros Islands could have been resulted from either lithospheric migration above a relatively stationary plume-related hot spot (Emerick and Duncan 1982; Class et al. 1996), or passive response of lithospheric break-up due to activation of a very slowly spreading ridge axis dissected by transform zones (Nougier et al. 1986; Courtillot et al. 2003).

Here we report the first ever analyses of light noble gases (He, Ne and Ar) in fluid inclusions coupled to the radiogenic isotopes (Sr, Nd and Pb) of mineral separates from peridotite xenoliths collected at La Grille volcano. Previous studies (i.e., Class and Goldstein 1997; Class et al. 2005) report the He isotopes measurements in fluid inclusions of La Grille xenoliths minerals together with Sr-Nd-Pb isotopic data of whole-rock samples. Moreover, investigation of Grand Comore rock lithotypes has been so far mainly focused on bulk samples and mineral separates from lavas, although petrological and geochemical data from clinopyroxenes and glasses of ultramafic mantle nodules from La Grille are reported in the literature (Coltorti et al. 1999).

The investigation of peridotite mantle xenoliths enclosed in alkaline lavas can help to shed light on the mechanisms that can modify mantle materials. In particular, mafic phenocrysts in mantle xenoliths have attained important consideration in terms of their

isotope compositions as they can provide useful insights on the evolution of the mantle sources and constrain the effects of hypothetical metasomatizing agents.

Several investigation have demonstrated that noble gases (He, Ne, and Ar) isotope systematics in fluid inclusions represent an useful tool for understanding the main the geochemical characteristics of the mantle (Gautheron and Moreira 2002; Gautheron et al. 2005; Martelli et al. 2011, 2014; Correale et al. 2012, 2016; Day et al. 2015).

Isotope geochemistry of fluid inclusions in ultramafic mantle xenoliths from La Grille has been performed with the goal to investigate the mantle heterogeneity and/or to trace additional chemical processes acting at modifying the pristine signature of the mantle source. Furthermore, these results can also contribute to the geochemical background of the Gran Comore volcanic system (La Grille-Karthala) being useful for future geochemical monitoring of an active, dangerous and very poorly-explored volcanic system. Indeed, it is well recognized in literature (more details in Chapter I) that the noble gases systematics, are powerful tools for the geochemical monitoring of active volcanic systems (e.g., Mt Etna, Italy; Mt Ontake and Mt Hakone, Japan; Kilauea, Hawaii). However it is fundamental to characterize the composition of the source to recognize and interpret geochemical variation due to the degassing processes occurring during the uprise of magmas in the volcanic plumbing systems.

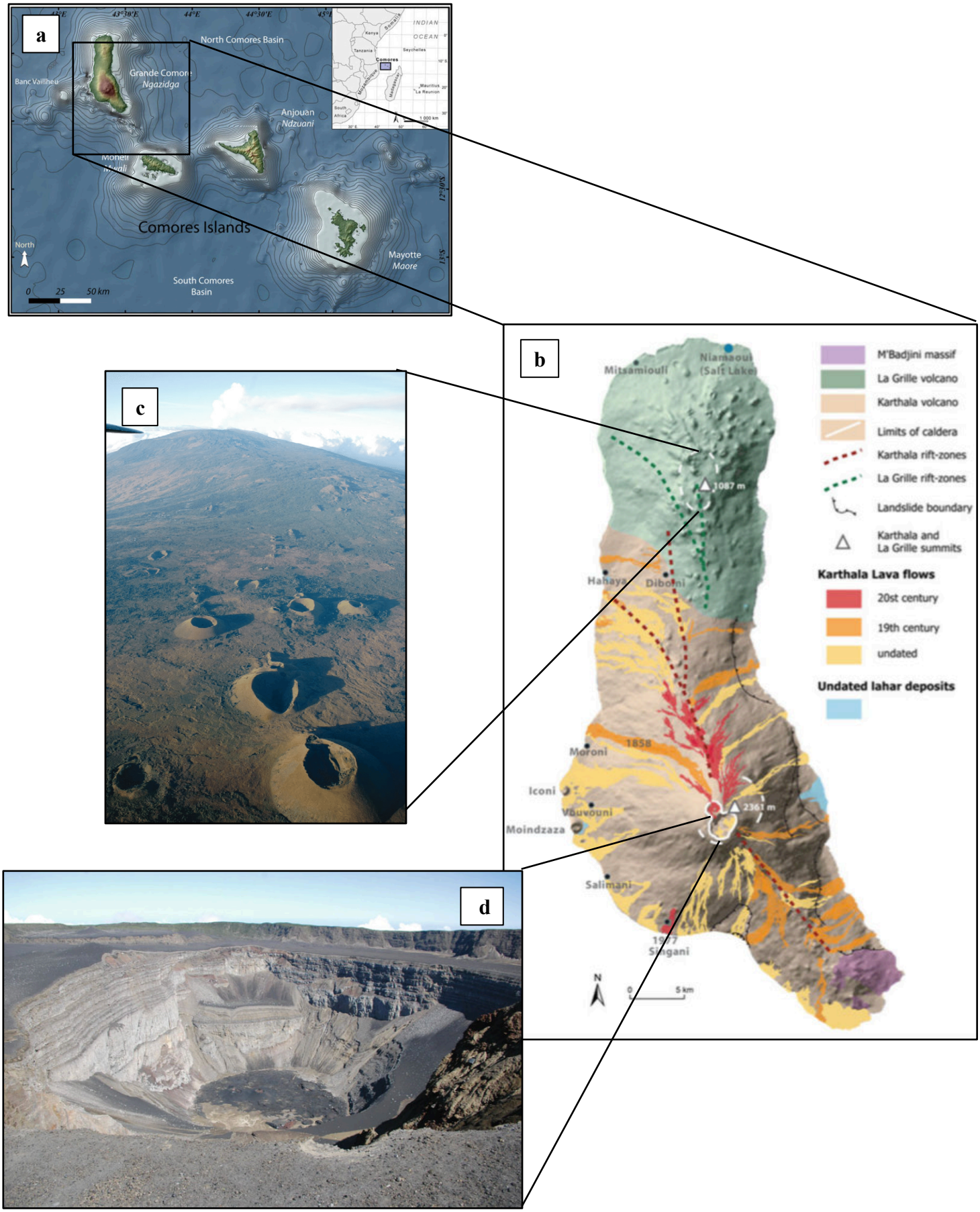

Fig. 1 – a) The Comoros Archipelago; bathymetry from GEBCO (General Bathymetric Chart of the Oceans, http://www.gebco.net/; topography from SRTM (Shuttle Radar Topography Mission, http://www2.jpl.nasa.gov/srtm/); isobaths every 200 m (Bachelery et al. 2016); **b)** Volcanological map of Grand Comore Island (Bachelery and Coudray 1993; Morin 2012); **c)** Monogenic scoriaceous cones at the summit of La Grille volcano (Photo J. Morin); **d)** The Choungou-Chahale crater of Karthala volcano (Photo J. Morin)

2. THE STUDY AREA

2.1 Geological setting

The Comoros Archipelago is an age-progressive volcanic chain located in the northern part of the Mozambique Channel in the Western Indian Ocean between Madagascar and East Africa (**Fig. 1a**). It is composed of four islands: from west to east these are Grand Comore, Moheli, Anjouan and Mayotte followed by two, poorly known submarine volcanic banks (Geiser and Leven; Daniel et al. 1972). Geochronological data indicate that magmatic activity in Comoros archipelago was diachronous (**Fig. 2**). It supposedly started in Mayotte around 11 Ma ago, then in Mohéli and Anjouan 3.9 and 5 Ma ago, respectively, and finally in Grande Comore approximately 0.13 Ma ago (Emerick and Duncan 1982; Nougier et al. 1986; Debeuf 2004). No geochronological and geochemical data are currently available for the submarine sector of each volcanic island where oldest rocks may occur. This magmatism is coeval with other volcanic provinces around the Mozambique Channel, namely the East African Rift System and the central-northern Madagascar, whose magmatic periods are dated back since Upper Oligocene.

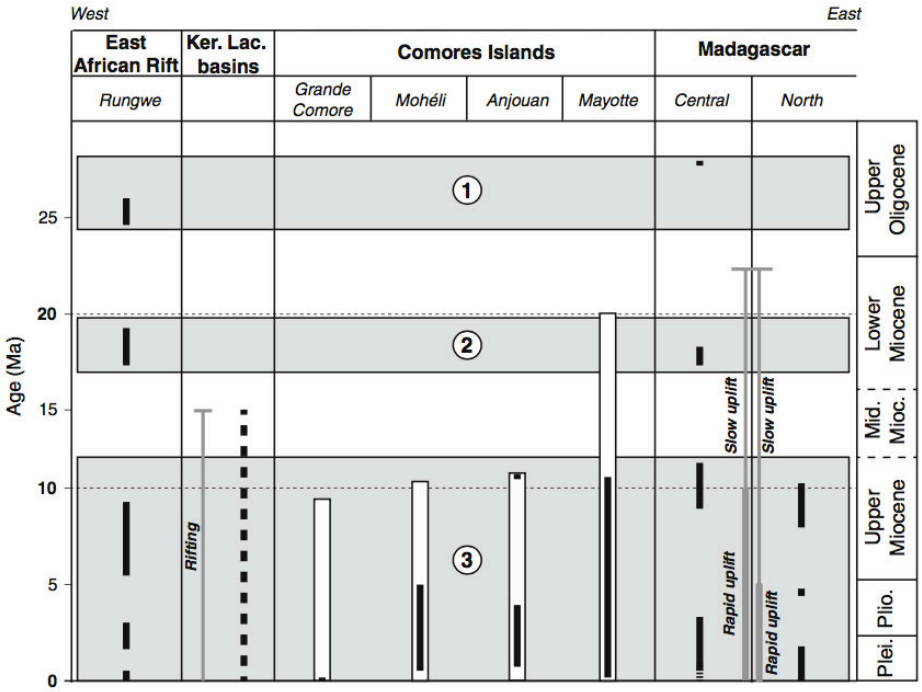

Fig. 2 – Age of the volcanism (*black bars*) in the Comoros archipelago and the sorrounding volcanic provinces. *White bars* account for the estimated volcanic activity for Mayotte, Moheli, Anjouan and Grand Comore based on calculations of the magma production rates. 1, 2 and 3 indicate the different magmatic periods developed at regional scale. Image taken from Michon 2016.

It is still poorly understood whether the volcanic activity in the Comoros Archipelago developed on either a continental or oceanic crust. The occurrence of xenoliths of sandstone and other continental rocks (e.g., granite and quartzarenite fragments; Lacroix 1922; Flower and Strong 1969) in lavas from all of four Comoros islands was used as evidence of a continental nature of the underlying crust. However, on the basis of magnetic data from Rabinowitz et al. 1983 and Coffin and Rabinowitz 1987, a Late Jurassic to Early Cretaceous oceanic crust (165-130 Ma), resulting from the N-S opening of the Somali Basin, is believed to lie beneath the Comoros Archipelago. The sedimentary enclaves could then represent crustal fragments resulting from erosion of continental units cropping out on the eastern or western coasts of Africa and Madagascar, respectively. Notwithstanding the nature of the crust, the Comoros Archipelago can be considered one of the most seismically active sector of the western Indian Ocean, whose volcanic edifices occur in a regional E-W seismic zone that link the northern tip of Madagascar in the east to the African coast in the west (Heidbach et al. 2008; Rindraharisaona et al. 2013; Franke et al. 2015).

Grand Comore Island consists of two shield volcanoes, La Grille (1087m) located in the north and Karthala (2361m) in the south (**Fig. 1b**). La Grille volcano is characterized by eroded and weathered lava flows associated with a series of monogenic cinder cones (**Fig. 1c**) mainly located in the summit area and aligned along structural fissures (Bachelery and Coudray 1990), while Karthala is the second most active volcano of the Indian Ocean (**Fig. 1d**; after Piton de la Fournaise at the Reunion Island) with last volcanic activity recorded in January 2007 (web source: *https://volcano.si.edu; Global Volcanism Program, Smithsonian Institution*). Alkali basalts including oceanites (olivine-rich basalts) and ankaramites (pyroxene-rich basalts) are the most common lithotypes at Karthala volcano, while La Grille products are markedly more silica-undersaturated than those of Karthala, ranging from basanites to nephelinites (Strong 1972; Späth et al. 1996). Contrary to those of Karthala, lavas from La Grille often enclose xenolithic mantle nodules of ultramafic rocks resulting from phreatomagmatic maar-like eruptions (Bachelery and Coudray 1993).

3. SAMPLING AND ANALYTICAL METHODS

Ultramafic mantle-derived xenoliths were collected on the north-eastern coast of Grand Comore during 2017-2018 field campaigns with the aim of characterizing and constraining the mantle source beneath La Grille volcano. Olivine, clinopyroxene and orthopyroxene (hereafter Ol, Cpx and Opx) crystals of 1-mm size-fraction were handpicked from crushed ultramafic xenoliths with binocular microscope for noble gas (He, Ne, and Ar) and radiogenic isotopes (Sr, Nd, and Pb) measurements.

The selected minerals were cleaned with acetone to remove all the impurities and were loaded into a stainless-steel crusher capable of holding up to six samples simultaneously for noble gas analysis. Fluid inclusions were released by in-vacuum single-step crushing at about 200 bar. The released gases from the fluid inclusions were then cleaned in an ultra-high-vacuum (10^{-9}-10^{-10} mbar) purification line and all the unwanted species in the gas mixture were removed, so at the end of the purification the only noble gases (He, Ne and Ar) are in the line and ready for the measurements. Ar is trapped in a cold finger by using the nitrogen liquid and He and Ne are trapped separately by using a cryogenic pump. Hence, Ar is released from the trap removing the liquid nitrogen and successively it has been measured for its isotopes by a multi-collector mass spectrometer *Argus GVI (Thermofisher).* Hence, He isotopes (^{3}He and ^{4}He), Ne isotopes (^{20}Ne, ^{21}Ne and ^{22}Ne) were released in two times and were measured separately using two different split-flight-tube mass spectrometers (*GVI-Helix STF Thermo Scientific*). The concentration and isotope composition of He, Ne, and Ar in Ol, Cpx and Opx fluid inclusions were determined at the laboratories of INGV-Palermo (Italy). Helium isotope ratios are expressed in R/Ra units, where Ra is the ^{3}He/^{4}He ratio in air (1.4×10^{-6}). The values of Ne-isotope ratios are corrected for isobaric interferences at m/z values of 20 ($^{40}Ar^{2+}$) and 22 ($^{44}CO^{2+}$). Corrections are performed by measuring ^{20}Ne, ^{21}Ne, ^{22}Ne, ^{40}Ar, and $^{44}CO_2$ during the same analysis, and considering the previously determined $^{40}Ar^{2+}$ /$^{40}Ar^{+}$ and ^{44} CO^{2+}/CO^{+} ratios on the same Helix SFT that run FI samples. For each analytical session we analyzed at least one standard of each of He, Ne, and Ar that had previously been purified from air and stored in tanks. The analytical uncertainty (1σ) values for the ^{3}He/^{4} He, ^{20}Ne/^{22}Ne, ^{21}Ne/^{22}Ne, ^{40}Ar/^{36}Ar were <0.94%, <0.07%, <0.3%, <0.05%, respectively. Typical blanks for He, Ne, and Ar were $<10^{-15}$, $<10^{-16}$,

and $<10^{-14}$ mol, respectively. Further details about the sample preparation and analytical procedures are given in Martelli et al. 2014 and Rizzo et al. 2015.

Radiogenic isotopes of Sr, Nd and Pb were determined only on clinopyroxene and orthopyroxene mineral phases as olivines contain abundances of these elements below detection limits. Two whole-rock samples have been also analyses to seek for potential differences with monomineralic fractions. The Cpx and Opx mineral separates were powdered in an agate mortar and pestle (or agate mill). After each pounding, the agate mill was scrubbed with a silicic sand (sable de Fontainebleau) to remove any residues, and then washed with distilled water and ethanol. Mineral and whole rock powders were dissolved for 72h on a hot plate at 120°C in a mixture of 1.5 ml HF and 1.5 ml HNO_3. After evaporation, 3 ml of 6N HCL were added to the mineral residue at 120°C for 72h before evaporation to dryness, then digested samples were re-dissolved in 1 ml of HBr. Chemical separation was carried out on Teflon columns with exchange resin using a HBr-HCL-HNO_3 exchange procedure. Sr, Nd and Pb isotope analyses of Cpx and Opx separates were performed at the Centre de Recherches Pétrographiques et Géochimiques (Nancy, France). Sr isotope ratios were measured with thermal-ionization mass spectrometer (TIMS) *Thermo Scientific Triton*, whereas Pb and Nd isotope ratios were measured with multi-collector inductively coupled plasma mass spectrometer (MC-ICP-MS) *Thermo Scientific Neptune Plus*.

Sr and Nd isotope ratios were corrected for mass fractionation by normalizing to $^{86}Sr/^{88}Sr = 0{\cdot}11938$ and $^{146}Nd/^{144}Nd = 0{\cdot}74049$. Over the course of this study, the NBS 987 Sr standard gave a mean value of $^{87}Sr/^{86}Sr = 0{\cdot}710256 \pm 9$ ($2\sigma_m$, $n = 5$) and the La Jolla Nd standard gave a mean value of $^{143}Nd/^{144}Nd = 0{\cdot}512097 \pm 6$ ($2\sigma_m$, $n = 10$). NIST-981 Pb standard yielded average values of $^{206}Pb/^{204}Pb = 16.93 \pm 0.0054$, $^{207}Pb/^{204}Pb = 15.48 \pm 0.0074$, $^{208}Pb/^{204}Pb = 36.66 \pm 0.0083$.

4. CLASSIFICATION AND PETROGRAPHY OF THE LA GRILLE MANTLE XENOLITHS

According to the classification of Coltorti et al. 1999, La Grille xenoliths can be classified into three different groups on the basis on petrography, modal compositions and textures: one group of lherzolites (Lh Group) and two groups of weherlites (Wh1 and Wh2 Groups). The only occurring aluminous phase is spinel. Any hydrous mineral (amphibole or phlogopite) was found in the La Grille xenoliths.

Consistent with the definitions of Mercier and Nicholas (1975), two textures have been petrographically observed: protogranular and porphyroclastic, with some xenolithic samples showing transitional features between the two. Xenoliths belonging to the first textural group show olivine and orthopyroxene up to 2 mm in size with curvilinear grain boundaries, and small clinopyroxene (up to 0.6 mm) and spinel (up to 0.4 mm) crystals occurring interstitially or included within the orthopyroxene. Xenoliths belonging to the second textural group have large porphyroclasts of olivine and orthopyroxene with small neoblasts of olivine and clinopyroxene. Superimposed on both the protogranular and porphyroclastic textures, three pyrometamorphic textures have been recognized on the basis of size and relative proportions of the secondary minerals and glass (Coltorti et al. 1999):

- *Type A* shows primary orthopyroxenes with clear evidence of destabilization and reaction processes, and irregular, fine-grained (<0·10–0·15 mm) rims on clinopyroxene, olivine, orthopyroxene, spinel and glass. Tiny crystals of olivine and clinopyroxene are forming at the expense of a large orthopyroxene. Glass-forming reactions may have occurred at the boundaries of, or within, the orthopyroxene.
- *Type B* contains elongate, glassy patches with a secondary assemblage of clinopyroxene, olivine, and spinel. The clinopyroxene and olivine grains are larger (0.1–0.6 mm) than in Types A and C, and spinels are typically globular.
- *Type C* displays secondary olivines, irregularly shaped spinels within glass, and tiny clinopyroxene aggregates (0·1–0·3 mm), aligned and oriented in optical continuity, suggesting growth at the expense of a primary phases as clinopyroxene.

In Lh Group, large primary orthopyroxenes (0·5–1·0 mm) are homogeneous and contain exsolution lamellae. All clinopyroxenes are presumed to be secondary, as no petrographic evidence for primary clinopyroxene was found. Most of the spinels are

secondary phases associated with clinopyroxene and olivine in the recrystallized domains. In Wh1 Group, either veins or patches of clinopyroxene are always associated with olivine, glass and secondary spinel. In Wh2 Group, both primary and secondary olivines are present. Clinopyroxene is present only in the recrystallized areas and glassy patches.

5. RESULTS

Noble gas analyses are reported in **Table 1**. The $^{3}He/^{4}He$ ratio not corrected for air contamination (R/Ra) is 5.67-7.34 in Ol, 6.46-7.25 in Cpx, and 5.11-7.01 in Opx (**Fig 3a**). The $^{4}He/^{20}Ne$ ratios are in the range 3-180 in Ol, 77-1855 in Cpx, and 9-601 in Opx (**Fig 3a**). The $^{40}Ar/^{36}Ar$ ratio is 310-1501 in Ol, 501-3161 in Cpx, and 568-7747 in Opx (**Fig 3b**). The $^{20}Ne/^{22}Ne$ and $^{21}Ne/^{22}Ne$ ratios are respectively 9.81-9.94 and 0.0291-0.0314 in Ol, 9.80-10.38 and 0.0292-0.0345 in Cpx, and 9.89-10.36 and 0.0290-0.0347 in Opx (**Fig. 3b-c**). All the measured $^{4}He/^{20}Ne$ ratios in the La Grille samples are higher, at least one order of magnitude, than the same ratio in atmosphere (0.318; Ozima & Podosek, 2002), so these samples suffer of low-He air contamination and the correction of the He isotopes are low and often negligible (**Table1; Fig. 3a**). The $^{3}He/^{4}He$ ratio corrected for air contamination (expressed as Rc/Ra values) is 6.30-7.36 in Ol, 6.48-7.25 in Cpx, and 5.27-7.02 in Opx (**Table 1**). Helium and neon concentrations (expressed as 10^{-9} $cm^{3}STP/g$) are 8.15-325.46 and 1.20-6.07, respectively, in Ol, 7.12-860.16 and 0.09-7.66 in Cpx, and 7.01-963.20 and 0.31-15.28 in Opx (**Table 1**).

Sr, Nd and Pb isotope ratios for Cpx and Opx phenocrysts are given in **Table 2**. The $^{87}Sr/^{86}Sr$ ratios vary between 0.703225 and 0.703480, and 0.703239 and 0.704260 in Cpx and Opx, respectively, while $^{143}Nd/^{144}Nd$ ratios range between 0.51281 and 0.51285, and 0.51279 and 0.51286 in Cpx and Opx, respectively (**Fig. 4a-b-c**). The $^{206}Pb/^{204}Pb$, $^{207}Pb/^{204}Pb$ and $^{208}Pb/^{204}Pb$ ratios are 18.63-19 and 18.24-19.45, 15.62-15.66 and 15.63-16.31, and 38.60-38.93 and 38.47-40.21 in Cpx and Opx, respectively (**Fig. 4a-b-c**). The two analysed whole-rock samples NDR17-9-WR1 and NDR17-9-WR2 show nearly indistinguishable $^{87}Sr/^{86}Sr$, $^{143}Nd/^{144}Nd$ and $^{206}Pb/^{204}Pb$, $^{207}Pb/^{204}Pb$ and $^{208}Pb/^{204}Pb$ ratios (**Table 2**).

Table 1. He, Ne and Ar isotope ratios and abundance of mineral separates in La Grille xenoliths

Sample	Phase	Weight (mg)	$^{3}He/^{4}He$ (R/Ra)	$^{3}He/^{4}He$ (Rc/Ra)	[He] $10^{-9}cm^{3}STP/g$	[Ne] $10^{-9}cm^{3}STP/g$	$^{40}Ar/^{36}Ar$	$^{20}Ne/^{22}Ne$	$^{21}Ne/^{22}Ne$
NDR17-1	Ol	436	6.94	6.96	180.38	1.46	551.40	9.82	0.0297
NDR17-2	Ol	434	6.76	6.88	77.46	4.64	701.18	9.85	0.0294
	Cpx		7.06	7.06	360.64	0.43	1114.17		
	Opx		7.01	7.01	227.19	0.57	1703.97	9.93	0.0302
NDR17-3	Ol	636	6.57	6.60	168.15	2.57	984.07	9.84	0.0296
	Cpx		6.88	6.89	242.12	0.43	1157.50		
	Opx		7.01	7.02	98.23	0.56	1627.45	9.89	0.0299
NDR17-5	Ol		7.34	7.36	325.46	2.60	1501.54	9.82	0.0291
	Cpx		7.03	7.06	624.96	7.66	501.39	9.80	0.0292
	Opx		6.68	6.72	712.32	15.28			
NDR17-6	Ol	315	6.58	6.63	64.59	2.02	1416.17	9.90	0.0304
	Cpx		6.55	6.56	31.02	0.14	2562.41		
	Opx		6.91	6.92	963.20	1.60	7747.47	10.36	0.0347
NDR17-7	Ol	417	6.26	6.48	40.58	4.85	310.30		
	Cpx		6.99	7.00	68.25	0.27	1062.46	9.93	0.0312
	Opx		6.82	6.83	688.31	2.51	1860.89	9.96	0.0299
NDR17-8	Ol		5.67	6.3	17.11	6.07	392.19	9.81	0.0292
NDR17-9	Ol	401	6.96	7.01	130.51	3.22	585.85	9.84	0.0296
	Cpx		6.69	6.70	108.53	0.39	1608.11	9.92	0.0295
	Opx		6.90	6.91	507.30	1.09	2378.55	9.94	0.0312
NDR17-11	Ol	428	6.63	6.77	73.77	5.15	482.01	9.84	0.0294
	Cpx		6.63	6.65	57.98	0.53	822.29		
	Opx		5.11	5.27	23.41	2.47	568.41	9.96	0.0290
NDR17-12	Ol		6.34	6.41	33.66	1.20	341.27	9.84	0.0295
	Cpx		7.25	7.25	860.16	0.46	3161.71	10.38	0.0345
NDR17-13	Ol	424	7.01	7.06	128.36	3.57	1459.50	9.94	0.0314
	Opx		6.57	6.60	185.66	2.47	625.57	9.95	0.0299
NDR17-14	Ol	347	6.84	6.88	165.95	3.81	852.92	9.89	0.0294
NDR17-16	Ol	321	6.62	6.98	8.15	1.48	400.86	9.83	0.0292
	Cpx		6.46	6.48	7.12	0.09	1740.85	10.21	0.0314
	Opx		6.24	6.32	7.01	0.31	1550.37	9.96	0.0293

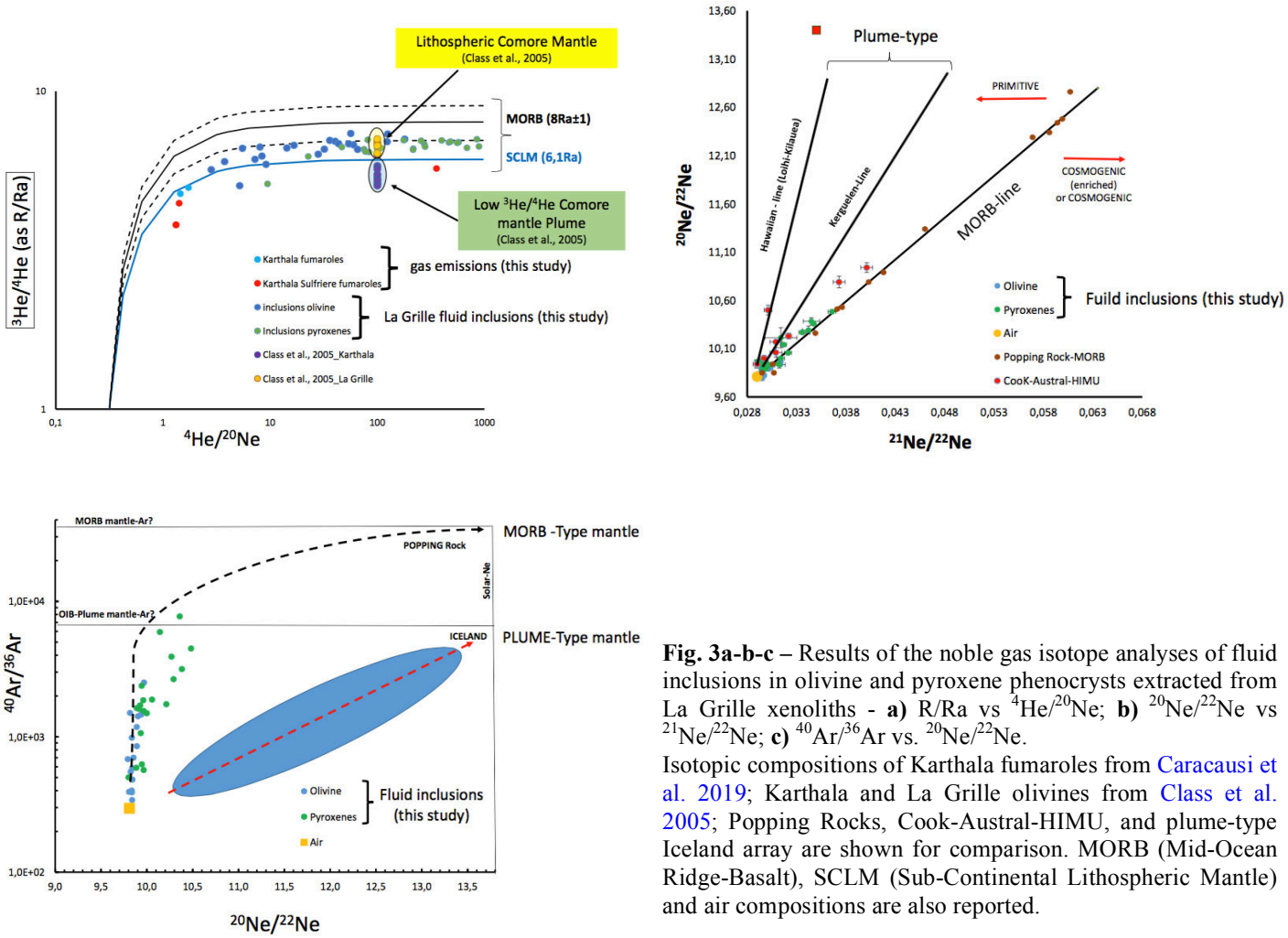

Fig. 3a-b-c – Results of the noble gas isotope analyses of fluid inclusions in olivine and pyroxene phenocrysts extracted from La Grille xenoliths - **a)** R/Ra vs $^{4}He/^{20}Ne$; **b)** $^{20}Ne/^{22}Ne$ vs $^{21}Ne/^{22}Ne$; **c)** $^{40}Ar/^{36}Ar$ vs. $^{20}Ne/^{22}Ne$.
Isotopic compositions of Karthala fumaroles from Caracausi et al. 2019; Karthala and La Grille olivines from Class et al. 2005; Popping Rocks, Cook-Austral-HIMU, and plume-type Iceland array are shown for comparison. MORB (Mid-Ocean Ridge-Basalt), SCLM (Sub-Continental Lithospheric Mantle) and air compositions are also reported.

The He-Ne-Ar isotope systematics of fluid inclusions in La Grille ultramafic nodules clearly indicates a mantle-type reservoir. The He isotopic signature of fluid inclusions in Ol, Cpx and Opx (up to 7.3Ra) is in good agreement with that from literature (Class et al. 2005; yellow-filled circles in **Fig. 3a**) and plot in a range that overlap the SCLM 6.1± 0.9 (Sub Continental Lithospheric Mantle; Gautheron and Moreira 2002) and the MORB mantle signatures (8±1Ra; Graham, 2002). Moreover, the $^{3}He/^{4}He$ ratios of La Grille samples (**Fig. 3a**) are systematically higher than those measured in gases from crater fumaroles (Istituto Nazionale di Geofisica e Vulcanologia and Institute de Physique du Globe de Paris dataset; Caracausi et al. 2019), consistent with the $^{3}He/^{4}He$ ratios in fluid inclusions from minerals of the Karthala volcano lavas (Class et al., 2005). The Ne and Ar isotopes in the volatiles trapped in the fluid inclusions of the La Grille xenoliths are well-solved respect to the atmospheric composition (**Fig. 3b and c**). In fact, the $^{21}Ne/^{22}Ne$ and $^{20}Ne/^{22}Ne$ ratios are higher than 9.86 and 0.029 (Graham, 2002) and the $^{40}Ar/^{36}Ar$ and $^{38}Ar/^{36}Ar$ ratios are higher than 298.56 (± 0.31) and

0.1885 (± 0.0003) respectively (Lee et al. 2006) (**Table 1 and Fig. 3b and c**). Hence, the Ne and Ar isotopes furnish new elements to investigate the composition of the mantle feeding the magmatic activity at Gran Comore. In general, the neon isotopes measurements in mantle-derived fluids have a relative large composition. However, MORBs (Mid Oceanic Ridge Basalts) and OIBs (Oceanic Island Basalts) are systematically different in their Ne isotope composition (e.g., Sarda et al., 1988; Moreira and Allegre, 1998; Graham, 2002; Mukhopadhyay, 2012). In comparison to MORBs, some OIB show a much steeper correlation in the Ne three isotopes diagram (**Fig. 3b**), where samples from Hawaii, Le Reunion and Iceland show the steeper correlation (**Fig. 3b).** These trends reveal that the OIB mantle source, at least for these volcanic systems, have less nucleogenic Ne, hence lower $^{21}Ne/^{22}Ne$ than for the MORB mantle sources. These evidences coupled to 1) the lower He isotope ratios in the MORB–derived fluids than in the OIB-derived fluids ($^{3}He/^{4}He$ up to ~ 50Ra) and 2) the trace element-depletion of the MORB mantle sources respect to the OIB mantle sources indicate that the OIB mantle is less degassed than the upper MORB mantle. These evidences support that OIB-volcanism is fed by deep mantle plume (e.g., Graham, 2002; Mukhopadhyay, 2012; Parai and Mukhopadhyay, 2015). The $^{20}Ne/^{22}Ne$ and $^{21}Ne/^{22}Ne$ ratios in the La Grille fluid inclusions are along the MORB line, being indistinguishable for the same ratios in MORB-derived volatiles (**Fig. 3b**) and it indicates that the mantle Ne source at La Grille is the Typical MORB-type.

^{40}Ar is generated by radioactive decay of ^{40}K and it is commonly assumed that all ^{36}Ar in MORB and OIB samples could be derived from air contamination (Graham, 2002). Hence on the basis of the Ar isotopes, it possible to assess the amount of mantle derived Ar present in a sample. Furthermore, the $^{40}Ar/^{36}Ar$ ratios is also variable due to time integrated variations in $K/^{36}Ar$. MORBs show $^{40}Ar/^{36}Ar$ ratios that are up to 40.000. In contrast, the highest $^{40}Ar/^{36}Ar$ ratios at OIBs are in xenolithes from Samoa and the values are from 8000 to 21.500 (Farley et al., 1994; Trieloff et al., 2000). Ne and Ar isotope systematic are key-tools that highlight the difference between the OIB and MORB mantle sources, with the OIBs sources being less degassed. The $^{40}Ar/^{36}Ar$ ratios in the La Grille samples coupled to the $^{20}Ne/^{22}Ne$ in the same samples are always along the MORBs lines. Hence the He-Ne-Ar systematic in the fluid inclusion of the La Grille xenoliths highlight that the mantle in the region has MORB affinities. It is worthy-noting that the $^{40}Ar/^{36}Ar$ and $^{20}Ne/^{22}Ne$ in the pyroxenes from La Grille are generally higher than the same ratios in the olivine from the same rocks. So, the petrology of

these products can help to understand these differences to provide new insight about the composition of the mantle at regional scale and the processes that can modify it.

Table 2. Sr, Nd, Pb isotope ratios of Cpx, Opx and whole rock from La Grille xenoliths

Sample	Phase	Weight (mg)	$^{87}Sr/^{86}Sr$	$^{143}Nd/^{144}Nd$	$^{206}Pb/^{204}Pb$	$^{207}Pb/^{204}Pb$	$^{208}Pb/^{204}Pb$
NDR17-2	Opx	106	0.703457	0.512860	18.70272	15.81844	38.87053
NDR17-3	Cpx	105	0.703366	b.d.l.	18.96369	15.63418	38.84940
	Opx	112	0.703505	0.512860	19.45659	15.71536	38.95679
NDR17-6	Cpx	113	0.703225	0.512865	18.88801	15.66725	38.60478
NDR17-7	Cpx	119	0.703415	0.51283	18.63343	15.63393	38.72688
	Opx	107	0.703495	0.51284	18.24854	15.63232	38.47741
NDR17-9	Cpx	118	0.703449	0.51280	18.97451	15.63035	38.93015
	Opx	101	0.703551	0.51279	18.52713	15.69310	38.59701
NDR17-11	Cpx	109	0.703444	0.51281	18.87393	15.63196	38.81141
	Opx	103	0.704260	0.51284	18.74541	15.63733	38.67977
NDR17-13	Opx	103	0.704096	0.51284	19.38905	16.31723	40.21247
NDR17-14	Cpx	106	0.703480	0.51285	19.00550	15.62991	38.93248
	Opx	107	0.703239	0.51286	18.77215	15.63393	38.73309
NDR17-9-WR1	Whole-rock	113	0.703426	0.51284	18.93276	15.61580	38.87953
NDR17-9-WR1	Whole-rock	101	0.703452	0.51284	18.93285	15.61465	38.87726

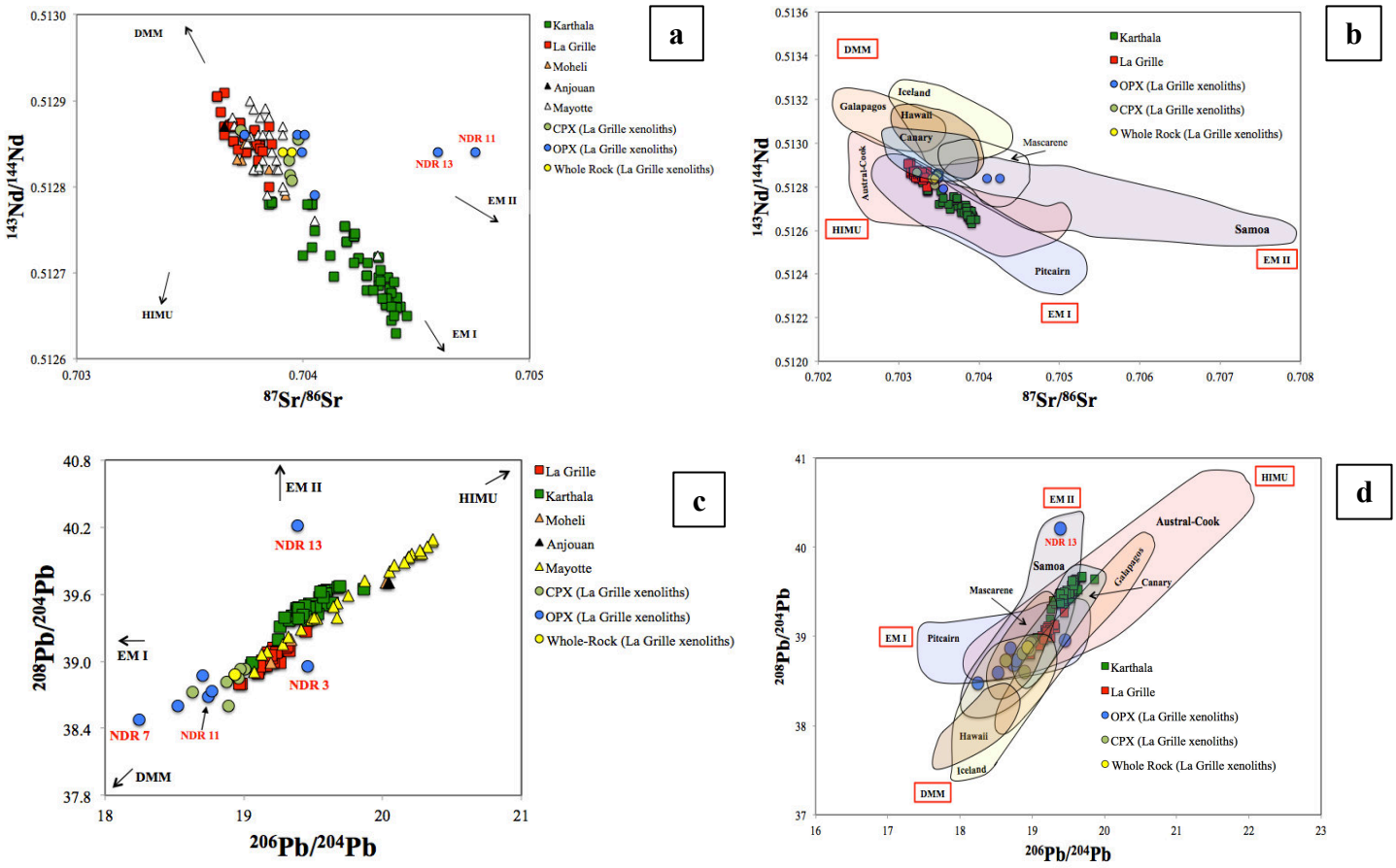

Fig. 4 a-b-c-d – a-b) $^{87}Sr/^{86}Sr$ vs. $^{143}Nd/^{144}Nd$ and **c-d)** $^{208}Pb/^{204}Pb$ vs. $^{206}Pb/^{204}Pb$ binary diagrams of Cpx, Opx and Whole-rock of La Grille xenoliths. Karthala whole-rock lavas (green squares) from Class et al. 1998; La Grille whole-rock lavas (red squares) from Class and Goldstein 1997 and Class et al. 1998; Moheli, Anjouan and Mayotte whole-rock lavas (orange, black and white triangles, respectively) from GEOROC Database; Data of OIB lavas (Iceland, Hawaii, Canary, Galapagos, Austral-Cook, Mascarene Archipelago, Pitcairn and Samoa) from GEOROC Database. End-member values for DMM (Depleted Morb Mantle), HIMU (high-μ = $^{238}U/^{204}Pb$ ratio), EMI and EMII (Enriched Mantle) are taken from Stracke 2012 and reference therein.

An important objective of geochemistry is to unravel how the Earth developed from its primordial to its present-day state. In particular, radiogenic isotope geochemistry represents a unique tool since isotope ratios such as $^{87}Sr/^{86}Sr$ and $^{143}Nd/^{144}Nd$ are a function of the time at which both the differentiation processes and fractionation of Rb from Sr and Sm from Nd occurred, respectively. Isotope systematics play a powerful role in mantle investigations precisely because Earth's mantle cannot be accessible for direct sampling so that much of the information about the geochemistry of the Earth's mantle stems from studies of mantle-derived products such as lavas and ultramafic peridotite xenoliths which provide a snapshot of the compositions and heterogeneities of the different mantle reservoirs.

Previous studies (e.g., Class et al., 1998) of the Sr-Nd-Pb isotopic relationships at Gran Comore show that the Karthala and La Grille sample suites have different isotopic compositions, demonstrating involvement of different sources in their formation (**Fig. 4a**) and indicating mantle heterogeneity below Grand Comore Island. La Grille lavas show a very small isotopic variation, suggesting derivation from a common mantle source ($^{87}Sr/^{86}Sr$ 0.70312–0.70332; $^{143}Nd/^{144}Nd$ 0.51284–0.51291; $^{206}Pb/^{204}Pb$ 19.1–19.27; $^{208}Pb/^{204}Pb$ 38.89–39.15). The overall isotopic variation of La Grille lavas has been explained by mixing between a plume component and alkali low-degree melts of metasomatized oceanic lithospheric mantle (Class and Goldstein 1997; Class et al. 1998), while Karthala alkali basalts are the result of mixing between plume-derived melts and high-degree melting of the metasomatized oceanic lithospheric mantle (Class et al. 1998). However, all the previous studies were based on measurements carried out on whole rocks samples.

Here we present for the first time data of the Sr-Nd-Pb isotopes on the different minerals of the La Grille xenoliths (i.e., clinopyroxene and orthopyroxene; hereafter Cpx and Opx). Furthermore, we also analysed some whole-rock samples for Sr-Nd-Pb isotopes, and our results fit well with those from previous investigations.

6. DISCUSSION

Overall, the Sr-Nd-Pb isotope signatures of Opx are more variable than Cpx (**Fig. 4 a-b-c-d**). The Sr-Nd-Pb isotope compositions of Cpx and Opx phenocrysts from La Grille xenoliths show higher variability than La Grille bulk lavas (**Fig. 4a-c**). As a whole, Cpx and Opx samples have Sr-Nd isotopic ratios that fall along a mixing between DMM and EM1 reservoir, but for two Opx samples (NDR17-11 and NDR17-13) whose higher Sr isotope signatures point towards an EM2 source for a given Nd isotope ratio (**Fig. 4a**). All together, these data are in agreement with previous investigations, however the behaviour of the two Opx samples (NDR17-11 and NDR17-13) has to be explained. Class et al. 1998 point out that the small isotopic variation observed in La Grille lavas indicates a derivation from a common mantle source. In Sr-Nd binary diagrams for OIB lavas (**Fig. 4b**), Cpx and Opx of La Grille xenoliths straddle mostly between the fields of Canary, Austral-Cook and Pitcairn lavas, while the two Opx samples NDR17-11 and NDR17-13 have compositions that overlap with those of Mascarene Archipelago (which includes La Reunion and Mauritius islands) and the least Sr radiogenic values of Samoan lavas. As seen for Sr and Nd element pairs, Pb isotope compositions of Opx show higher variability than Cpx. Most of the mineral samples exhibit highly un-radiogenic $^{208}Pb/^{204}Pb$ and $^{206}Pb/^{204}Pb$ ratios with respect to all Comoros lavas (**Fig 4c**), except for sample NDR17-13 (Opx) that shows the highest radiogenic Pb signature. The sample NDR17-3 (Opx) displays Pb isotope ratios close to those of La Grille whole-rock lavas (**Fig. 4c**). The sample NDR17-11 (Opx) shows Sr-Pb decoupling with highly radiogenic $^{87}Sr/^{86}Sr$ (**Fig. 4a**) and unradiogenic Pb isotope ratios (**Fig. 4c**). Furthermore, the Sr-Nd-Pb compositions of two whole-rock samples (NDR17-9-WR1 and NDR17-9-WR2) approach those of the Cpx (**Fig. 4a-b-c-d**). In Pb isotope diagrams for OIB lavas (**Fig. 4d**), Cpx and Opx of La Grille xenoliths fall in a wider range that overlaps the fields of Canary, Iceland, Austral-Cook and Pitcairn lavas, whereas the Opx sample NDR17-13 shows ratios pointing to EM2 reservoir.

Helium isotope compositions of Ol, Cpx and Opx from La Grille xenoliths, with few exceptions, are similar to those of the olivines separated from La Grille lavas and cover a wide range of [He] contents (7-963 $x10^{-9}$ cm^3STP/g) at almost uniform $^3He/^4He$ ratios (**Fig. 5**). NDR17-8 (Ol) and NDR17-11 (Opx) have the lowest R/Ra ratios (5.67 and 5.11, respectively.

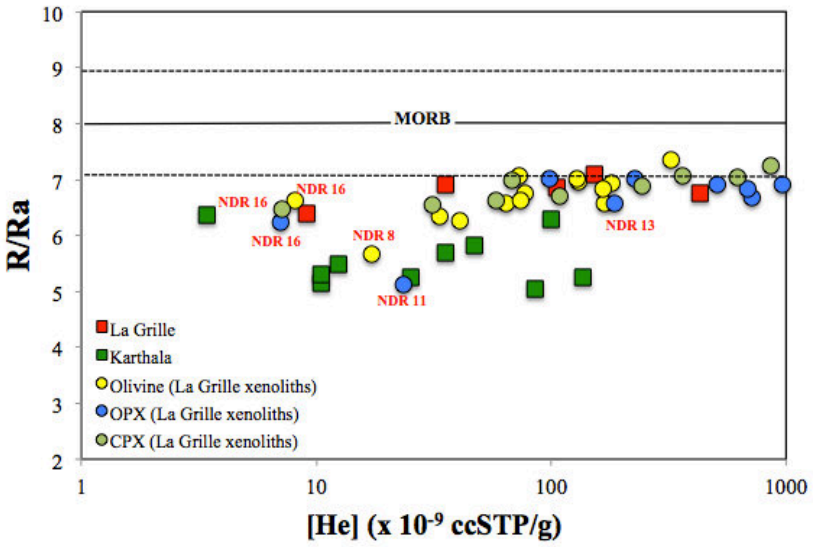

Fig. 5 – $^{3}He/^{4}He$ (R/Ra) vs [He] of crushed olivine, clinopyroxene and orthopyroxene phenocrysts. Where multiple analyses were carried out, the sample with the highest He concentration is shown. Red and green squares represent olivines separated from La Grille and Karthala lavas, respectively (Class et al. 2005).

Plotting helium vs. radiogenic isotopes (**Fig. 6a-b**) reveals that most of the La Grille xenoliths show variability lower than literature data, whereas the two Opx samples NDR17-13 and NDR17-11 display isotopic decoupling with NDR17-13 having R/Ra and $^{143}Nd/^{144}Nd$ ratios in the range of the other xenolithic samples but higher $^{87}Sr/^{86}Sr$ values, and NDR17-11 showing R/Ra and $^{87}Sr/^{86}Sr$ ratios pointing towards values close to Karthala and $^{143}Nd/^{144}Nd$ ratios indistinguishable from the other xenoliths.

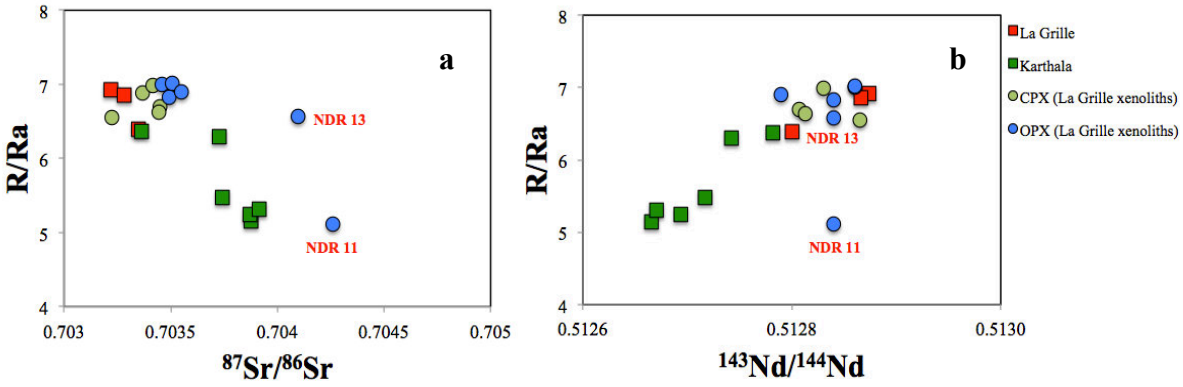

Fig. 6 a-b – $^{3}He/^{4}He$ (R/Ra) vs. (**a**) $^{87}Sr/^{86}Sr$ and (**b**) $^{143}Nd/^{144}Nd$ isotope ratios measured in orthopyroxene and clinopyroxene phenocrysts from La Grille xenoliths. Helium and Sr-Nd isotope data of La Grille (red squares) and Karthala (green squares) were measured in olivines and whole rock lavas, respectively (Class et al. 1997, 1998, 2005).

Fig. 7 shows clear evidence of contamination of NDR17-13 and NDR17-11 since their Sr-Nd isotopic compositions fall within and very close to the fields of Cenozoic alkaline rocks of central-northern Madagascar (Melluso e al. 2016 and reference therein) and of carbonatite rocks from East African Rift System (EARS), respectively.

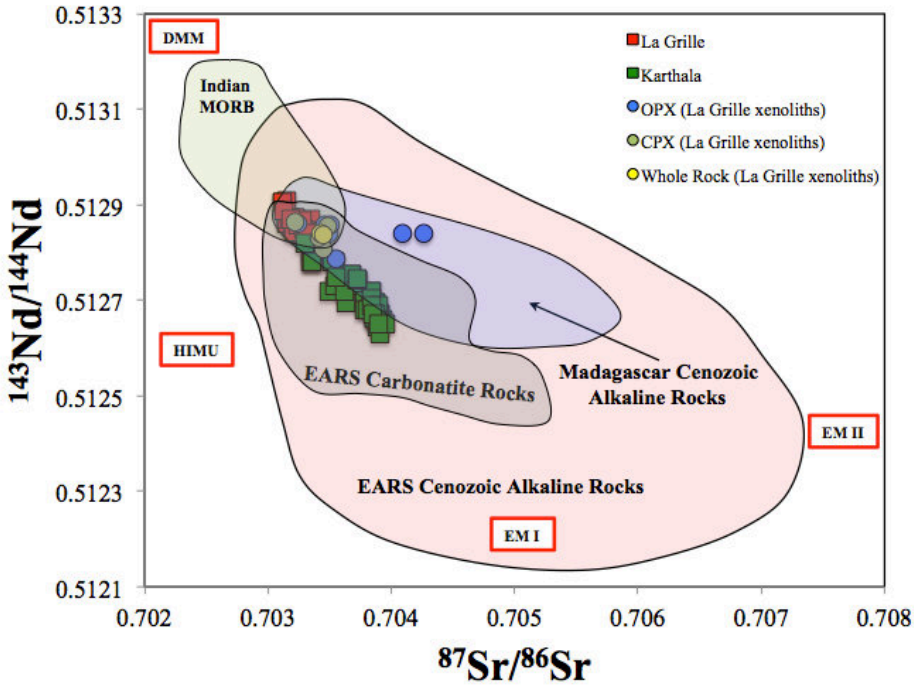

Fig. 7 - $^{87}Sr/^{86}Sr$ vs. $^{143}Nd/^{144}Nd$ of Cpx, Opx and whole-rock of La Grille xenoliths compared to EARS and Madagascar volcanic rocks. Karthala whole-rock lavas (green squares) from Class et al. 1998; La Grille whole-rock lavas (red squares) from Class and Goldstein 1997 and Class et al. 1998; Moheli, Anjouan and Mayotte whole-rock lavas (orange, black and white triangles, respectively) EARS Carbonatite Rocks, EARS Cenozoic Alkaline Rocks, Madagascar Cenozoic Alkaline Rocks and Indian MORB from GEOROC Database; EARS rocks comprise Ethiopia, Kenya, Uganda, Tanzania and Malawi. Madagascar Cenozoic Alkaline rocks include volcanic products from Nosy Be, Itasy and Ankaratra.

On the basis on petrological and geochemical constrains, Coltorti et al. (1999) bring evidence of a metasomatic episode in the oceanic mantle beneath La Grille volcano. They argue that the variable compositions of clinopyroxene phenocrysts and glasses extracted from spinel lherzolite and wehrlite xenoliths was due to an "ephemeral" alkali-rich carbonatitic metasomatizing agent with composition very close to those of natural carbonatites such as those found at Oldoinyo Lengai volcano.

Although NDR17-11, which has the highest Sr isotope composition along with a low $^{3}He/^{4}He$ ratio (then strongly degassed), might have been possibly contaminated by a He-rich metasomatizing melt more easily than the NDR17-13, which had originally a higher He content, it is unlikely that the supposed contaminant fluid was the volatiles associated to the an Oldoinyo Lengai-type carbonatitic melt since fumarolic fluids collected at Oldoinyo Lengai volcano have noble gases isotopic compositions indistinguishable from a mantle MORB reservoirs (Fischer et al. 2009). This could indicate that 1) the supposed metasomatizing agent responsible of the Opx variability may not be attributed to carbonatite-like compositions; 2) there could be a gas-magma decoupling with magma showing compositional values different from those of the emitted gases. Alternatively, if we try to discuss this Sr variability at regional scale, we observe isotopic similarities between the La Grille and the central-northern sector of Madagascar (**Fig. 8**) that may suggest rafts of lithospheric mantle, drifting behind during the southeastward separation of Madagascar from Africa, resulting in the opening of the Somali basin (Rabinowitz et al. 1983), might have affected mantle-derived materials erupted at La Grille volcano in the Grand Comore Island.

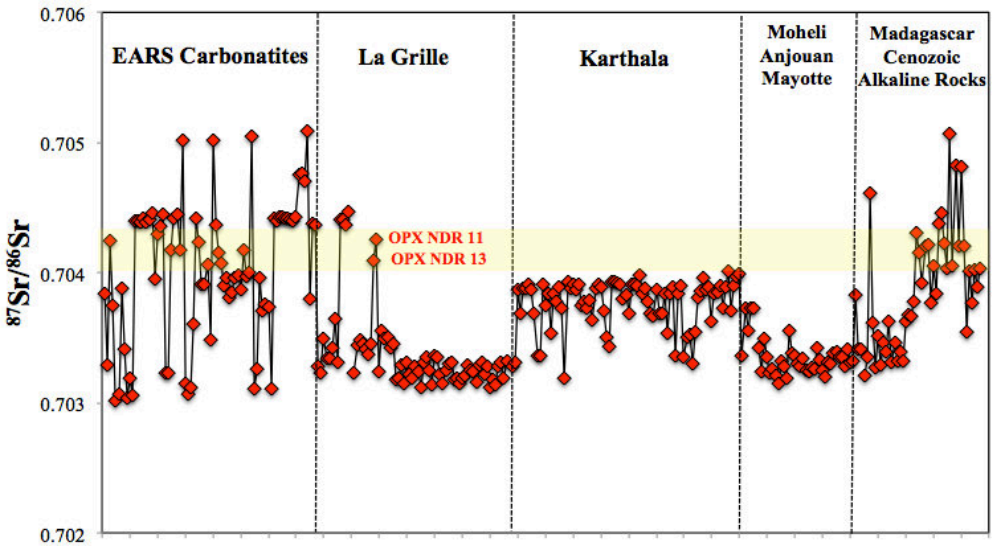

Fig. 8 – $^{87}Sr/^{86}Sr$ variation patterns showing comparison between Comoros archipelago and EARS Carbonatites and central-northern Madagascar alkaline rocks. Karthala whole-rock lavas from Class et al. 1998; La Grille Sr isotope ratios includes data of this study as well as of whole-rock lavas from Class and Goldstein 1997 and Class et al. 1998; Moheli, Anjouan and Mayotte whole-rock lavas EARS Carbonatites and Madagascar Cenozoic Alkaline Rocks from GEOROC Database; EARS: East African Rift System. Yellow shaded area highlights the volcanic products showing $^{87}Sr/^{86}Sr$ ratios nearly identical with those of the two Opx samples NDR17-13 and NDR17-11

7. SUMMARY AND CONCLUSIONS

The first ever measurements of the noble gas isotopes (He, Ne and Ar) in fluid inclusions combined to radiogenic isotopes (Sr, Nd and Pb) of olivine, clinopyroxene and orthopyroxene mineral separates from ultramafic peridotite xenoliths collected at La Grille volcano during 2017-2018 field campaigns were here presented with the purpose of constraining the mantle source beneath Grand Comore Island. Xenoliths are lherzolites, harzburgites, dunites and wehrlites with a protogranular to porphyroclastic texture, overprinted by Type A, B and C metasomatic reactions (Coltorti et al. 1999). Previous investigations of Grand Comore lithotypes were focused on bulk samples and mineral separates from lavas (i.e., Class et al. 1998; Class et al. 2005), while major and trace element data from clinopyroxenes and glasses from La Grille mantle xenoliths were reported in the literature by Coltorti et al. (1999). Previous geochemical investigations of Grand Comore lithotypes were focused on bulk samples and mineral separates from lavas, while major and trace element data from clinopyroxenes and glasses from La Grille xenoliths are reported in the literature.

Sr-Nd-Pb isotope systematics in clinopyroxene and orthopyroxene phenocrysts displays higher variability than La Grille bulk lavas, with orthopyroxenes more variable than clinopyroxenes. The $^{86}Sr/^{87}Sr$ and $^{143}Nd/^{144}Nd$ ratios of these mantle minerals fall along a mixing line between Depleted MORB and Enriched Mantle reservoirs, but for two samples whose higher Sr isotope signatures point towards an EM2 source. They show isotopic similarities with carbonatite rocks from the East African Rift System and central-northern Madagascar Cenozoic alkaline rocks. Most of the mineral samples exhibit highly un-radiogenic Pb isotope ratios with respect to all Comoros lavas, but for one orthopyroxene sample that shows the highest radiogenic Pb signature. Additionally, the observed variability in terms of Sr-Nd-Pb isotope compositions might induce to think that the compositions of bulk mineral separates from ultramafic mantle nodules could somewhat represent average values of heterogeneous monomineralic populations.

Noble gas isotopes in fluid inclusions of La Grille indicate a MORB-type mantle reservoir. In particular, the $^{3}He/^{4}He$ isotope compositions (up to 7.3Ra) fall in a range that overlaps the MORB mantle signature and the SCLM. These values are

systematically higher than those measured on crater fumaroles and fluid inclusions in olivine phenocrysts from Karthala lavas, indicating that Karthala volcano is still degassing volatiles with a He isotopic signature similar to those in volcanic products of the last eruption. The $^{20}Ne/^{22}Ne$, $^{21}Ne/^{22}Ne$ and $^{40}Ar/^{36}Ar$ isotope ratios plot along a mixing between air and a typical MORB-type reservoir.

REFERENCES

- **Bachelery P. and Coudray J. (1990)** – La Grande Comore et son volcan actif: Le Karthala, Journal of Nature 2, pp. 32-48
- **Bachelery P. and Coudray J. (1993)** - Carte geologique des Comores: Carte volcano-tectonique de la Grande Comore (Ngazidja), Laboratoire de Cartographie et d'informations geographiques, Cultures Annuelles, St. Denis de la Reunion, 1993.
- **Bachelery P. and Hémond C. (2016)** – Geochemical and Petrological Aspects of Karthala Volcano. In: Bachelery, P., Lénat, J. F., Di Muro, A. and Michon, L. (Eds.), Active Volcanoes of the Southwest Indian Ocean: Piton de la Fournaise and Karthala, Springer-Verlag, pp. 333-344
- **Caracausi A., Bafakih S., Boudoire G., Coltorti M., Di Muro A., Faccini B., Grassa F., Lauret F., Lemarchand A., Liuzzo M., Rizzo A. L. and Ventura Bordenca C. (2019)** – Preliminary results of an on-going geochemical study at Karthala Volcano, Grand Comore Islands (Indian Ocean), Geophysical Research Abstracts, vol. 21, EGU 2019-15978, Vienna (Austria).
- **Class C., Goldstein S. L. and Kurtz M. D. (1996)** - Significance of lower mantle entrainment or plume–lithosphere interaction in oceanic islands basalts: helium isotope evidence from Grande Comore, Goldschmidt Conference, Journal of Conference Abstracts 1, 112.
- **Class C. and Goldstein S. L. (1997)** – Plume-lithosphere interactions in the ocean basins: constrains from the source mineralogy, Earth and Planetary Science Letters 150, pp. 245-160.
- **Class C., Goldstein S. L., Altherr R. and Bachelery P (1998)** – The process of plume-lithosphere interaction in the ocean basins: the case of Grand Comore, Journal

of Petrology 39, pp. 881-903.

- **Class C., Goldstein S. L., Stute M., Kurz M. D. and Schlosser P. (2005)** - Grand Comore Island: A well-constrained "low $^{3}He/^{4}He$" mantle plume, Earth and Planetary Science Letters 233, pp. 391-409.
- **Coffin M. F. and Rabinowitz P. D. (1987)** - Reconstruction of Madagascar and Africa: evidence from the Davie fracture zone and western Somali basin. J Geophys Res 92, 9385–9406
- **Coltorti M., Bonadiman C., Hinton R. W., Siena F. and Upton B. (1999)** – Carbonatite metasomatism of the oceanic upper mantle: evidence from clinopyroxenes and glasses in ultramafic xenoliths of Grande Comore, Indian Ocean, Journal of Petrology 40, pp. 133-165
- **Correale A., Martelli M., Paonita A., Rizzo A., Brusca L., and Scribano V. (2012)** - New evidence of mantle heterogeneity beneath the Hyblean Plateau (southeast Sicily, Italy) as inferred from noble gases and geochemistry of ultramafic xenoliths. Lithos 132, 70–81.
- **Correale A., Rizzo A., Barry P. H., Lu J., and Zheng J. (2016)** - Refertilization of lithospheric mantle beneath the Yangtze craton in south-east China: evidence from noble gases geochemistry. *Gondwana Res*. 38, 289–303.
- **Courtillot V, Davaille A, Besse J, Stock J (2003)** - Three distinct types of hotspots in the Earth's mantle. Earth Planet Sci Lett 205:295–308
- **Daniel J., Dupont J. and Jouannic Ch. (1972)** – Relations Madagascar-Archipel des Comores (Nord-Est du Canal du Mozambique). Sur la nature volcanique du Banc de Leven. C R Acad Sci Paris 274, pp. 1874-1877
- **Day J. M. D., Barry P. H., Hilton D. R., Burgess R., Pearson D. G., and Taylor L. A. (2015)** - The helium flux from the continents and ubiquity of low-$^{3}He/^{4}He$ recycled

crust and lithosphere. *Geochim. Cosmochim. Acta* 153,

- **Debeuf D. (2004)** - Etude de l'évolution volcano-structurale et magmatique de Mayotte (Archipel des Comores, Océan Indien), PhD Thesis, La Réunion Univ., p277
- **Emerick, C. M. & Duncan, R. A. (1982)** - Age progressive volcanism in the Comore Archipelago, Western Indian Ocean, and implications for Somali plate tectonics, Earth and Planetary Science Letters 60, pp. 415–428.
- **Farley K.A., Poreda R.J., Onstott T.C. (1994)** - Noble gases in deformed xenoliths from an ocean island: charcterization of a metasomatic fluid. *In* Matsuda J (ed) Noble Gas Geochemistry and Cosmochemistry. Terra Scientific, Tokyo, p 159-178
- **Fischer T. P., Burnard P., Mart B., Hilton D. R., Füri E., Palhol F., Sharp Z. D. and Mangasini F. (2009)** – Upper-mantle volatile chemistry at Oldoinyo Lengai volcano and the origin of carbonatites, Nature Letters, vol. 459
- **Flower M. F. J. and Strong D. F. (1969)** - The significance of sandstone inclusions in lavas of the Comores archipelago. Earth Planet Sci Lett 7:47–50
- **Franke D., Jokat W., Ladage S., Stollhofen H., Klimke J., Lutz R., Mahanjane E. S., Ehrhardt A. and Schreckenberger B. (2015)** – The offshore East African Rift System: Structural framework at the toe of a juvenile rift, Tectonics 34, pp. 2086-2104
- **Gautheron C., & Moreira M. (2002)** - Helium signature of the sub-continental lithospheric mantle. Earth and Planetary Science Letters, 199, pp. 39–47.
- **Gautheron C., Moreira M., and Allègre C. J. (2005)** - He, Ne and Ar composition of the European lithospheric mantle - *Chem. Geol.* 217, pp. 97–112
- **Graham D.W (2002)** – Noble Gases Isotope Geochemistry of Mid-Ocean Ridge and Ocean Island Basalts: Characterization of mantle Source Reservoirs. In Noble Gases in Geochemistry and Cosmochemistry, vol., 47, Reviews in Mineralogy & Geochemistry, Mineralogical Society of America, Washington, DC Porcelli D., C.J. Ballentine. R.

Wieler Editors

- **Heidbach O, Tingay M, Barth A, Reinecker J, Kurfeß D, Müller B (2008)** - The World Stress Map database release 2008.
- **Honda M, Reynolds J, Roedder E, Epstein S (1987)** - Noble gases in diamonds: occurrences of solar like helium and neon. J Geophys Res 92:12507-12521
- **Lacroix A. (1922)** - La constitution lithologique de l'archipel des Comores. C R XIIIème congrès Int Géol Bruxelle 2:949–979
- **Lee J. Y., Marti K., Severinghaus K., Kawamura K., Yoo H. S., Lee J. B. and Kim J. S. (2006)** - A redetermination of the isotopic abundances of atmospheric Ar. Geochim. Cosmochim. Acta 70, 4507–4512.
- **Martelli M., Bianchini G., Beccaluva L., and Rizzo A. (2011)** - Helium and argon isotopic compositions of mantle xenoliths from Tallante and Calatrava, Spain - *J. Volcanol. Geotherm. Res.* 200, 18–26.
- **Martelli, M., Rizzo, A. L., Renzulli, a., Ridolfi, F., Arienzo, I., and Rosciglione, A. (2014)** - Noble-gas signature of magmas from a heterogeneous mantle wedge: the case of Stromboli volcano (Aeolian Islands, Italy). *Chemical. Geology, vol.* 368, pp. 39–53.
- **Melluso L. Cuccinello C., le Roex A. P. and Morra V. (2016)** – The Geochemistry of primitive volcanic rocks of the Ankaratra volcanic complex, and source enrichment processes in the genesis of the Cenozoic magmatism in Madagascar, Geochimica and Cosmochmica Acta, vol. 185, pp. 435-452
- **Mercier J-C. C. and Nicolas A. (1975)** - Textures and fabrics of upper mantle peridotites as illustrated by xenoliths from basalts. *Journal of Petrology* 16, 454–487.
- **Michon L. (2016)** - The volcanism of the Comoros archipelago integrated at a regional scale. In: Bachelery, P., Lénat, J. F., Di Muro, A. and Michon, L. (Eds.), Active Volcanoes of the Southwest Indian Ocean: Piton de la Fournaise and Karthala,

Springer-Verlag, pp. 333-344

- **Moreira M. and Allegre C. (1998)** – Helium-neon systematics and the structure of the mantle. Chem. Geol. 147, 53-59
- **Morin J. (2012)** - Gestion institutionnelle et réponses des populations face aux crises volcaniques: études de cas à La Réunion et en Grande Comore. PhD thesis, University of La Réunion, p 358 + annexes
- **Mukhopadhyay, S. (2012)** - Early differentiation and volatile accretion recorded in deep-mantle neon and xenon - Nature 486 (7401), 101
- **Nougier, J., Cantagrel, J. M. & Karchie J. P. (1986)** - The Comores archipelago in the western Indian Ocean: volcanology, geo- chronology and geodynamic setting. Journal of African Earth Sciences 5, 135–145.
- **Parai, R., Mukhopadhyay and S. (2015)** - The evolution of MORB and plume mantle volatile budgets: constraints from fission Xe isotopes in Southwest Indian Ridge basalts. Geochem. Geophys. Geosyst.16 (3), 719–735.
- **Rabinowitz, P. D., Coffin, M. F., Falvey, D. (1983)** - The separation of Madagascar and Africa, Science 220, 67–69.
- **Rindraharisaona EJ, Guidarelli M, Aoudia A, Rambola- manana G (2013)** - Earth structure and instrumental of Madagascar: implications on the seismotectonics. Tectonophysics 594:165–181. doi:10.1016/j.tecto. 2013.03.033
- **Rizzo A. L., Barberi F., Carapezza M. L., Di Piazza A., Francalanci L., Sortino F. and D'Alessandro W. (2015)** - New mafic magma refilling a quiescent volcano: evidence from He-Ne-Ar isotopes during the 2011-2012 unrest at Santorini, Greece. *Geochem. Geophys. Geosyst.* 16, 798–814. doi: 10.1002/2014GC005653
- **Sarda P.**, **Staudacher T., Allegre C. J., (1988)** - Neon isotopes in submarine basalts. Earth Planet. Sci. Lett., 91, 73-88

- **Sarda P., Moreira M., Staudacher T., Schilling J-G, Allègre C. J. (2000)** - Rare gas systematics on the southernmost Mid-Atlantic Ridge: constraints on the lower mantle and the Dupal source. J Geophys Res 105:5973-5996
- **Späth A., Le Roex A. P. and Duncan R. A. (1996)** – The geochemistry of lavas from the Comores Archipelago, Western Indian Ocean: petrogenesis and mantle source region characteristics, Journal of Petrology 37, pp. 961-991
- **Stracke A. (2012)** – Earth's heterogeneous mantle: A product of convection-driven interaction between crust and mantle, Chemical Geology 330-331, pp. 274-299
- **Strong D. F. (1972)** – The petrology of the lavas of Grande Comore, Journal of Petrology 13, pp. 181-217.
- **Trieloff M., Kunz J., Clague D.A., Harrison D., Allegre C.J. (2000) -** The nature of pristine noble gases in mantle plumes. Science, 288, 1036-1038
- **Vlastelic I. and Pietruszka A. J. (2016)** – A review of the recent geochemical evolution of Piton de la Fournaise volcano (1927-2010) - In: Bachelery, P., Lénat, J. F., Di Muro, A. and Michon, L. (Eds.), Active Volcanoes of the Southwest Indian Ocean: Piton de la Fournaise and Karthala, Springer-Verlag, pp. 185-201

Zindler, A. & Hart, S. (1986) - Chemical geodynamics. – Ann. Rev. Earth Planet. Sci. **14:** 493 – 571.

General conclusions of the PhD dissertation

In this PhD dissertation, noble gases (He, Ne, Ar) were the main subjects of study. The objective was to provide new contributions to the comprehension of the origin and behavior of natural fluids both in active seismic and volcanic settings by means of noble gases. It has discussed: **1)** The application of a field-based auto-sampler (SPARTAH) in a seismic region (Umbria region, Italy) to acquire high-frequency noble gas data and laboratory advances concerning the in-vacuum extraction of noble gases dissolved in thermal waters sampled with SPARTAH; **2)** A model of fluid circulation and secondary processes in a seismic region (Umbria region, Italy), based on the combination of noble gases and major volatiles (e.g., CO_2, N_2) necessary for interpreting possible geochemical anomalies carried by uprising fluids across the crust and their relationship between rock deformation, fracturing and the stress field of the area; **3)** First ever analyses of noble gases in fluid inclusions coupled to radiogenic isotopes (Sr, Nd and Pb) in olivine, clinopyroxene and orthopyroxene mineral separates from ultramafic mantle xenoliths from Grande Comore Island (Indian Ocean) performed with the goal to constrain mantle heterogeneity at depth and/or to trace potential chemical processes acting at modifying the pristine signature of the volatiles.

The outcomes of this PhD research offer some broad perspectives that help raising some fundamental questions for future lines of investigation.

As it is shown in Chapter II, SPARTAH apparatus has the potential to reinvigorate the approach to short-time series with implications for geochemical monitoring. A deployment of SPARTAH has been successfully tested in the field and showed the potentials of this type of equipments for capturing geochemical perturbations. Fluid samples were continously drawn into the copper tubings by means of a syringe-pump, although some logistic enhancements are needed in the future with the purpose of increase the on-field operative efficiency of the instrument. In order to improve the probability of recording pre-seismic anomalies, the field distribution of several SPARTAH devices must be extended. For this purpose, new sites of deployment are currently being sought for installation such as Iceland, Stromboli and Etna volcanoes as well as earthquake-prone areas with intense intercontinental seismicity such as eastern and southern China in order to determine short-term temporal patterns of noble

gases and, potentially, also other geochemical indicators. These sites can be considered potentially ideal localities for future deployments. The goal of these applications will be determining the respond of dissolved noble gases to any magmatic input and/or crustal perturbations.

As far as concern Chapter III, further elaborations of background geochemical models are strongly required in both seismically- and volcanically-active regions and must be considered as solid pre-requisite aimed at the recognition and investigation of any potential pre-event signals that can be straightforwardly correlated to geochemical anomalies due to volcanic and seismic activity.

From Chapter IV additional perspectives stem from the importance of coupling of noble gas (He, Ne, and Ar) to radiogenic components (Sr, Nd, and Pb) in fluid inclusions entrapped in primary mantle minerals that might carry to the surface the isotopic fingerprints of different geochemical reservoir disseminated in the Earth's mantle. However, more Sr-Nd-Pb isotope analyses on mineral phenocrysts, bulk xenolith and host lavas are required in order to extend the Comoros geochemical dataset. These results contribute to highlight the geochemical features of Gran Comore volcanic system (La Grille-Karthala) and its relationships with the underlying mantle, providing useful tools for future geochemical monitoring of an active, dangerous and very poorly explored natural system.